RADIAL DISTRIBUTION FUNCTIONS FOR AN HYDROGENOUS PLASMA IN EQUILIBRIUM

by

A.A. BARKER. M.Sc. (Adel.)

A thesis submitted in accordance with the requirements of the Degree of Doctor of Philosophy.

Mathematical Physics Department
University of Adelaide.
South Australia.

Submitted September 1968.

CONTENTS

CONTENTS

SUMMARY

Radial distribution functions $g_{ab}(r)$ for a dense hydrogenous plasma in equilibrium near the ionization temperature are obtained by two methods. The first is the Monte Carlo (MC) method originally applied to fluids by Metropolis et al, and recently extended to plasmas by Brush, Sahlin and Teller, and Barker. Although the technique seems readily applicable to high and low temperatures, the MC results near the ionization temperature show that in this region the $g_{ab}(r)$ obtained are unusually sensitive to two parameters. The first is the cut off imposed at small radii on the Coulomb potential between unlike particles, and it is found that it is necessary to consider quantum effects at these radii. The second is the maximum step length Δ through which the particles are allowed to move in the MC procedure. Near the ionization temperature the plasma behaves as a variable mixture of two phases, one ionized, the other unionized, and the magnitude chosen for Δ influences which phase dominates, in the relatively small sample of configurations selected by the Monte Carlo procedure.

The second technique applied is the solution of integral equations, and in particular the solution of a modified Percus-Yevick (MPY) equation. Early

investigation of the Percus-Yevick (PY) equation showed that in an asymptotic form for large radii it was inconsistent for systems interacting with attractive forces, and to overcome this difficulty terms suggested by Green were included to obtain the MPY equation.

The numerical solution of the MPY equation immediately showed the importance of the quantum mechanical effects at small radii, and that it would be necessary to calculate these accurately. An expression is obtained for the quantum mechanical distribution function in a dilute plasma, and from this an effective quantum mechanical potential is defined, which merges into the Coulomb potential at large radii. Results are given for the temperature range 9×10^{3}°K - 8×10^{4}°K for a neutral plasma.

Using shielded quantum mechanical $g_{ab}(r)$ as input to the PY equation, solutions are obtained for temperatures of 4×10^{4}°K and 3×10^{4}°K with an electron density of $10^{16}/c^{3}$. For temperatures below this the second-order inconsistency mentioned above causes divergence. Solutions of the MPY equation are also presented. These are found to improve on the PY results and to also increase slightly the temperature range over which the equation can be applied. The

percentage ionization present, and the difficulties encountered as the plasma tends towards a neutral gas are discussed in detail.

STATEMENT

I hereby declare that this thesis contains no material which has been accepted for the award of any other degree or diploma in any University, and that to the best of my knowledge and belief, the thesis contains no material previously published or written by any other person, except where due reference is made in the text.

A. A. Barker

ACKNOWLEDGEMENTS

Throughout this work the author has been greatly stimulated and encouraged by Professor H.S. Green, with whom many valuable discussions have been held. The author is also particularly grateful to Dr. P.W. Seymour for numerous helpful suggestions, and indeed wishes to acknowledge useful discussion with many visitors and members of the Adelaide University Mathematical Physics Department, especially Dr. R. Storer and Miss P. Tong.

Further this work could not have been completed without the generous grant from the Australian Institute of Nuclear Science and Engineering for computing. The computation was performed at the Adelaide University Computing centre and the cooperation of its staff was invaluable.

The author would also like to acknowledge the support of the Commonwealth Government in providing a Commonwealth Post Graduate Award from 1965 to 1968.

Thanks are also given to Miss M. Dodgson for her close cooperation in the production of this thesis.

I INTRODUCTION

The aim of this thesis is to determine accurate radial distribution functions for a neutral hydrogenous plasma of electron number density 10^{18}e/cc in the temperature region near ionization (i.e. 10^{4}°K to 5×10^{4}°K). So far there has been relatively little work on determination of distribution functions for plasmas, especially for the density-temperature region to be considered. We apply the Monte Carlo and the integral equation techniques, which have previously proved successful for non-ionized gases, to obtain distribution functions in plasmas.

1.1 The radial distribution function

Before 1900 the theoretical work on fluids was mainly based on the perfect gas law of Boyle and Charles, and its extension by Clausius and Van der Waals. In the early 1900's statistical mechanics was put on a much firmer basis by the systematic approach of Gibbs, whose theory of ensembles forms the basis of certain powerful techniques in use today. Then, in 1920, the application of X-ray diffraction techniques to fluids gave rise to the concept of the radial distribution function. The radial distribution function $g_{ab}(r)$ between two particles of types a and b is defined as

$$g_{ab}(r) = \frac{n_{b(a)}(r)}{n_b} \quad , \qquad (1.1)$$

where n_b is the average number density of particles of type b in the fluid (a macroscopic quantity), and $n_{b(a)}$ is the mean number density of particles of type b at a distance r from the ath particle (a microscopic quantity). The distance r is usually of microscopic order, and in this work will be expressed in units of Bohr radii. Thus $g_{ab}(r)$ is a measure of the correlation in the positions of particles of type a and b, and though not a strict probability, it is proportional to the probability of finding a particle of type b at a distance r from a particle of type a. About this time Ornstein and Zernike [1] also introduced their concept of the 'Indirect correlation function' $h_{ab}(r)$ (equal to $g_{ab}(r)-1$), which is composed of a 'direct correlation function' $c_{ab}(r)$ between the two particles a and b, plus a contribution from interactions with other particles. The importance of the concept of the radial distribution function (and hence the correlation functions) was realized when it was shown that most thermodynamic variables can be expressed in terms of $g_{ab}(r)$. Comprehensive treatments of the properties of $g_{ab}(r)$ and its relation to thermodynamic properties are given by Green [2], Hill [3], and Fisher [4].

1.2 Early work on Liquids

Several theories arose to predict g(r) for fluids. Initially these were associated particularly with crystal lattices and were known as 'cell or lattice' theories. These have become quite refined and have been extended to 'hole' theories, where the liquid is imagined to resemble a crystal lattice from which some of the particles are missing. Such significant structure theories have been particularly successful in predicting the properties of dense fluids, and are discussed fully by Guggenheim [5], Prigogine [6] and Barker [7] and references therein.

In the 1940's interest revived in fluid theory when Mayer and Mayer [8] proposed a 'cluster model' to calculate the virial coefficients accurately. The radial distribution function can be also expressed as a power series in the density, and for developments of this approach see references [9] and [10].

In the late 1940's, an integral equation for g(r) was proposed by Born and Green [11], who closed the sets of equations obtained previously by Yvon [14] by using the superposition approximation of Kirkwood [12]. Yvon's equations result from more general dynamical equations, by making substitutions appropriate to equilibrium, and

very similar dynamical equations were also proposed by Kirkwood [14a] and Bogoliubov [13] about this time. The integral equation for equilibrium is usually referred to as the BBGKY or BGY equation. It was solved numerically by a number of authors [14b] who obtained good agreement with experiment for tenuous fluids. An excellent review of this field is given by Green [14c].

In the 1950's the theorist received a setback when the results of reliable machine calculations became available for dense fluids, as the results disagreed with those of the cell theories, the BGY equation, and the virial expansion, which does not converge at liquid densities. The computing technique, developed by Metropolis et al. [15], is called the Monte Carlo method. The approach involves very few assumptions and applies for a wide temperature density range, and hence can be used to compare other theories. It has been applied to hard sphere fluids by Rosenbluth and Rosenbluth [16] and Alder, Frankel and Lewinson [17], and extended to particles interacting with a Lennard-Jones potential by Wood and Parker [18]. A similar approach called 'molecular dynamics' has been developed by Alder and Wainwright [19]. Recent papers by Hoover and Alder [20], Verlet [21] and Wood [22] give results which are in excellent agreement

with the experimental data available. The main disadvantage of the method is that it takes excessive computing time to obtain accurate radial distribution functions for a given temperature and density.

To improve upon this situation, in the last decade attention has reverted to the integral equation approach. In 1958 Percus and Yevick [23] proposed a new integral equation (PY) based on a collective coordinate procedure, which has since been elegantly derived by Percus [24] using a functional derivative technique. The PY equation was applied to hard spheres by Thiele, Helfand, Reiss, Frisch and Lebowitz [25] and an exact solution found for hard spheres by Wertheim [26] and Lebowitz [27]. Wertheim [28] has also obtained an analytic solution for a pair potential consisting of a hard core plus a short-range tail. A number of authors (see [29] to [33]) have extended the application of the PY equation to fluids interacting with the Lennard-Jones potential, several using the numerical solution procedure suggested by Broyles [34]. Comprehensive calculations have been completed recently for binary mixtures by Throop and Bearman [35] and Ashcroft and Langreth [36].

About the same time as the PY equation was proposed, another integral equation called the 'convoluted hyper-

netted chain' (CHNC) was introduced almost simultaneously by several authors, see [37] to [40]. This equation attempts to avoid the convergence difficulties arising from the series expansions in powers of density at high densities (see references [41] to [43]). It has been applied to Lennard-Jones fluids by Verlet and Levesque [44]; and Klein and Green [45] have also presented extensive results for this case. There have been recent papers by Helfand and Kornegay [46] and Hurst [47] extending the equation to take into account higher-order effects. Baxter [48] has numerically solved the CHNC equation involving the three particle term, and Khan [49] gives extensive results for liquid Ar, Kr, Ne and Xe.

Several approximate and perturbation theories have been suggested, most of which treat a region of the interaction by one of the equations mentioned above, see references [50] to [53]. Modern computer techniques have also enabled the BGY equation to be solved more accurately ([54] and [55]).

Recent experimental data has been published by Michels, et al [56] and Mikolaj and Pings [57], these results being principally for Argon and Neon, though Khan and Broyles [58] have considered liquid Xenon.

Even though several of the theories for fluids outlined above are quite comprehensive, there is still some

disagreement with experiment. This has led to papers on the relationship between pair potentials and distribution functions (e.g. Strong and Kaplow [59]) and also to some work on inequalities that g(r) must satisfy. (see [60] to [62]). Discussions of the determination of intermolecular forces from macroscopic properties are given by Rowlinson [63] and Hanley and Klein [64].

The main hope for further improvement in liquid theory seems to lie in the inclusion of three-body forces. There is considerable work being done in this field at present, and recent papers by Rushbrooke and Silbert [65], Rowlinson [66], Henderson [67], Lee, Jackson and Feenberg [68], Sinanoglu [69], and Graben [70] are of interest.

1.3 Extension to Plasmas

Prior to 1950, the work on electrolytes and plasmas in equilibrium was dominated by the famous work of Debye and Hückel in 1923 [71]. In 1950 Mayer [72] showed that the divergence due to the Coulomb interaction could be eliminated from the cluster expansion for the equation of state, and shortly after this several authors developed this approach to higher orders of accuracy (see [73] to [77]). There was also at this time considerable research, principally in Russia, directed at

extension of the BGY equation to plasmas, and this is discussed in detail in an excellent review article by Brush, De Witt and Trulio [78], which includes an extensive bibliography.

The difficulty in extending fluid theories to plasmas lies in the nature of the Coulomb force, because firstly, it contains a singularity at the origin, and secondly it has long-range effects. The stability of a system of particles interacting with such forces has been the subject of recent reviews and papers by Yang [79], Ter Haar [80], McWeeney [81], Fisher and Ruelle [82], and Dyson and Lenard [83]. The latter authors have shown that a necessary condition for stability of the system is the inclusion of quantum statistics. It is also well known that the more obvious difficulties associated with the short range of the Coulomb potential can be removed by taking into account quantum effects. The author at first attempted to treat these very approximately in extending fluid theories to plasmas. However, they proved to be so important that it became necessary to make more exact calculations.

Chapter II presents the results of extending the Monte Carlo approach to plasmas. The theory of extending the Monte Carlo approach to long-range forces has been developed independently by Brush, Sahlin and Teller [84]

for a one component plasma, and by Barker [85] for a two-component plasma, so only a brief description of the method is given. The results are presented in a series of tables and graphs, and show that for temperatures near ionization it is very difficult and expensive to obtain accurate distribution functions.

Chapter III describes the extension of the PY equation to a hydrogenous system. It is shown that the PY equation is in fact inconsistent for such a system, and to ensure consistency, higher-order terms such as those suggested by Green must be included. This equation is referred to as a modified Percus-Yevick equation (MPY), and is expressed in a form suitable for solution on a computer. An initial attempt to solve the MPY equation showed the importance of quantal effects, a feature which had already been indicated by the MC results.

To take account of the quantal effects, an expression for the two-particle distribution function is presented in Chapter IV. This expression is then evaluated numerically, results are presented, and then discussed in detail. References to research on the inclusion of quantal effects in fluids and plasmas are given in the introductory section 4.1.

In Chapter V, using the results of Chapter IV,

solutions of the PY and MPY equations are obtained. Some emphasis is placed on the numerical techniques used, for if a straightforward iteration procedure is adopted, the method diverges. Accurate distribution functions for 4×10^4°K are obtained, and somewhat less accurate results for 3×10^4°K. At 2×10^4°K it is found that, even when appropriate stabilizing techniques are employed in the computer program, both the PY and MPY equations diverge.

Before proceeding to the application of the MC method and MPY equation to plasmas, the author should mention in particular two other current lines of research in this field. The first is the systematic development of the diagrammatic method* to include quantal effects. Recent papers on this technique have been published by Bowers and Salpeter [86], De Witt [87], Hirt [88], Gaskell [89] and Diesendorf and Ninham [90]. The second line of approach extends the theory of integral equations to take into account long-range forces. The short-range divergence for the BGY equation was treated some time ago by Glauberman and Yukhnovski [91]. The higher-order terms, however (e.g. Green [92]), prove quite important as indicated by O'Neil and Rostoker [93]. Hirt [94] and Guernsey [95] have recently applied the BGY equation to plasmas. The quantal effects are incorporated

* Mentioned previously in a fluid context, this cluster expansion approach yields the DH result as a first approximation.

into the BGY equation in papers by Matsudaira [95] and in an elegant paper by Matsuda [96]. Extensions of the PY and, CHNC methods to a one component plasma have been made by Broyles, Sahlin and Carley [97], and Carley [98].

At the present time there are few plasma experimental values for g(r), and even the thermodynamic functions prove very difficult to obtain. Most of the experimental work completed so far has given g(r) for liquid metals (see Johnson and March [99]: here theoretical results are given by Villars [100]). The experimental thermodynamic properties of Hydrogen are discussed by Oppenheim and Hafemann [101] and Theimer and Kepple [102]. Numerical results are also given by Rasaiah and Friedman [103] for the application of integral equations to ionic solutions.

References to Chapter 1

[1] Ornstein, L.S and Zernike, F. (1944) Proc. Acad. Sci. (Amst) 17, 793.

[2] Green, H.S. (1952) 'Molecular theory of Fluids' (North-Holland Pub. Co. Amsterdam).

[3] Hill, T.L. (1956) Statistical Mechanics (McGraw-Hill, London)

(1960) Statistical Thermodynamics (Addison-Wesley, London).

[4] Fisher, I.Z. (1963) Statistical Theory of Liquids (Chicago Press, London).

[5] Guggenheim, E.A. (1952) Mixtures (Oxford Uni. Press, London).

[6] Prigogine, M. (1957) Molecular theory of solutions (North-Holland Pub. Co., Amsterdam).

[7] Barker, J.A. (1963) Lattice Theories of the Liquid State (Permagon Press Ltd., London).

[8] Mayer, J.E. and Mayer, M.G. (1940) Statistical Mechanics (J. Wiley and Sons, New York).

[9] Meixner, J, editor (1964) Proc. of Int. Symp. on Stat. Mechs. Germany 1964. (North-Holland Pub. Co. Amsterdam).

[10] De Boer, J. and Uhlenbeck, G.E. (1964) Studies in St. Mechs. Vol. I and II (North Holland Pub. Co. Amsterdam).

[11] Born, M. and Green, H.S. (1946) Proc. Roy. Soc. A188, 10.

[12] Kirkwood, J.G. (1935) J. Chem. Phys. 3, 300

(1939) J. Chem. Phys. 7, 919.

[13] Bogoliubov, N.N. 'Problems of Dynamical Theory of Statistical Physics ' (English translation by E.K. Core Air Force Cambridge Research Centre, Publication TR-59-23).

[14] Yvon, J. (1937) Fluctuations en Densité; La Propogation et la Diffusion de la Luminiére (Herman and Cie).

[14a] Kirkwood, J.G. (1946) J. Chem. Phys. 14, 180.

Kirkwood, J.G. and Boggs, M. (1941). J. Chem. Phys. 9, 514.

10, 394.

[14b] Rodriguez, A.E. (1948) Proc. Roy. Soc. London. Ser. A. 196, 73.

McLellan, A.G. (1952) Proc. Roy. Soc. London 210, 509

Cheng, K.C. (1950) Proc. Roy. Phys. Soc. Ser.A. 63, 428.

Kirkwood, J.G., Maun, E.K. and Alder, B.J. (1950) J. Chem. Phys. 18, 1040.

Kirkwood, J.G. Lewinson, V.A. and Alder, B.J. (1952) J. Chem. Phys. 20, 949.

[14c] Green, H.S. (1960) 'Encylopedia of Physics, Vol.X. p.14' Ed. by S. Flügge.

[15] Metropolis, N.M., Rosenbluth, A.W., Rosenbluth, M.N., Teller, A.H. and Teller, E. (1953) Jour. Chem. Phys. 21, 1087.

[16] Rosenbluth, M.N. and Rosenbluth, A.W. (1954) J. Chem. Phys. 22, 881.

[17] Alder, B.J., Frankel, S.P. and Lewinson, V.A. (1955) J. Chem. Phys. 23, 417.

[18] Wood, W.W. and Parker, F.R. (1957) J. Chem. Phys. 27, 720.

[19] Alder, B.J. and Wainwright, A.W. (1959) J. Chem. Phys. 31, 459.

[20] Hoover, W.G. and Alder, B.J. (1967) J. Chem. Phys. 153, 250.

[21] Verlet, L. (1967) Phys. Rev. 159, 98
(1968) 165, 201.

[22] Wood, W.W. (1968) J. Chem. Phys. 48, 415.

[23] Percus, J.K. and Yevick, G.J. (1958) Phys. Rev. 110, 1.

[24] Percus, J.K. (1962) Phys. Rev. Letters 8, 462.
(1963) J. Math. Phys. 4, 116. See also Lebowitz, J.L. (1963) J. Math. Phys. 4, 248.

[25] Thiele, E. (1963) J. Chem. Phys. 38, 1959 and 39, 474.

Reiss, H., Frisch, H.L. and Lebowitz, J.L. (1959) J. Chem. Phys. 31, 369.

Helfand, E., Frisch, H.L. and Lebowitz, J.L. (1961) J. Chem. Phys. 34, 1037.

[26] Wertheim, M.S. (1963) Phys. Rev. Letters 10, 321, and E501.

[27] Lebowitz, J.L. (1964) Phys. Rev. 133, A895.

[28] Wertheim, M.S. (1964) J. Math. Phys. 5, 643.

[29] Broyles, A.A. (1961) J. Chem. Phys. 34, 1068 and 35, 493.

[30] Verlet, L. (1964) Physica 30, 95.

[31] Broyles, A.A. Chung, S.U. and Sahlin, H.L. (1962) J. Chem. Phys. 37, 2462.

[32] Verlet, L. and Levesque, D. (1962) Physica 28, 1124.

[33] Rowlinson, J.S. (1963) Molec. Phys. 7, 349.

[34] Broyles, A.A. (1960) J. Chem. Phys. 33, 456.
34, 359.

[35] Throop, G.J. and Bearman, R.J. (1966) J. Chem. Phys. 44, 1423.
(1967) J. Chem. Phys. (47), 3036.

[36] Ashcroft, N.W. and Langreth, D.C. (1967) Phys. Rev. 156, 685.

Meeron, E. (1958) Phys. Fluids 1, 246.

[37] Meeron, E. (1960) J. Math. Phys. 1, 192.

Morita, T. (1958) Prog. Theor. Phys. Kyoto. 20,920.

[38] Morita, T. and Hiroike, K. (1960) Prog. Theor. Phys. Kyoto 23, 385, 829 and 1003; 24, 317; 25, 537.

[39] Van Leeuwen, J.M.J., Groenweld, J. and De Boer, J. (1959) Physica 25, 792.

[40] Green, M.S. (1960) J. Chem. Phys. 33, 1403.

[41] Rushbrooke, G.S. (1960) Physica 26, 259.

[42] Verlet, L. (1960) Nuovo Cimento 18, 77.

[43] Salpeter, E.E. (1958) Ann. Phys. 5, 183.

[44] Verlet, L. and Levesque, D. (1962) Physica 28, 1124.

[45] Klein, M. and Green, M.S. (1963) J. Chem. Phys. 39, 493, 1367, 1388.

[46] Helfand, E and Kornegay, R.L. (1964) Physica 30, 1481.

[47] Hurst, C. (1965) Proc. Phys. Soc. 86, 193.

[48] Baxter, R.J. (1967) Preprint.

[49] Khan, A.A. (1964) Phys. Rev. 134, A367; 136, A1260 (1966) Preprints

[50] Carley, D.D. and Lado, F. (1965) Phys. Rev. 137, A42.

Lado, F. (1964) Phys. Rev. 135, A1013.

(1967) J. Chem. Phys. 47, 4828.

[51] Wertheim, M.S. (1965) J. Chem. Phys. 43, 1370.
(1967) J. Chem. Phys. 46, 2551.
(1967) J. Maths. Phys. 8, 927.

[52] Barker, J.A. and Henderson, D. (1967) J. Chem. Phys. 47, 2856 and 4714.

[53] Kazak, J.J. and Rice, S.A. (1968) J. Chem. Phys. 48, 1226.

[54] Young, D.A. and Rice, S.A. (1967) J. Chem. Phys. 47, 5061.

[55] Andrews, F.C. Preprint.

[56] Michels, A., Levelt, J.M.H. and Wolkers, G.J. (1958) Physica 24, 769.
Michels, A., Levelt, J.M.H. and De Graaf, W. (1958) Physica 24, 659.

[57] Pings, C.J. (1967) Disc. Farad. Soc. 43, 89.
Molec. Phys. 12, 501.
Mikoloj, P.G. and Pings, C.J. (1967) J. Chem. Phys. 46, 1401, 1412.

[58] Khan, A.A. and Broyles, A.A. (1965) J. Chem. Phys. 43, 43.

[59] Strong, S.L. and Kaplow, R. (1966) J. Chem. Phys. 45, 1840.

[60] Yamada, M. (1961) Prog. Theor. Phys. Kyoto 25, 579.

[61] Garrod, C. and Percus, J.K. (1964) J. Math. Phys. 5, 1756.

[62] Feenberg, E. (1965) J. Math. Phys. 6, 658.

[63] Rowlinson, J.S. (1965) Disc. Farad. Soc. 40, 19.

[64] Hanley, H.J.M. and Klein, M. (1967) N.B.S. technical note 360.

[65] Rushbrooke, G.S. and Silbert, M. (1967) Molec. Phys. 12, 505.

[66] Rowlinson, J.S. (1967) Molec. Phys. 12, 513.

[67] Henderson, D. (1967) J. Chem. Phys. 46, 4306.

[68] Lee, D.K., Jackson, H.W. and Feenberg, E. (1967) Ann. Phys. 44, 84.

[69] Sinanoglu, L. (1967) Adv. in Chem. Phys. 12, 283.

[70] Graben, H.W. (1968) Phys. Rev. Letters 20, 529.

[71] Debye, P. and Hückel, E. (1923) Phys. Zeits. 24, 185, 305. 'The collected papers of P.J.W. Debye' (Interscience Pub., New York, 1954).

[72] Mayer, J.E. (1950) J. Chem. Phys. 18, 1426.

[73] Montroll, E.W. and Ward, J.C. (1958) Phys. Fluids 1, 55.

[74] Friedman, H.L. (1959) Molec. Phys. 2, 23, 190 and 436

[75] Meeron, E. (1957) J. Chem. Phys. 26, 804.
(1958) Phys. Fluids 1, 139.

[76] Abe, R. (1959) Progr. Theor. Phys. Kyoto 21, 475 and 22, 213.

[77] Landau, L.D. and Lifshitz, E.M. (1958) 'Statistical Physics' p.229 (Permagon Press. New York).

[78] Brush, S.G., De Witt, H.E. and Trulio, J.G. (1963) Nuc. Fusion 3, 5.

[79] Yang, C.N. (1962) Rev. Mod. Phys. 34, 694.

[80] Ter Haar, D. (1961) Rept. Prog. Phys. 24, 304.

[81] Mc Weeney, R. (1960) Rev. Mod. Phys. 32, 335.

[82] Fisher, M.E. and Ruelle, D. (1966) J. Math. Phys. 7, 260.

[83] Dyson, F.J. and Lenard, A. (1967) J. Math. Phys. 8, 423, 1538.

[84] Brush, S.G., Sahlin, H.L. and Teller, E. (1966) J. Chem. Phys. 45, 2102.

[85] Barker, A.A. (1965) Aust. J. Phys. 18, 119 - see Appendix A.

[86] Bowers, D.L. and Salpeter, E.E. (1960) Phys. Rev. 119, 1180.

[87] De Witt, H. (1962) J. Math. Phys. 3, 1003, 1216.
(1965) Phys. Rev. 140, A466.
(1966) J. Math. Phys. 7, 616.

[88] Hirt, C.W. (1965) Phys. Fluids 8, 693, 1109.

[89] Gaskell, T. (1968) Proc. Phys. Soc. Ser 2 1, 213.

[90] Diesendorf, M.O. and Ninham, B.W. (1968) J. Maths. Phys. (to be published).

[91] Glauberman, A.E. (1951) Doklady Akad Nauk SSR 78, 88
Glauberman, A.E. and Yukhnovski (1952) Zhur. Ekop. Teor. Fiz. 22. 562.

[92] Green, H.S. (1961) Nuclear Fusion 1, 69.

[93] ONiel, T. and Rostoker (1965) Phys. Fluids 8, 1109.

[94] Hirt, C.W. (1965) Phys. Fluids 8, 693.
(1967) 10, 565.

[95] Matsudaira, N. (1966) Phys. Fluids 9, 539.

[96] Matsuda, K. (1968) Phys. Fluids 11, 328.

[97] Broyles, A.A., Sahlin, H.L. and Carley, D.D. (1963) Phys. Rev. Lett. 10, 319.

[98] Carley, D.D. (1963) Phys. Rev. 131, 1406.
(1965) J. Chem. Phys. 41, 3489
(1967) 46, 3783

[99] Johnson, M.D. and March, N.H. (1963) Phys. Lett. 3, 313.

[100] Villars, D.S. (1963) Phys. Fluids 6, 745.

[101] Oppenheim, I. and Hafemann, D.R. (1963) J. Chem. Phys. 39, 101.

[102] Theimer, O. and Kepple, P. (1967) Phys. Rev. 165, 168.

[103] Rasaiah, J.C. and Friedman, H.L. (1968) J. Chem. Phys. 48, 2742.

II THE MONTE CARLO METHOD

The extension of the Monte Carlo (MC) method to plasmas is described in detail by Brush, Sahlin and Teller [1], and Barker [2]. Emphasis in this chapter is placed on the results of this author's recent extensive computer calculations for a hydrogenous plasma of density 10^{18} ions/cc at a temperature of 10^{4}°K.

2.1 An outline of the method

A system composed of N individual particles is confined in a volume V at a temperature T. The particles are assumed to obey classical statistics and to interact in accordance with the Coulomb potential. The problem is reduced to a feasible size by considering only a finite number of particles N, and in this case N=32, a value which proves convenient and gives reasonable accuracy (see Alder and Wainright [3]). In the initial configuration the particles can be either placed randomly or in an ordered fashion in the unit cell of volume $V=L^3$, and in the case of an electrically neutral plasma they can also be initially paired as neutral particles or dissociated as ions. The unit cell is surrounded by a network of identical cells, thus enabling the energy of a configuration to be calculated conveniently as

described in detail in [1] and [2]. Another configuration is obtained by displacing a particle by a random amount, which can have a maximum value Δ. The energy of the new configuration is calculated, and the MC procedure decides if the move is acceptable or not, (see [2]). In the present calculation each particle is displaced systematically (although they can be moved randomly) in this manner, until the energy of the system approaches its equilibrium value. The criterion for the choice of Δ is such that the rate of approach of the system to equilibrium is minimised. In previous MC calculations [1], [2], [4], it has been found convenient to use $\Delta \sim L/\sqrt{3N})$, where L is the unit cell length, and N is the number of particles in the cell for then Δ has the right order of magnitude to secure near-optimum convergence. In this work this implies a value of Δ of order 9 Bohr radii.

Another parameter which proves important in the calculation is the cut-off AO imposed on the attractive Coulomb potential at short radii. This limits the closeness of approach of two particles, and hence the potential energy between them. The value given to AO is twice the Bohr radius, for at this radius (by Bohr's orbit theory) a particle has its lowest potential energy possible without any kinetic energy, and the value of the

potential energy is the same as the ionization energy for the particle. Here pairing is considered to occur between two particles when they are closer than A0, i.e. in their ground state, and particles are not considered paired when they are in excited states.

The computer program used for the calculation is given in [2], although several modifications were necessary to adapt it to the C.D.C. 6400 computer on which the present calculations were completed. The computing time involved was found to be excessive, 3000 iterations taking one hour on the 6400 computer (each iteration gives every particle in the unit cell a chance to move up to the maximum distance Δ). For this reason the study has been confined to a single temperature of 10^4°K, and density, 10^{18}ions/cc.

2.2 Results

Three main computer runs were made. The first started the particles from a random configuration of protons and electrons and initially put $\Delta = 12.5\ a_o$, and proceeded for 50,000 iterations. Then the energy of the system appeared to have settled down to the equilibrium value, and to check this, a second run was carried through, starting the particles as pairs of

protons and electrons approximately equidistant from each other in the cell. Again the maximum displacement was chosen as $\Delta = 12.5a_o$, but here the run covered 12,000 iterations. This run seemed to approach a slightly different energy equilibrium value, and so a third run was completed, again starting the particles as pairs, distributed evenly throughout the cell, but now allowing them to move with $\Delta = 50a_o$ for 10,000 iterations.

Fig 2.1 shows the variation of the normalised cell energy per particle E/NkT with the number of iterations completed for the three runs mentioned above. The energy is averaged over 1000 iterations for each point plotted, and this smooths out many of the extreme energy fluctuations which occur from iteration to iteration. It can be seen that with such fluctuations it becomes difficult to obtain comprehensive sampling of all states using the MC procedure unless a very long run is taken. On the right-hand side of the figure levels are presented which show approximately the number of pairs in the unit cell corresponding to a selected value of E/NkT. In Fig 2.2 the like and unlike distribution functions are drawn (on a log scale) by considering iterations 30,000 to 50,000 of run 1, in which region the system seemed to be near equilibrium.

The corresponding classical distribution functions are also drawn; to incorporate the required cut-off at small radii, they have been given a constant value below 2.0 Bohr Radii. The data for these characteristics are given to the nearest three figures in Table 2.1, where the subscript U refers to the unlike case, L the like case and C refers to the classical distribution function.

Fig 2.3 shows unlike distribution functions taken from selected sections of Fig 2.1. The results to 2 places of decimals are given numerically in Table 2.2 with the corresponding Debye Huckel distribution function. For a plasma of this temperature and density the Debye shielding distance is 92.4 Bohr radii, and is denoted on the graphs by λ_D. Fig 2.4 and Table 2.3 present the distribution functions between the like particles for the corresponding sections of Fig 2.1. The non-integral values of r appearing in the Table arise because the program (see [2], Appendix B) was run in mesh units, and 1 Bohr radius = 2.100 mesh units. The energy has also been expressed as a dimensionless number, where the energy in cell units E is converted into the dimensionless E/NkT by multiplying it by 2.072×10^{-3} for the Temp of 10^4°K and electron density of 10^{18}e/cc.

Fig 2.5 isolates the unlike distribution functions at small radii, and the values are obtained by taking

logs to the base ten of the figures given in Table 2.2.

Again the classical curve $g_{UC} = e^{\beta\phi_U(r)}$ is given with the $\phi_U(r)$ used in the Monte Carlo calculation (i.e. Coulomb for $r>2a_o$, and const for $r<2a_o$.)

Distribution functions taken from iterations 13000 to 23000 of run (1) are denoted in the Tables as 13000-23000 (1).

TABLE 2.1

RADIAL DISTRIBUTION FUNCTIONS for Like and Unlike cases from iterations 30,000 to 50,000 of Run 1.

r (Bohr Radii)	$Log_{10}(g_L(r))$	$Log_{10}(g_{LC}(r))$	$Log_{10}(g_U(r))$	$Log_{10}(g_{UC}(r))$
1.19	-.576	-6.857	4.740	6.857
2.00		-6.857		6.857
3.57	.339	-3.841	3.2940	3.841
5.95	.139	-2.305	2.321	2.305
8.33	.214	-1.646	1.918	1.646
10.71	.150	-1.280	1.659	1.280
13.10	.072	-1.047	1.504	1.047
15.48	.083	-0.886	1.365	0.886
17.85	.007	-0.786	1.244	0.768
20.24	.059	-0.678	1.166	0.678
22.6	.028	-0.607	1.041	0.607
25.0	.055	-0.549	.959	0.549
27.4	.095	-0.500	.846	0.500
29.8	.065	-0.460	.778	0.460
32.2	.097	-0.426	.730	0.426
34.5	.103	-0.397	.640	0.397
36.9	.051	-0.372	.579	0.3[illegible]
39.3	.047	-0.349	.517	0.349

r	Log_{10} $(g_L(r))$	Log_{10} $(g_{LC}(r))$	Log_{10} $(g_U(r))$	Log_{10} $(g_{UC}(r))$
41.7	.051	-0.329	.459	0.329
44.0	.088	-0.312	.430	0.312
46.4	.140	-0.296	.407	0.296
48.8	.134	-0.281	.372	0.281
51.2	.113	-0.268	.334	0.268
53.5	.140	-0.256	.297	0.256
55.9	.087	-0.245	.268	0.245
58.3	.064	-0.235	.224	0.235
60.7	.038	-0.226	.179	0.226
63.1	.020	-0.217	.139	0.217
65.5	.018	-0.209	.127	0.209
67.8	.061	-0.202	.117	0.202
70.2	.036	-0.195	.097	0.195
72.6	.017	-0.188	.072	0.188
75.0	.020	-0.183	.045	0.183
77.4	.010	-0.177	.045	0.177
79.8	.016	-0.172	.046	0.172
82.1	-.009	-0.167	.015	0.167
84.5	.012	-0.162	.011	0.162
86.9	.036	-0.158	.033	0.158
89.3	.020	-0.154	.012	0.154
91.6	.012	-0.150	.014	0.150
94.0	.003	-0.146	.017	0.146
96.4	1044	-0.142	.031	0.142

r	$\text{Log}_{10}(g_L(r))$	$\text{Log}_{10}(g_{LC}(r))$	$\text{Log}_{10}(g_U(r))$	$\text{Log}_{10}(g_{UC}(r))$
98.8	.027	-0.139	-.006	0.139
101.1	.034	-0.136	.017	0.136
103.6	.039	-0.132	.012	0.132
105.9	.022	-0.129	.002	0.129
108.3	.015	-0.127	-.014	0.127
110.7	-.020	-0.124	-.026	0.124
113.1	-.009	-0.121	-.043	0.121
115.5	-.032	-0.119	-.056	0.119
117.9	-.022	-0.116	-.044	0.116
119.1	-.056	-0.115	-.077	0.115
122.6	-.052	-0.112	-.077	0.112
125	-.051	-0.110	-.078	0.110
127.4	-.031	-0.108	-.061	0.108
129.8	-.047	-0.106	-.082	0.106
132.1	-.047	-0.104	-.067	0.104
134.5	-.046	-0.102	-.075	0.102
136.9	-.050	-0.100	-.075	0.100
139.3	-.047	-0.099	-.061	0.099
141.7	-.048	-0.097	-.067	0.097
144.0	-.034	-0.045	-.060	0.095
146.4	-.043	-0.094	-.068	0.094
148.8	-.038	-0.092	-.068	0.092
151.2	-.053	-0.091	-.068	0.091
153.6	-.032	-0.089	-.064	0.089

r	$\text{Log}_{10}(g_L(r))$	$\text{Log}_{10}(g_{LC}(r))$	$\text{Log}_{10}(g_U(r))$	$\text{Log}_{10}(g_{UC}(r))$
156.0	- .035	-0.088	- .053	0.088
158.4	- .044	-0.086	- .076	0.086
160.7	- .049	- 0.085	- .072	0.085
163.1	- .024	- 0.084	- .044	0.084
165.5	- .038	- 0.083	- .065	0.083
167.9	- .016	- 0.082	- .044	0.082
170.2	- .016	- 0.081	- .047	0.081
172.6	- .005	- 0.079	- .034	0.079
175.0	- .012	- 0.078	- .037	0.078

TABLE 2.2

Unlike radial distribution functions taken from various runs as shown and compared with the corresponding Debye Huckel distribution Function.

$r(a_o)$	D.H.	13000-2300(1)	30000-40000(1)	40000-50000(1)	40000-50000(3)
1.19	2.35×10^{11}	2.95×10^{4}	5.51×10^{4}	5.47×10^{4}	6.75×10^{3}
3.57	4.94×10^{3}	1.24×10^{3}	1.98×10^{3}	1.96×10^{3}	2.00×10^{2}
5.95	1.45×10^{2}	1.30×10^{2}	2.15×10^{2}	2.04×10^{2}	2.58×10
8.33	3.19×10	5.44×10	8.31×10	8.25×10	9.98
10.71	1.38×10	367×10	4.59×10	4.52×10	6.51
13.10	8.10	2.63×10	3.27×10	3.11×10	5.36
15.48	5.61	2.01×10	2.33×10	2.30×10	5.01
17.85	4.29	1.58×10	1.79×10	1.72×10	3.85
20.24	3.50	1.27×10	1.48×10	1.45×10	3.44
22.6	2.98	1.07×10	1.08×10	1.19×10	2.89
25.0	2.62	8.64	9.10	9.08	2.64
27.4	2.36	6.73	6.85	7.34	2.62
29.8	2.16	5.54	5.88	6.12	2.39
32.2	2.00	4.84	5.32	5.41	2.23
34.5	1.88	4.03	4.45	4.26	2.09
36.9	1.77	3.37	3.82	3.76	1.98
39.3	1.69	2.84	3.14	3.44	1.99

$r(a_o)$	D.H.	13000-23000(1)	30000-40000(1)	40000-50000(1)	40000-50000(3)
41.7	1.62	2.43	3.10	2.66	1.95
44.0	1.56	2.15	2.91	2.47	1.80
46.4	1.51	1.86	2.81	2.31	1.75
48.8	1.46	1.76	2.56	2.16	1.70
51.2	1.42	1.58	2.33	1.99	1.67
53.5	1.39	1.53	2.10	1.86	1.64
55.9	1.36	1.44	2.11	1.59	1.54
58.3	1.33	1.41	1.83	1.51	1.54
60.7	1.31	1.38	1.64	1.38	1.51
63.1	1.29	1.47	1.53	1.23	1.49
65.5	1.27	1.45	1.42	1.26	1.41
67.8	1.25	1.55	1.44	1.18	1.38
70.2	1.23	1.34	1.37	1.13	1.41
72.6	1.22	1.32	1.32	1.04	1.35
75.0	1.21	1.27	1.22	.98	1.31
77.3	1.19	1.29	1.32	.90	1.31
79.8	1.18	1.30	1.23	.99	1.29
82.10	1.17	1.29	1.12	.96	1.26
84.5	1.16	1.30	1.08	.98	1.31
86.9	1.15	1.22	1.14	1.02	1.25
89.3	1.14	1.18	1.13	.93	1.26
91.6	1.14	1.17	1.08	.98	1.24

$r(a_o)$	D.H.	13000-23000(1)	30000-40000(1)	40000-50000(1)	40000-50000(3)
94.0	1.13	1.14	1.09	.99	1.23
96.4	1.12	1.13	1.14	1.00	1.21
98.8	1.12	1.11	1.06	.97	1.20
101.2	1.11	1.09	1.09	.99	1.21
103.6	1.10	1.05	1.11	.95	1.18
105.9	1.10	1.05	1.13	.90	1.18
108.3	1.09	1.06	1.09	.83	1.20
110.7	1.09	.98	1.05	.83	1.20
113.1	1.09	1.02	1.02	.78	1.16
115.5	1.08	1.03	1.04	.72	1.14
117.9	1.08	1.00	1.08	.72	1.16
120.2	1.07	.99	1.03	.64	1.12
122.6	1.07	1.03	1.00	.68	1.10
125.0	1.07	1.03	1.00	.67	1.09
127.4	1.06	1.03	1.02	.71	1.11
129.8	1.06	.99	.96	.70	1.14
132.1	1.06	1.04	1.02	.70	1.11
134.5	1.06	1.05	.98	.71	1.12
136.9	1.05	1.06	.95	.73	1.07
139.3	1.05	1.05	1.00	.74	1.12
141.7	1.05	1.03	.98	.74	1.09
144.0	1.05	1.07	1.02	.72	1.08
146.4	1.05	1.06	.99	.71	1.08

$r(a_o)$	D.H.	13000-23000(1)	30000-40000(1)	40000-50000(1)	40000-50000(3)
148.8	1.04	1.05	.97	.73	1.05
151.2	1.04	1.07	.99	.70	1.05
153.6	1.04	1.04	1.01	.71	1.04
156.0	1.04	1.03	.99	.77	1.06
158.4	1.04	1.05	.95	.73	1.05
160.7	1.04	1.08	.98	.72	1.04
163.1	1.03	1.01	1.01	.79	1.03
165.5	1.03	1.02	.99	.73	1.04
167.9	1.03	1.00	1.05	.75	1.04
170.2	1.03	.98	1.01	.79	1.04
172.6	1.03	.95	1.04	.81	1.04
175.0	1.03	.97	1.01	.83	1.03
177.4	1.03	.92	.98	.84	1.02
179.8	1.03	.93	.98	.83	1.02
182.1	1.02	.90	.97	.81	1.00
184.5	1.02	.88	.97	.79	1.02
186.9	1.02	.89	.92	.82	1.01
189.3	1.02	.87	.90	.83	1.01
191.7	1.02	.87	.87	.84	1.00
194.1	1.02	.87	.93	.85	1.01
196.4	1.02	.90	.98	.83	1.00
198.8	1.02	.89	.93	.85	.99
201.2	1.02	.88	.90	.87	1.00

$r(a_o)$	D.H.	13000–23000(1)	30000–40000(1)	40000–50000(1)	40000–50000(3)
203.6	1.02	.89	.89	.89	.99
206.0	1.02	.92	.89	.86	.99
208.3	1.02	.92	.91	.88	.98
210.7	1.02	.91	.85	.88	.99
213.1	1.01	.90	.86	.97	.99
215.5	1.01	.92	.94	.94	.97
217.9	1.01	.93	.88	.95	.97
220.2	1.01	.93	.90	.96	.97
222.6	1.01	.94	.87	1.01	.99
225.0	1.01	.93	.89	1.03	.98
227.4	1.01	.92	.90	.99	.97
229.8	1.01	.93	.91	1.00	.96
232.1	1.01	.92	.95	1.00	.96
234.5	1.01	.95	.95	1.04	.98

TABLE 2.3

Like radial distribution functions taken from iterations as shown, and compared with the corresponding Debye-Huckel distribution function.

$r(a_o)$	D.H.	13000-2300(1)	30000-40000(1)	40000-50000(1)	40000-50000(3)
1.19	4.25×10^{-12}	0.00	0.53	0.00	0.00
3.57	2.02×10^{-4}	.00	3.06	1.30	.18
5.95	6.92×10^{-3}	.00	1.44	1.32	.08
8.33	3.14×10^{-2}	.01	1.60	1.66	.19
10.71	7.25×10^{-2}	.05	1.03	1.79	.35
13.10	.12	.13	1.11	1.25	.39
15.48	.18	.18	1.21	1.21	.38
17.85	.23	.13	1.09	.95	.64
20.24	.29	.14	1.10	1.18	.58
22.6	.34	.14	1.10	1.02	.55
25.0	.38	.15	1.07	1.20	.61
27.4	.42	.16	1.03	1.45	.62
29.8	.46	.20	1.13	1.19	.69
32.2	.50	.25	1.31	1.19	.63
34.5	.53	.29	1.28	1.24	.77
36.9	.56	.37	1.22	1.02	.67
39.3	.59	.32	1.17	1.05	.68
41.7	.62	.39	1.32	.92	.75
44.0	.64	.38	1.41	1.05	.77
46.4	.66	.43	1.74	1.35	.83

$r(a_o)$	D.H.	13000-23000(1)	30000-40000(1)	40000-50000(1)	40000 50000(3)
48.8	.68	.40	1.56	1.16	.84
51.2	.70	.49	1.51	1.09	.85
53.5	.72	.53	1.49	1.27	.81
55.9	.74	.65	1.46	.98	.86
58.3	.75	.69	1.30	1.00	.84
60.7	.76	.74	1.28	.90	.85
63.1	.78	.91	1.22	.88	.85
65.5	.79	1.02	1.20	.88	.89
67.8	.80	1.14	1.31	.99	.90
70.2	.81	1.09	1.28	.80	.90
72.6	.82	1.03	1.23	.85	.91
75.0	.83	1.00	1.18	.72	.88
77.34	.84	1.11	1.23	.82	.90
79.8	.85	1.18	1.19	.89	.93
82.10	.85	1.16	1.06	.90	.93
84.5	.86	1.15	1.14	.90	.93
86.9	.87	1.13	1.15	1.02	.92
89.3	.87	1.11	1.15	.94	.90
91.6	.88	1.13	1.12	.92	.95
94.0	.89	1.09	1.10	1.01	.97
96.4	.89	1.09	1.20	1.01	.95
98.8	.90	1.13	1.14	.98	.97

$r(a_o)$	D.H.	13000-23000(1)	30000-40000(1)	40000-50000(1)	40000-50000(3)
101.2	.90	1.09	1.14	1.02	.97
103.6	.91	1.07	1.22	.99	.96
105.9	.91	1.06	1.16	.94	.99
108.3	.91	1.07	1.16	.90	.99
110.7	.92	.99	1.05	.85	1.03
113.1	.92	1.00	1.10	.86	1.00
115.5	.92	1.01	1.09	.77	.97
117.9	.93	.96	1.15	.75	.99
120.2	.93	.99	1.08	.68	.99
122.6	.93	.98	1.05	.72	.97
125	.94	1.03	1.03	.75	1.00
127.4	.94	1.04	1.08	.78	.99
129.8	.94	1.01	1.02	.78	1.02
132.1	.94	1.05	1.06	.73	1.00
134.5	.95	1.08	1.01	.79	1.03
136.9	.95	1.07	.99	.79	1.00
139.3	.95	1.06	1.01	.79	1.00
141.7	.95	1.04	1.03	.75	1.03
144.0	.96	1.08	1.10	.74	1.01
146.4	.96	1.11	1.06	.74	1.01
148.8	.96	1.08	1.04	.80	1.00
151.2	.96	1.08	1.03	.73	1.01
153.6	.96	1.06	1.08	.78	1.01

$r(a_o)$	D.H.	13000-23000(1)	30000-40000(1)	40000-50000(1)	40000-50000(3)
156.0	.96	1.05	1.04	.80	1.02
158.4	.96	1.08	1.04	.76	1.02
160.7	.97	1.06	1.03	.75	1.02
163.1	.97	1.03	1.07	.83	1.02
165.5	.97	1.04	1.05	.77	1.04
167.9	.97	1.02	1.11	.81	1.03
170.2	.97	.98	1.09	.83	1.03
172.6	.97	.97	1.09	.89	1.02
175.0	.97	.98	1.06	.88	1.01
177.4	.97	.96	1.06	.90	1.02
179.8	.98	.95	1.06	.88	1.01
182.1	.98	.95	1.04	.88	1.02
184.5	.98	.92	1.05	.85	1.02
186.9	.98	.91	1.00	.86	1.02
189.3	.98	.87	.97	.87	1.00
191.7	.98	.89	.95	.89	1.02
194.1	.98	.92	.99	.89	1.02
196.4	.98	.91	1.05	.89	1.01
198.8	.98	.92	1.00	.90	1.03
201.2	.98	.93	.97	.91	1.03
203.6	.98	.95	.97	.93	1.01
206.0	.98	.95	.95	.93	1.01

$r(a_o)$	D.H.	13000-23000(1)	30000-40000(1)	40000-50000(1)	40000-50000(3)
208.3	.98	.96	.95	.93	1.01
210.7	.98	.98	.90	.95	1.01
213.1	.99	.96	.93	.99	1.00
215.5	.99	1.00	.98	.99	.98
217.9	.99	1.00	.94	1.00	1.01
220.2	.99	.99	.96	1.00	1.00
222.6	.99	.99	.93	1.06	1.01
225.0	.99	1.00	.94	1.07	.99
227.4	.99	.98	.94	1.06	1.00
229.8	.99	1.00	.97	1.07	.99
232.1	.99	1.01	.99	1.06	1.00
234.5	.99	1.01	1.01	1.10	.99

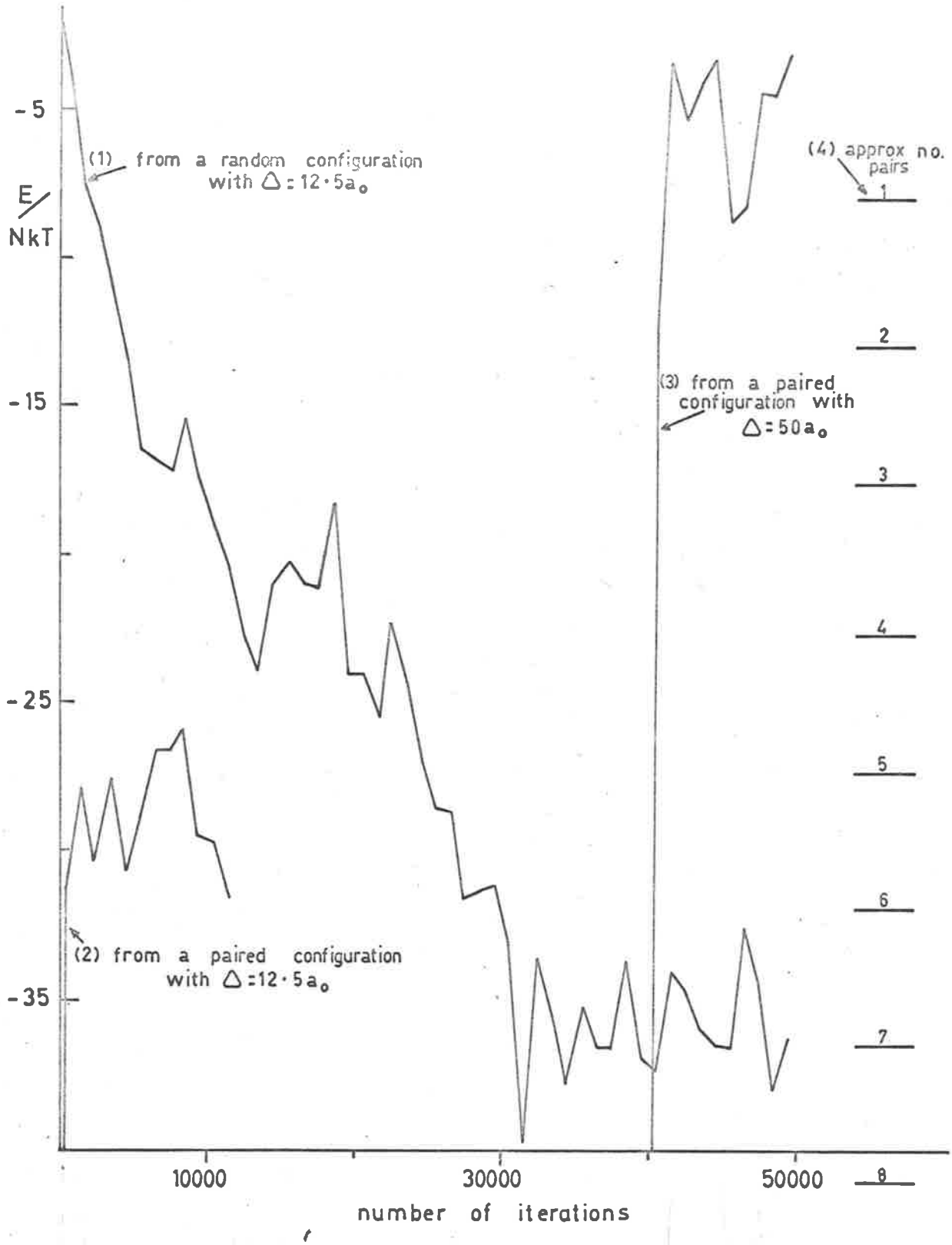

FIG. 2·1. APPROACH TO EQUILIBRIUM

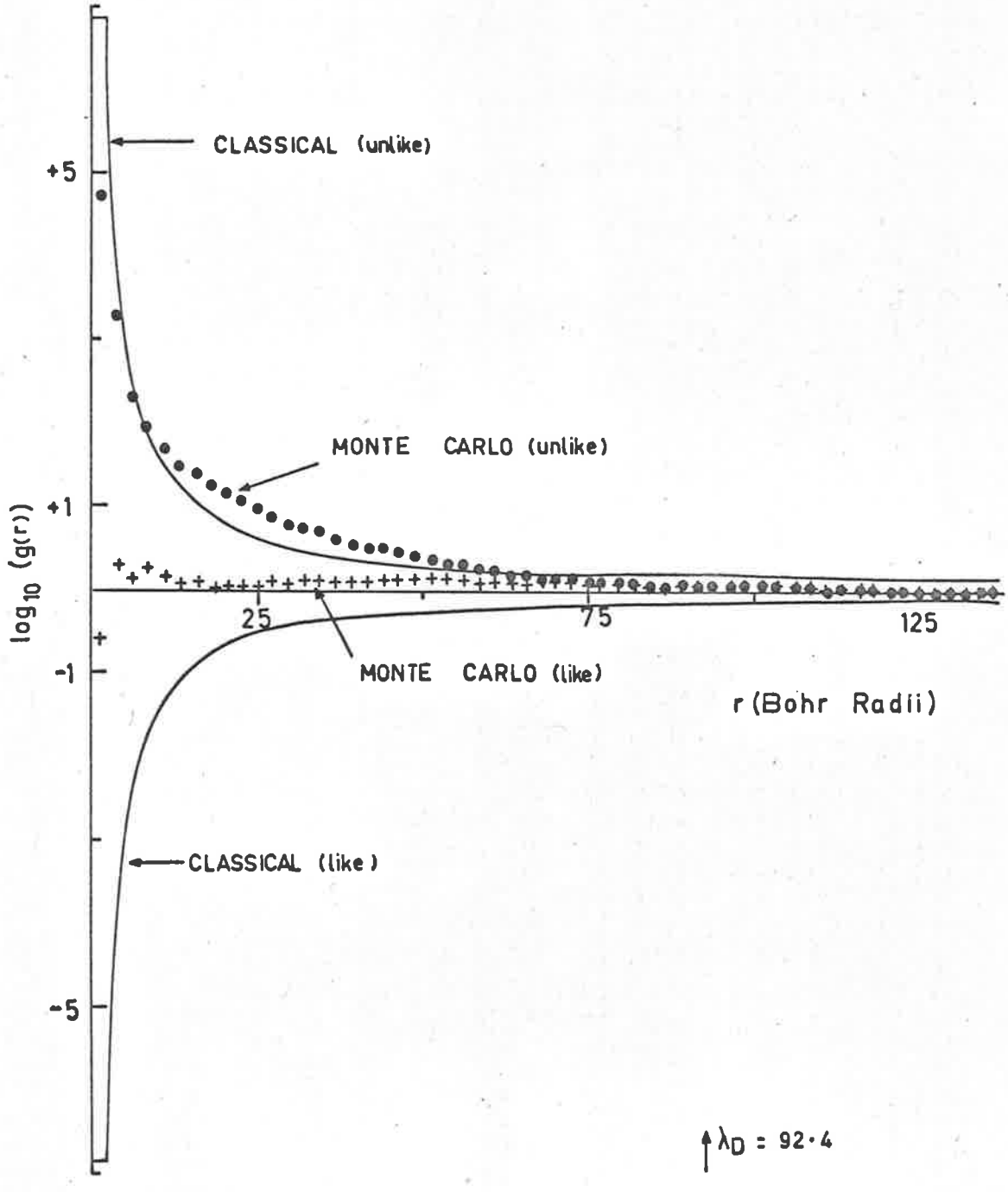

FIG. 2·2 RADIAL DISTRIBUTION FUNCTIONS (drawn on a log scale) FOR LIKE AND UNLIKE CASES, WITH THEIR CORRESPONDING CLASSICAL GRAPHS, TAKEN FROM ITERATIONS 30000 TO 50000 OF RUN 1.

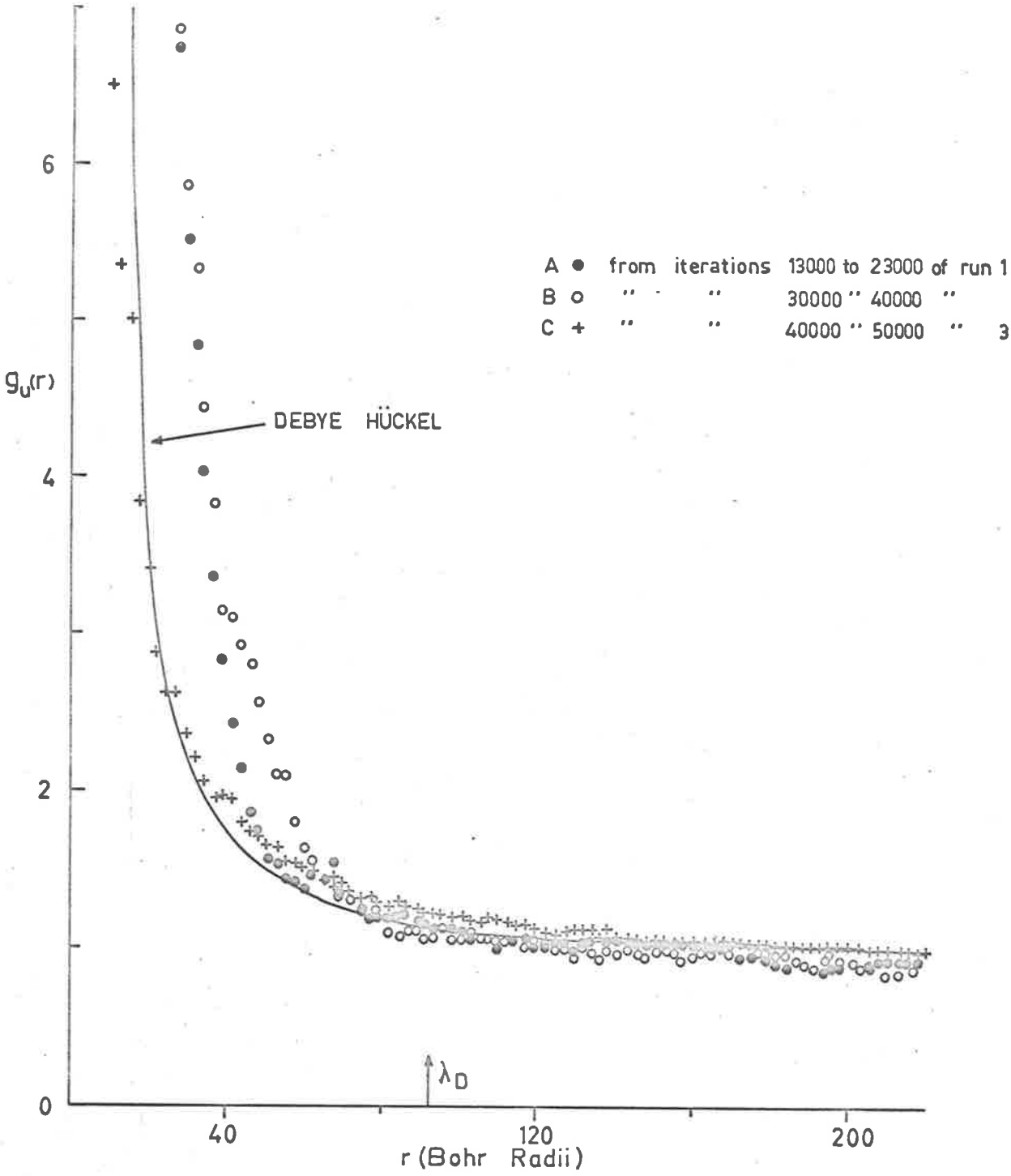

FIG. 2·3 UNLIKE DISTRIBUTION FUNCTIONS COMPARED WITH THE CORRESPONDING DEBYE HÜCKEL DISTRIBUTION FUNCTION FOR $10^{4°}$K AND 10^{18} e/cc.

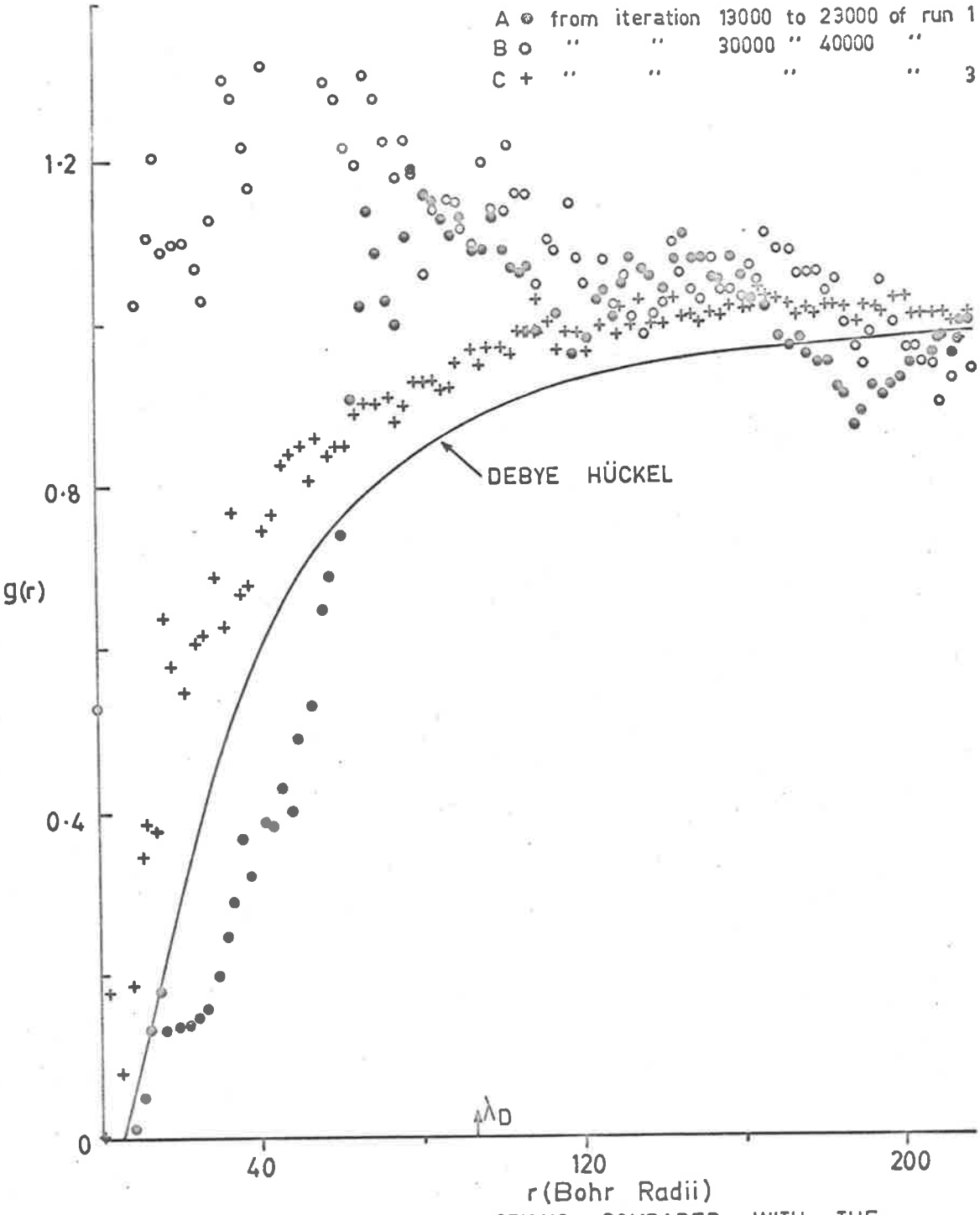

FIG. 2·4 LIKE DISTRIBUTION FUNCTIONS COMPARED WITH THE CORRESPONDING DEBYE HÜCKEL DISTRIBUTION FOR $10^{4°}$K AND 10^{18} e/cc.

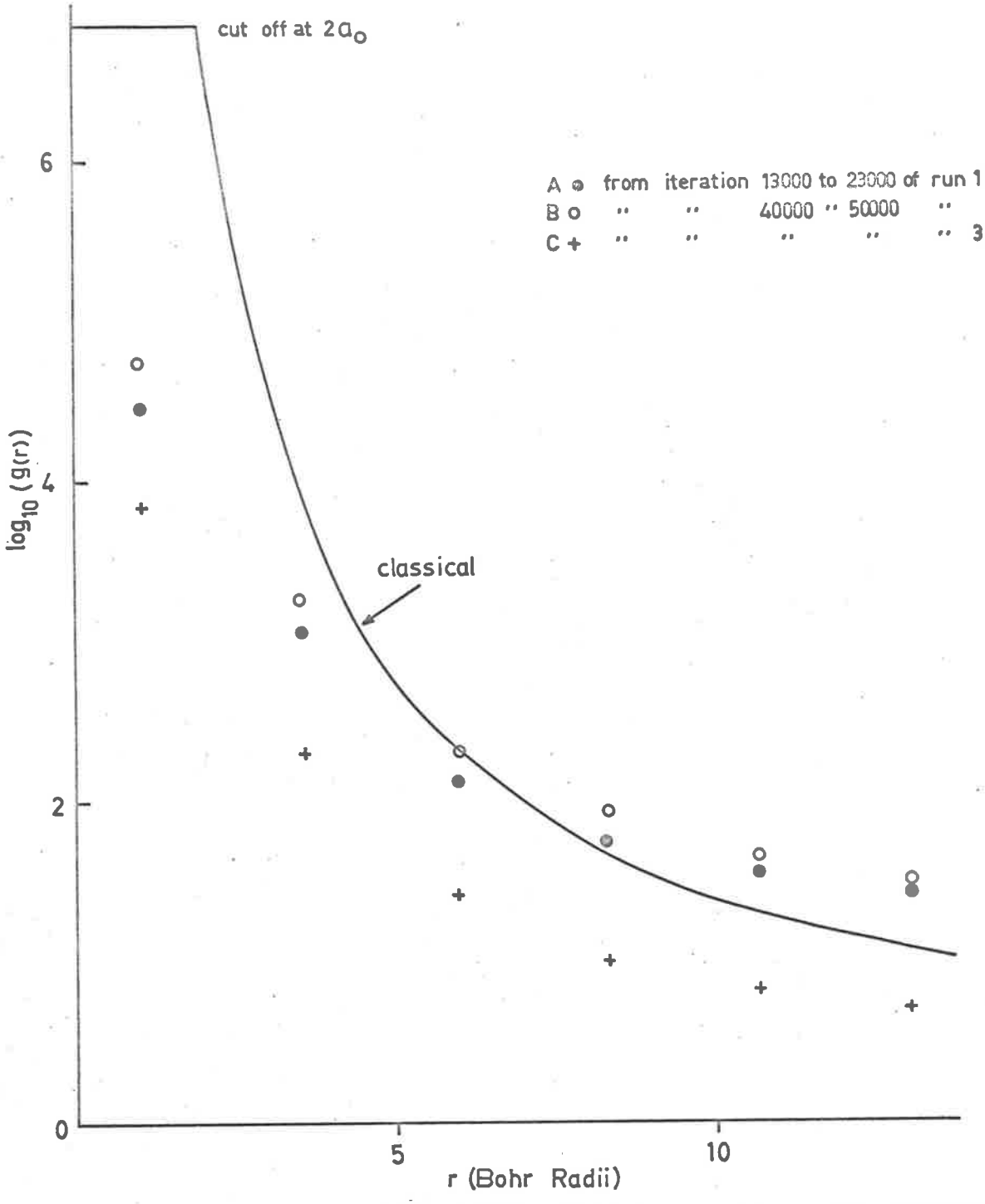

FIG. 2·5 LOGS OF UNLIKE DISTRIBUTION FUNCTIONS AT SMALL RADII COMPARED WITH THE CLASSICAL DISTRIBUTION FUNCTION FOR 10^{4°K AND 10^{18} e/cc.

2.3 Discussion and Conclusion

From Fig 2.1 it can be seen that the approach of the system to its equilibrium energy value is influenced drastically by both the parameter Δ, and the initial configuration chosen. At the present temperature and density, run 2 shows that equilibrium is obtained much faster from a configuration with all particles paired. It can also be seen that with Run 3 Δ not only influences the rate of approach to equilibrium, but the equilibrium energy value attained. This contrasts with the results of Wood and Parker [4] who, working with a fluid interacting with a Lennard-Jones potential, noted that their results were independent of Δ. On closer examination of the results presented it was found that this difficulty occurs in the temperature range 10^4°K to 3×10^4°K, where the plasma appears to behave as a variable mixture of two phases, ionized and unionized, which phase dominate is influenced rather sensitively by the parameter Δ for the relatively small sample of configurations considered in this work. The levels (4) on the right of Fig 2.1 give approximately the number of pairs (i.e. unlike particles closer than $2a_o$), in the unit cell for corresponding E/NkT. A detailed study of particle movements shows that it is the number of particles paired that is so dependant

on the size of Δ.

The distribution functions taken from run 1 as it approaches a constant energy value, i.e. from iterations 30,000 onwards as in Fig 2.2, show a marked difference from the classical and the Debye-Huckel cases. The rapid rise of $g_L(r)$ to a value above unity is due to a proton or an electron colliding with a pair. This occurs particularly when there is a relatively large number of pairs present, and is evident in B when Δ is less than fifteen Bohr radii. Fig 2.4 illustrates this situation very clearly. In run 3 ($\Delta = 50a_o$) when, from the energy graph, there are usually no pairs, and occasionally one pair is found, $g_L(r)$ is similar to the Debye-Huckel case, but approaches unity much faster. In run 1, where the particles were started as randomly distributed ions, and were in the process of approaching equilibrium, but initially there were few collisions between pairs and ions, $g_L(r)$ was small for $r<60$. However, already the tendency of ions to collide with pairs is indicated by the appearance of a sharp peak at $r = 80\ a_o$. In run 2 taken from near equilibrium there are peaks at $r = 5a_o$ and $r = 40a_o$, and from a study of the particle movements, these peaks appear following a collision between a pair and an ion.

The number of pairs present also has a marked effect on $g_U(r)$. Run 3 in Fig 2.3 shows that for Δ large, $g_U(r)$ is quite similar to the Debye-Huckel curve, but falls appreciably below it at small radii, while in the range $r = 40a_o$ to $r = 80a_o$ it lies above. For $\Delta = 12.5\ a_o$ as in 2 there is a tendency for unlike particles to stay about $10a_o$ to $60a_o$ apart. Examination of particle movements confirm that two unlike ions do tend to wander around the cell together, sometimes coming close as a pair, and sometimes straying $40a_o$ or $50a_o$ apart, but rarely escaping fully the other's influence. However, if Δ is increased they do escape fully, and if Δ is decreased to $5a_o$, they tend to fall into pairing completely.

Fig 2.5 illustrates the importance of the choice of another parameter used in the calculation, the cut-off AO imposed on the Coulomb potential at small radii. If the cut-off were applied at one instead of at two Bohr radii say, then an unlike ion on moving to 2 Bohr radii apart would be subject to a considerable change in potential energy, and this move would be most improbable by the MC procedure. On the other hand, if the inter-particle potential was cut off to make the well shallow, then unlike particles could escape each other's influence quite easily. To rigorously determine the

form of the interparticle potential at small radii it would be necessary to treat the close interactions quantum mechanically. The present choice AO = $2a_o$ is based on classical considerations only. It was also noticed from Fig 2.5 that as Δ became smaller the distribution function at small radii tends to approach the classical curve. Further, examination of particle movements showed that if Δ were large, then almost every trial movement took one ion well away from another, and although this meant a large potential energy change, eventually a move was allowed; whereas for small Δ, the particles tend to move apart and together frequently, but rarely to escape very far from each other.

Tables 2.2 and 2.3 present the distribution functions obtained from iterations 30,000 to 40,000 and 40,000 to 50,000 of run 1, to show the variance that occurs within a run of 10,000 iterations. It can be seen that this variance is quite large, being regularly greater than 0.2 and although a long run would tend to smooth out these fluctuations, it seems unlikely that such a run would improve the distribution functions much beyond the first place of decimals.

In conclusion then, it appears that the Monte Carlo approach is not particularly successful in

obtaining accurate distribution functions for a two component plasma in the temperature region near ionization. In this region the maximum step length parameter Δ is analagous to a limit of the energy of quanta absorbed or emitted from the radiation field, and if Δ is small one particle may move slightly away from the interacting particle, but rarely escapes fully; whereas if Δ is relatively large the particles completely separate. This behaviour is peculiar to the temperature range near ionization as at low and high temperatures the results are independent of Δ for a long enough run. It is in this respect that the plasma appears to behave as a variable mixture of two phases in the region of ionization, with the choice of Δ determining which phase dominates. It also appears highly desirable to include quantum mechanical interactions between protons and electrons at small radii in the M.C. calculation. Because of the excessive computing time involved (3000 iterations taking one hour on a C.D.C.6400 computer), distribution functions should be obtained more economically in this region by solving a modified Percus-Yevick equation. Using this latter approach it is hoped by comparing results to resolve the dilemma of the choice of Δ and hence improve the MC results.

References to Chapter II

[1] Brush, S.G., Sahlin, H.L., and Teller, E. J. Chem. Phys. 45, 2102 (1966).

[2] Barker, A.A. M.Sc. Thesis, University of Adelaide, S.A. (1964); Aust. J. Phys. 18, 119 (1965).

[3] Alder, B.J., and Wainwright, T. J. Chem. Phys. 33, 5 (1960).

[4] Wood, W.W., and Parker, T.R., J. Chem. Phys. 27, 720 (1957).

[5] Metropolis, N., Rosenbluth, A.W., Rosenbluth, M.N., Teller, A.W., and Teller, E. J. Chem. Phys. 21, 1087 (1953).

[6] Barker, A.A. To be published in Phys. Rev. July 1968.

III THE INTEGRAL EQUATION METHOD

3.1 Introduction - The Percus-Yevick Equation

In Chapter I the extension of integral equations to deal with plasmas was discussed generally. The three main integral equations which have been applied to fluids are the Born-Green-Yvon (BGY) equation, the Percus-Yevick (PY) equation, and the Convoluted Hypernetted Chain (CHNC) equation. In deciding that the Percus-Yevick equation could be applied best to a plasma of 10^{18}e/cc at temperatures near 10^{4}°K, the author was influenced by a number of factors. Firstly Green [1], and Stell [2] had developed higher order equations which contained the PY equation as a first approximation. Subsequently Verlet [3], Verlet and Levesque [4], Allnat [5], Wertheim [6] and Henderson [7] have all proposed higher order terms to improve the PY equation. Secondly several comparisons of the three approaches with the Monte Carlo method for fluids [8], and for the electron gas [9], indicated the superiority of the PY equation in most cases. A recent paper by Watts [10] confirms that the PY equation is superior near the critical region for a Lennard-Jones fluid. However, little is known about the merits of PY equation where attractive forces are involved.

3.2 An Asymptotic form of the Percus-Yevick equation for large r

The Percus-Yevick equation, generalised for a fluid mixture, has the form

$$g_{ab}\, e_{ab} = 1 - \sum_n n_c \int (e_{ac}-1)\, g_{ac}\, (g_{bc}-1)\, d^3x_c \,, \tag{3.1}$$

where $e_{ab} = \exp(\beta\phi_{ab})$. This can further be written in the form

$$g_{ab}(r)\, e_{ab}(r) = 1 - \frac{2\pi}{r} \sum_c n_c \int_o^\infty \int_{|s-r|}^{s+r} [e_{ac}(s)-1]\, g_{ac}(s)\, [g_{bc}(t)-1]\, t\, dt\, s\, ds, \tag{3.2}$$

where n_c is the number density of particles of type c per unit volume, Σ_c sums over all types of particles in the mixture, and d^3x_c ranges over the volume of particles of the cth type. Let the integral term be imagined to physically correspond to a particle of type a at $\underline{x}_a$, a particle of type b at $\underline{x}_b$, and a particle of type c at $\underline{x}_c$; and further, let $\underline{r} = |\underline{x}_a - \underline{x}_b|$ $\underline{s} = |\underline{x}_a - \underline{x}_c|$ and $\underline{t} = |\underline{x}_b - x_c|$. Because of the spherical symmetry, the integration over the range 0 to 2π due to the rotation of the $\underline{r}\underline{s}\,\underline{t}$ plane about $\underline{r}$ can be done immediately. Further,

since $\underline{r} = \underline{s} + \underline{t}$ we can use the sine rule to change the variable and write the integrations over lengths only as in (3.2). Broyles [11], by differentiating over r, rewrote this equation in the form

$$\frac{d}{dr}[r\, g_{ab}(r)\, e_{ab}(r)] - 1 = 2\pi \sum_c n_c \int_{-\infty}^{\infty} (s+r) g_{ac}(|s|) \cdot [g_{bc}(|s+r|-1)]\,[1-e_{ac}(s)]\, sds\,, \qquad (3.3)$$

which is much easier to handle computationally.

To obtain an asymptotic form of equation (3.2) for large r, we make the following assumptions: (i) That for large r and the integer $n>0$, $\beta\phi_{ab}\ O(r^{-n})$; and for attractive forces at small r, $\beta\phi_{ab}$ is finite. These assumptions exclude gravitational forces, and require a cut off at small r for Coulomb forces. They imply that we can express $g_{ab}(r) = 1 + \epsilon_{ab}(r)$, where $\epsilon_{ab}(r)$ will be finite for small r, and will be small for large r; and without these conditions statistical mechanics is probably inapplicable here. (ii) That $\epsilon_{ab}(r)\, r^m \to 0$ for large r and for sufficiently small m. (iii) That $\left|\int_o^{\infty} \epsilon_{\text{attractive}}(r)\, dr\right| > \left|\int_o^{\infty} \epsilon_{\text{repulsive}}(r)\, dr\right|$ for mixtures, which in a plasma is a consequence of screening between particles.

Now by (i) above it is possible to expand in powers of ϕ for large r, and with retention of terms involving

only small powers of ϕ, equation (3.2) becomes

$$[1 + \epsilon_{ab}(r)]\,[1+\beta\phi_{ab}(r) + \tfrac{1}{2}\beta^2\,\phi_{ab}{}^2(r) + \ldots] = 1 + \frac{2\pi}{r}\sum_c n_c \int_o^\infty [1-e_{ac}(s)]\cdot[1+\epsilon_{ac}(s)] \int_{|s-r|}^{s+r} \epsilon_{bc}(t)\,t\,dt\,s\,ds. \tag{3.4}$$

Changing the variable to $y = s-r$, and neglecting $\epsilon_{ab}(r)$ by assumptions (i) and (ii), equation (3.4) reduces to

$$\beta\phi_{ab}(r) + \tfrac{1}{2}\beta^2\phi_{ab}(r)^2 + \ldots = \frac{2\pi}{r}\sum_c n_c \int_{-r}^{\infty} [1-e_{ac}(y+r)]\,[1+\epsilon_{ac}(y+r)]\cdot\int_{|y|}^{y+2r} \epsilon_{bc}(t)\,t\,dt\,(y+r)\,dy\,. \tag{3.5}$$

Using assumption (ii) it can be seen that the most important contributions to the right-hand side integral in equation (3.5) arise when y is small, and hence, a cut-off parameter "a" is introduced, where $a<r$ for large r, beyond which contributions to the integral are assumed negligible. Further by assumption (i) the right-hand side is finite, and since r is large and y small, $\epsilon_{ac}(y+r)$ can be neglected; so the right-hand side can be expanded in powers of $\phi(y+r)$, to give

$$\beta\phi_{ab}(r) + \tfrac{1}{2}\beta^2\phi_{ab}{}^2(r) + \cdots = 2\pi \sum_c n_c \int_{-a}^{a} [-\beta\ \phi_{ac}(y+r) -$$

$$\tfrac{1}{2}\beta^2\phi_{ac}{}^2(y+r)\cdots]\cdot \left(\frac{y+r}{r}\right) \int_{|y|}^{y+2r} \epsilon_{bc}(t)\ t\,dt\,dy \quad (3.6)$$

As there are no general existence theorems for solutions of non-linear integral equations, even if we obtain agreement from a comparison of the left-hand and right-hand sides of equation (3.6), we cannot be sure an exact solution to equation (3.2) exists. However, if we are able to satisfy the asymptotic equation (3.6), there may exist an accurate solution to equation (3.2), whereas if (3.6) has no solution, no exact solution of (3.2) can exist.

For a system of particles involving attractive forces only, it is evident from equation (3.6) that a solution is impossible; for then ϕ_{ac} is always negative, $\int_{|y|}^{y+2r} \epsilon_{\text{attractive}}(t)dt$ is positive for small y by physical considerations, and ϕ_{ab} is negative. Thus, to first order the left-hand side is negative, while the right-hand side is positive; and to second order the left hand side is positive, while the right-hand side is negative, both orders being mathematically inconsistent. However, by modifying the above reasoning for a system

of repulsive forces only, we see that ϕ_{ac} becomes positive, while $\int_{|y|}^{y+2r} \epsilon_{bc}(t)dt$ becomes negative; so that now both first- and second-order agreement in ϕ can be obtained. For a system of mixed forces, several cases arise, for ϕ_{ab} can now be positive or negative, and if ϕ_{ab} is positive, so that a particle "a" repels a particle "b", then particle "a" can attract a particle "c" while particle "b" may repel particle "c". Because many of these cases are unphysical, we shall, for definiteness, consider mixtures of charged particles. Then, if particle "a" repels particle "b" and attracts particle "c", particle "b" will attract particle "c" also. For these charged particle mixtures, first-order agreement follows by the same reasoning as above and using assumption (iii), but second order considerations lead to disagreement. The above discussion is summarised in Table 3.1.

TABLE 3.1

Summary of the consistency of the asymptotic equation (3.6) for various cases

Type of force present	Order in ϕ_{ac}	Whether (3.6) is consistent to this order
Attractive only	First	No
	Second	No
Repulsive only	First	Yes
	Second	Yes
Mixtures of Charges	First	Yes
	Second	No

For a Lennard-Jones type of interparticle potential, which is repulsive at short distances, and which falls off rapidly, the PY equation applies well, and not only is a solution to the asymptotic equation (3.6) possible, but solutions to the PY equation (3.2) have been found. However, for mixed Coulomb interparticle potentials an exact solution of (3.2) is clearly not possible due to the inconsistency in the second order terms of equation (3.6).

Because of this difficulty, the additional terms proposed by Green [1] were considered. The integral

equation resulting from the inclusion of the first additional term is referred to as a modified Percus-Yevick equation (MPY) and is discussed in detail in Chapter V' For the present we shall observe that by including this additional term the inconsistency in the second-order asymptotic equation for charged mixtures is removed. The main disadvantage of this additional term is that the equation can no longer be expressed in the convenient form of (3.3), and so computational solution of the equation will be correspondingly more difficult.

3.3 Deficiencies in the Approach

Before attempting to solve the MPY equation, the author decided to write a Fortran program to evaluate the first-order, or Percus-Yevick term, as in equation (3.2). This form of the equation was preferred to the form (3.3), as using equation (3.2) the program could be easily expanded to incorporate the additional term at a later stage.

The program used to solve the PY equation is incorporated in the final program used to solve the MPY, which latter program is presented in Appendix B, and thus most of the present discussion also applies to the final program. It was decided to initially store the $g_{ab}(r)$ and $\phi_{ab}(r)$ in intervals of 1 Bohr radius for

values of r from zero to three times the Debye shielding distance. It was further decided to use the Debye-Huckel $g_{ab}(r)$, (i.e. $g_{DH}(r)$), and the Coulomb $\phi_{ab}(r)$, (i.e. $\phi_c(r)$), in the following form

$$g_{ab}(r) = g_{DH}(r) \text{ and } \phi_{ab}(r) = \phi_c(r) \text{ for } r>2a_o$$

$$g_{ab}(r) = g_{DH}(2a_o) \text{ and } \phi_{ab}(r) = \phi_c(2a_o) \text{ for } r<2a_o$$

as input data to evaluate the integral on the right-hand side of equation (3.2). This choice of the cut-off value at $2a_o$ is identical with that used for the MC calculation (see 2.1, where the choice of the cut-off was discussed fully, and was referred to as A0), and to allow a complete comparison with the MC results, the initial data is chosen for the same temperature (10^4°K) and density (10^{18}e/cc).

At first an attempt was made to evaluate the integral by using a procedure suggested by Lyness [12], which could easily be extended to integrations of higher dimension without an excessive increase in the number of evaluation points. However, it was found that this technique could not be applied to the PY integral because of (1) the awkward range of integration in the inner integral, and (11) the non-smoothness of the $g_{DH}(r)$ and $\phi_c(r)$ that are used as input data. Hence finally it was decided to use a simple trapezoidal rule to evaluate the integral, and to increase the mesh ratio until the desired accuracy

was attained.

The initial interpolation procedure adopted for obtaining $g_{ab}(r)$ and $\phi_{ab}(r)$ at the mesh points, from the $g_{ab}(t)$ and $\phi_{ab}(r)$ stored at set values of r, was the usual linear interpolation. However, it was found that this caused large errors, especially for small r, unless a very fine mesh was used, and this proved time consuming. To avoid this difficulty the $g_{ab}(r)$ and $\phi_{ab}(r)$ stored were converted into logarithms and a linear interpolation made between the logarithmic values. This procedure gave reasonable accuracy without taking an excessive number of mesh points.

A further device employed in the evaluation of the integral was to divide it into several regions. This allows the use of different mesh ratios in the different regions, and it is then possible to see which regions are most important. The integral of equation (3.2) is also terminated by an upper limit (LBCUT) on the variable s, so that the integral becomes

$$I(r) = \int_{0}^{LBCUT} [e_{ac}(s) - 1]\, g_{ac}(s)\, s \int_{|s-r|}^{s+r} (g_{bc}(t)-1)\, t\, dt\, ds$$

It is divided into regions as shown in Fig.3.1.

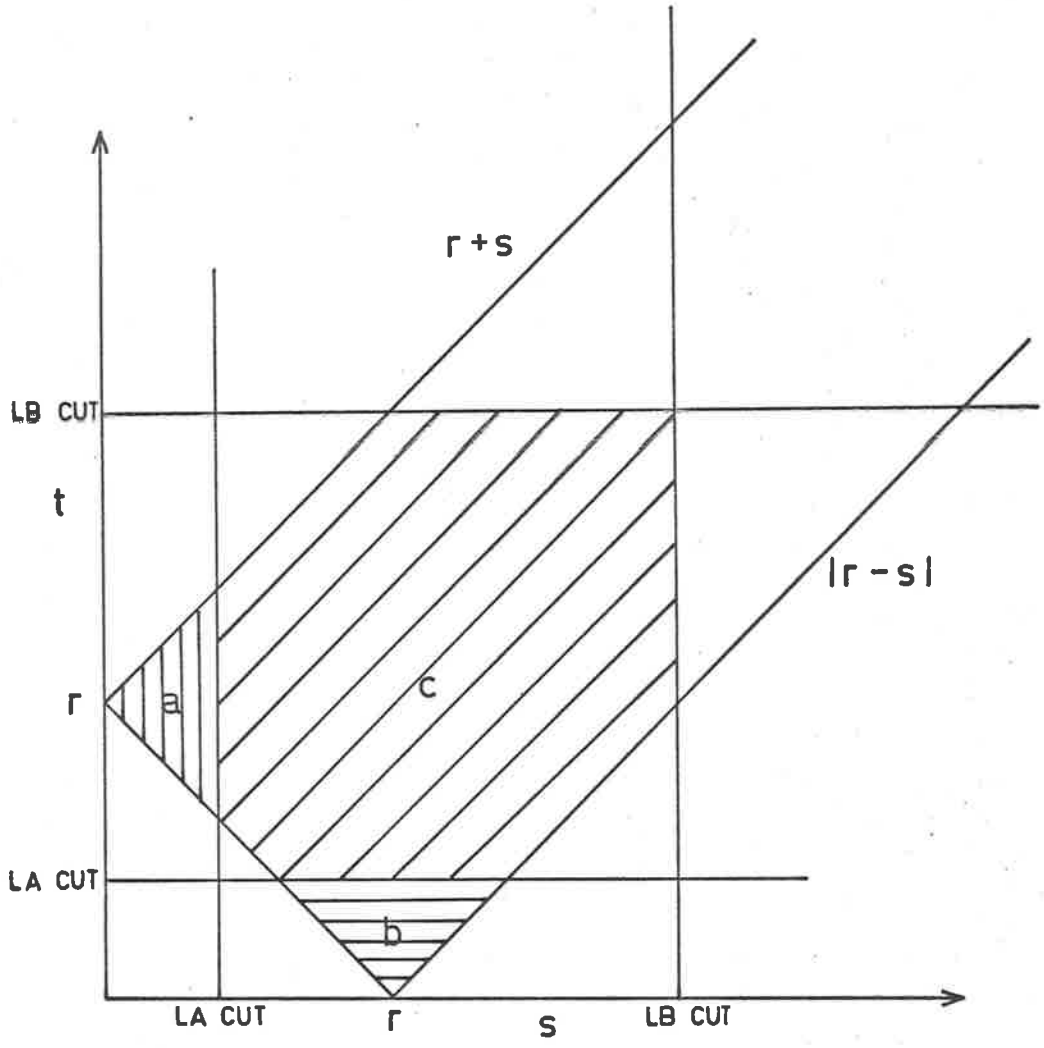

FIG. 3·1 SHOWING THE SEPARATE REGIONS OF INTEGRATION OF TDTM.

In 'Appendix B' region a is referred to as the "inner region", region b the "large r" region, and region c, the 'main region'. The mesh ratios used in each region have brackets after them, with (2D) to indicate that they refer to the two dimensional integral above, and (5D) to indicate they refer to mesh ratios for the five dimensional term considered in Chapter V.

The evaluation of the integral for a particular value of r showed that the results are extremely sensitive to the form of the distribution and potential used as input (let us denote these by g_{IN} and ϕ_{IN}), especially at small radii, and hence are extremely sensitive to the cut-off value AO. As the choice of AO is based on semi-classical criteria, the validity of which has been thrown into some doubt by the MC results, it appears necessary to determine the input accurately by taking into account quantum effects in detail. Further evaluations of I(r) show that this is so for all values of r from zero to LBCUT, though the dependence is most marked for r small. The next Chapter will take into account the quantal effects at small radii.

References to Chapter 3

[1] Green, H.S. (1965) Phys. Fluids 8,1.

[2] Stell, G. (1963) Physica 29, 517.

[3] Verlet, L. (1964) Physica 30, 95.
(1965) " 31, 959
(1966) " 32, 304.

[4] Verlet, L. and Levesque, D. (1967) Physica 36, 254. See also
Levesque, D. (1966) Physica 32, 1985.
(1967) " 36, 254.

[5] Allnat, A.R. (1966) Physica 32, 133.

[6] Wertheim, M.S. (1967) J. Math. Phys. 8, 927.

[7] Henderson, D. (1967) Disc. Farad. Soc. (GB) 43,26.

[8] Broyles, A.A., Chung, S.U. and Sahlin, H.L. (1962) J. Chem. Phys. 37, 2462.

[9] Carley, D.D. (1963) Phys. Rev. 131, 1406.

[10] Watts, R.O. (1968) J. Chem. Phys. 48, 50.

[11] Broyles, A.A. (1960) J. Chem. Phys. 33, 456, 1068.

[12] Lyness, J.N. Preprint
Mustard, D., Lyness, J.N. and Blatt, J.M. (1963) Comput. Jour. 6, 75
Lyness, J.N . (1965) Maths. Comput. 19, 260.

IV A QUANTUM MECHANICAL CALCULATION OF THE TWO PARTICLE DISTRIBUTION FUNCTION

4.1 Introduction

It is necessary to distinguish between two kinds of effects which are commonly referred to as quantum effects:

A - The effect due to quantum statistics which gives rise to the 'exchange' terms, or terms arising from the Pauli 'exclusion' principle; and which can lead to correlations even in the absence of interactions.

B - The effect due to the quantum dynamics which is directly associated with Heisenberg's uncertainty principle.

As early as 1930 quantum mechanical expressions for g(r) were proposed by Born and Oppenheimer [1], Slater [2], London [3], Kirkwood [4], Uhlenbeck and Gropper [5], Wigner [6] and others [7]. These were applied to real fluids i.e. see [8], to obtain the quantum corrections to their equation of state. Experimental evidence confirmed that quantum corrections for fluids were important (especially for Hydrogen and Helium) at low temperatures. Extensive reviews of later work have been made by De Boer [9], Coleman [10], and Mayer and

Band [11], to name but a few, and recently many papers discussing quantal effects in fluids have been published [12].

Recently however, with the increasing interest in plasma physics, it has been found that quantum effects are particularly important at low temperatures, where for an hydrogenous plasma "low" temperature is $O(10^4°K)$. As the quantal effects are also density dependent, for the case of atomic number $z=1$, many authors use the Debye shielding distance $\lambda_D = \left(\frac{kT}{8\pi n_e e^2} \right)^{\frac{1}{2}}$, where the neutrality condition $n_i = n_e$ applies; or some plasma length parameter which depends on both density and temperature, to obtain a criterion for the range of importance of the quantal effects. The differences in the quantal effects for interactions between various types of particles are very large, and frequently reference is made to the thermal De Broglie wavelength $\lambda = \bar{h} \left(\frac{\beta}{2m} \right)^{\frac{1}{2}}$. It is because of the presence of particles with relatively small mass m (electrons), and also the change of the dominant interparticle potential from the Lennard-Jones to the Coulombic type, that the quantal effects become so important for plasmas at low temperatures. In this thesis we are concerned

with a rather dense hydrogenous plasma, having an electron number density $n_e = 10^{18}$e/cc ($=n_p$, the proton number density), and temperatures ranging from 10^4°K (pre-ionization) to 5×10^4°K where the gas is fully ionized and is a true plasma.

The fact that the classical Coulomb potential $\phi_c(r) = \frac{e_a e_b}{r}$ has a divergence at the origin, and that this divergence can be removed by taking quantal considerations into account, has also increased the interest in this field. The three main approaches taken were:-

(a) Using 'bound-unbound'state considerations for interactions between unlike particles. This has been developed recently by a large number of authors (see [13] to [23]), and various criteria have been proposed for the transition from the bound region to the unbound region. Most of these references also refer to the degree of ionization present, and several ([17(c)], [19], [23]) offer improvements to the Saha equation.

(b) Extending the Montroll-Ward [24] perturbation expansion for plasmas by including quantal terms in the formulae (see [25] to [29]).

(c) By applying recent mathematical techniques to the expressions obtained for including quantal effects in fluids (i.e.[1] to [8]). At that time direct evaluation of the sums involved was impossible, but sophisticated mathematics and the advent of the computer has now made a direct evaluation feasible (see references [30] to [35]).

In this chapter a quantal expression is formulated for a two particle distribution function which specifically does not include the effect of other particles. The method takes into account the Heisenberg effect only, and is an extension of the Slater sum for $g_{ab}(r)$ [2]. The expression does not include quantum statistical effects, as even at $10^{4°}K$ the number of electrons approaching each other closely is expected to be small. However, there is some evidence from references [26], [28] and [30] that these are not negligible for the electron-electron (e-e) interactions at short distances. Quantum statistical effects fall away as M and M^2 for the electron-proton (e-p) and proton-proton (p-p) interactions, where M is the proton to electron mass ratio, and so the effect of statistics should be negligible in the calculation of g_{ep} and g_{pp}.

The two-particle distribution function is

evaluated on a CDC 6400 computer to obtain g_{pe} and g_{ee} over the range of temperatures 10^4 to 5×10^4. Because of the difficulties encountered in evaluating the Coulomb wave functions, g_{pp} could not be evaluated, but due to the large reduced mass for this system, the quantal effect should be quite negligible in this case. Results are presented in Tables 4.1 to 4.11, and corresponding graphs are drawn in Figs. 4.1 to 4.8. These are discussed in section 4.4, and conclusions made.

4.2 A formulation of the expression for $g_{ab}(r)$

The radial distribution function $g_{ab}(r)$ is usually defined by $g_{ab}(r) = D_{ab}(r)/D_b$ where $D_{ab}(r)$ is the number density of particles of type b at a distance r from a particle of type a, and D_b the average number density of type b throughout the fluid. However, $g_{ab}(r)$ can also be defined as the ratio of 'the conditional probability of finding particle b in the volume element dx(2) given particle a in volume element dx(1)' to 'the independent probability of finding particle b in volume dx(2) and also particle a in volume element dx(1)', i.e.

$$g_{ab}(r) = \frac{n_{ab}(r)\ dx(1)\ dx(2)}{n_a\ dx(1)\ n_b\ dx(2)} \ . \qquad (4.1)$$

Using the usual probability interpretation of the wave function and assuming that Boltzmann statistics apply to the system, the equation (4.1) can be written for a proton-electron system as:

$$g_{pe}(r) = \frac{\Sigma_n \exp(-\beta E_n)\ \psi_{nlm}\psi^*_{nlm} + \Sigma_{\underline{k}} \exp(-\beta \underline{k}^2\hbar^2/2m)\psi_{\underline{k}}\psi_{\underline{k}}^*}{\Sigma_{\underline{k}} \exp(-\beta \underline{k}^2\hbar^2/2m)\psi_o\psi_o^*} \quad ; \qquad (4.2)$$

where the summation over n sums over the bound states of energy E_n of the hydrogen atom, and ψ_{nlm} are the wave functions normalised so that $\int \psi_{nlm}\ \psi^*_{nlm}\ dV = 1$. The summation over $\underline{k}$ sums over scattered states of the hydrogen atom and the $\psi_{\underline{k}}$ are the wave functions normalised so that $\int \psi_{\underline{k}}\psi^*_{\underline{k}}\ dV=1$. ψ_o is the wave function of an electron without a proton present, that is, a plane wave, but normalised so that $\int \psi_o\psi_o^* dV=1$. Putting in the wave functions as given by Pauling and Wilson [36] for the bound states, and by Schiff [37] for the scattered states; and replacing the summation over $\underline{k}$ by an integral and removing the angular dependence we have:

$$g_{pe}(r) = \left\{ \sum_{n=1}^{\infty} \exp(-\beta E_n) \sum_{l=o}^{n-1} \frac{2l+1}{4\pi} \left(\frac{2z}{na_o}\right)^3 \frac{(n-l-1)!}{2n\{(n+l)!\}^3} \right.$$

$$\exp(-\rho)\rho^{2l}[L_{n+l}^{2l+1}(\rho)]^2 + \frac{4\pi}{(2\pi)^3} \int_o^{\infty} \exp(-\beta k^2\hbar^2/2m)$$

$$\left. \sum_{l=o}^{\infty} \frac{2l+1}{k^2r^2} [F_l(\alpha,kr)]^2 \, k^2dk \right\} / \frac{4\pi}{(2\pi)^3} \int_o^{\infty} \exp(-\beta k^2\hbar^2/2m)k^2dk$$

(4.3)

where $\rho = 2rZ/na_o$ (a_o being the first Bohr radius, Z the atomic number, and n the principal quantum number), L_{n+l}^{2l+1} are associated Laguerre polynomials, and $F_l(\alpha,kr)$ are the Coulomb wave functions with $\alpha = Zme^2/\hbar^2k$ for $k = mv/\hbar$ and m being the reduced mass of the particles. Evaluating the denominator directly gives $(2\pi\beta\hbar^2/m)^{-3/2}{}_{cm}{}^{-3}$, which can be conveniently expressed in units of (Bohr radii)$^{-3}$, and we have

$$g_{p\ e}(r) = \left(\frac{2\pi\beta\hbar^2}{m}\right)^{3/2} \left\{ \left(\frac{Z}{a_o}\right)^{3/2} \sum_{n=1}^{\infty} \frac{\exp(-\beta E_n - \rho)}{\pi n^4} \right.$$

$$\left. \sum_{l=o}^{n-1} \frac{(2l+1)(n+l+1)!}{\{(n+1)!\}^3} \rho^{2l} \left[L_{n+l}^{2l+1}(\rho)\right]^2 + \right.$$

$$+ \frac{}{2\pi r^2} \int_o^\infty \exp\left(- \frac{\beta k^2 \hbar^2}{2m}\right) \sum_{l=o}^{\infty} (2l+1) \left[F_l(\alpha, kr)\right]^2 dk \Bigg\}$$

(4.4)

We can interpret equation (4.4) as being composed of a normalisation constant $(2\pi\beta\hbar^2/m)^{3/2}$, which multiplies a bound state contribution (the first term) added to a scattered state contribution (second term) to give the radial distribution function between two particles. The equation can be applied to e-e and p-p interactions equally well but in these cases there are no bound states. Also, the Coulomb wave functions now refer to the e-e or p-p interactions, and the normalisation constant alters due to the change in the reduced mass m of the system. It should be emphasized that equation (4.4) refers to the distribution function between two particles only, and does not allow for the presence of other particles.

4.2B Evaluation of Equation (4.4)

The bound state contribution to g_{pe} is evaluated by generating the associated Laguerre polynomials by two methods, one using recurrence relations obtained from the differential equation, and the other using the power series provided by Pauling and Wilson [36], these

provide a consistency check. The summation over n is terminated when the contribution from the last nth state is less than one ten thousandth of the sum to ensure accuracy to three figures. The program was written to evaluate $g_{pe}(r)$ for r in intervals of half Bohr radii. The parameter ρ is dimensionless, as is the term $-\beta E_n$ which is expressed as $\frac{15.78044}{T}\left(\frac{Z}{n}\right)^2$. On multiplying the bound state contribution by the normalising constant (both expressed in units of Bohr radii) the dimensionless bound state contribution to $g_{pe}(r)$ is obtained.

The scattering contribution proves a little more difficult to evaluate, and differs for the three cases of proton-proton (p-p) proton-electron (p-e) and electron-electron (e-e) interactions. For the p-e and e-e cases the first few Coulomb wave functions can be generated by two methods, one using a power series, and the other using an asymptotic expansion, depending on the range of α and kr; the well known recurrence relation technique of Abramowitz [38] was then used to generate the functions of higher order. The summation over l is again terminated when the last term becomes small, and this occurs when l becomes much larger than $kr+|\alpha|$, for then the Coulomb wave functions fall off very sharply. The integral is evaluated using a trapezoidal rule with upper and lower

limits, which, when doubled and halved respectively, failed to alter the value of the integral by more than one ten thousandth of the value of the integral. Initially an attempt was made to express the Coulomb wave functions in their integral representations, and to then take the summation inside the integral, evaluate it analytically, and complete the integration. Unfortunately it was impossible to evaluate the sum analytically, and although a computer program was written using this approach, the final double integration over a summation proved time consuming, and this program was only used to check the scattered contribution.

Several points need to be noted concerning the scattered term in equation (4.4). As $\alpha \to 0$, i.e. for small charge or large k, then $\sum_{l=o}^{\infty} (2l+1)\, F_l(\alpha,kr)/k^2r^2 \to 1$, and the integral can be evaluated analytically. It can be easily shown that if the sum is of order 1 then the maximum value for the integrand occurs for $k \approx (\beta\hbar^2/2m)^{-\frac{1}{2}}$, and the integrand falls reasonably sharply for smaller or larger values of k. Even so, it is necessary to integrate over a fair range of k to obtain an accurate result. This in turn means the parameter kr in the Coulomb functions varies considerably. For the p-e and e-e case the

reduced mass m (used in α and the weighting term $\exp[-\beta k^2\hbar^2/(2m)]$) is of the order of the electron mass, α remains small, and the range of k is not excessive. However, in the p-p case, α becomes large, the maximum value for the integrand is large and accurate evaluation of the integral requires a large range of k to be considered. This in turn requires the evaluation of Coulomb functions over an extensive range of α and kr, and so would require many different generating techniques, as shown by Froberg [39], Abramowitz [38], Slater [40] and others [41]. For this reason the same method for calculating the p-p quantum mechanical distribution function is not appropriate here. It is possible to evaluate the p-p distribution using simplified wave functions of the W.K.B. approximation; but this simply shows that the quantal effects are not important. On physical grounds, and also from the high temperature results of references [26], [28] and [30], it is clear that the quantum mechanical corrections for the p-p distribution function are relatively small, and g_{pp} lies close to the corresponding classical $g_c(r)$.

As stated in Section 1.3, it is planned to use the two-particle $g_{pe}(r)$ and its associated effective potential, as inputs to a modified Percus-Yevick equation, to take into account the effects of other particles. However it

was decided to obtain an approximate estimate of the shielding of other particles on g(r) immediately by including a Debye-Hückel shielding factor in the charge so that Z in equation (4.4) is replaced by Ze^{-r/λ_D} where λ_D is the Debye shielding length. This involves the approximation that the wave functions obtained by solving the Schroedinger equation for a Debye-Huckel shielded potential are equal to the wave functions obtained by solving the usual hydrogen atom wave equation, with the charge in these wave functions modified by a Debye-Huckel shielding factor. This quasi-classical approximation seems reasonable and is supported by recent results of Rouse [23], Harris [16] and Storer [42].

The computer program is given in Appendix B, and is reasonably economical, one run to obtain g(r) (r going from zero to 200 a_o in steps of a_o) taking approximately 90 seconds on a CDC 6400 computer.

4.3 Results

The results are presented for five temperatures 10^4°K to 5×10^4°K in intervals of 10^4°K. Tables 4.1, 4.3, 4.5, 4.7, 4.9 give $\log_{10}(g_{pe})$ for the five temperatures, and for 10^4°K and 5×10^4°K the first bound state contribution is also given. Tables 4.2, 4.4, 4.6, 4.8,

4.10, are the corresponding $\log_{10}(g_{ee})$ values. In the tables only, $\log_{10}(g(r))$ is presented, and consequently the following abbreviations are made in the tables:

r - The radius in Bohr radii

$g_c(r)$ - Log_{10} of the corresponding classical distribution function.

$g_{1B}(r)$ - Log_{10} of the first bound state contribution.

$g_B(r)$ - Log_{10} of the total bound state contribution.

N - the number of bound states contributing to the total bound state contribution before contribution of a further state adds less than one ten thousandth of the total bound state contribution.

$g_{pe}(r)$ - Log_{10} of the proton-electron distribution function.

$g_{ee}(r)$ - Log_{10} of the electron-electron distribution function.

$g_{DH}(r)$ - Log_{10} of the corresponding Debye-Huckel distribution function.

$g_S(r)$ - Log_{10} of the appropriate distribution function including shielding effects.

Sometimes the description 'quantum mechanical' is added to the distribution functions, but largely this is assumed understood. The figures were calculated with an

estimated error of ±5 in the fourth figure.

The Tables 4.1 to 4.10 are represented graphically in Figs. 4.1 to 4.5, although most emphasis is placed on the temperature of 10^4°K where the quantum effects are most apparent. Table 4.11 presents (for the proton-electron case) for various temperatures, three parameters defined as follows:-

r_J - the radius in Bohr radii such that $(g_{pe}(r) - g_c(r))/g_c(r)$ is less than .05 for $r>r_J$. This in the text is referred to as the 'joining radius', as for $r>r_J$ the quantum mechanical curve is within 5% of the corresponding classical curve. Values are not given for the e-e case as they are very similar to the p-e values.

I - The percentage ionization =

$$\frac{\int_o^{R_I} g_{SCATT}(r) 4\pi r^2 dr}{\int_o^{R_I} g_{pe}(r) 4\pi r^2 dr} \times 100$$

where $g_{SCATT}(r)$ is the scattering contribution to $g_{pe}(r)$ and r_I is the radius chosen such that $\frac{3}{4\pi r_I^3}$ = electron number density, (i.e. $4\pi r_I^3/3$ is the volume which on the average contains one electron.)

For the present calculations using a number density of 10^{18}e/cc r_I has the value of 117.2 Bohr radii.

λ_D - The Debye shielding distance in Bohr radii defined in the usual manner as $\lambda_D = \left(\frac{kT}{8\pi n_e e^2}\right)^{\frac{1}{2}}$.

Figs. 4.6 and 4.7 present these results graphically. In Fig 4.7 a comparison is made with the percentage ionization predicted by the Saha equation [43]. Fig. 4.8 shows effective potentials V, (multiplied by β to make them dimensionless), for e-e and e-p interactions for $10^{4°}$K defined from the QM distribution function as follows:

$$g_{ee}(r) = \exp(-\beta\, V_{ee}(r))$$

$$g_{ep}(r) = \exp(-\beta\, V_{ep}(r)) \ .$$

Hence the effective potential values can be obtained from the logs of the corresponding distribution functions by multiplying them by -2.30259. The classical curves $g_c(r)$ using the Coulomb potential $\phi_c(r)$ are also drawn using $g_c(r) = \exp(-\beta\, \phi_c(r))$,

where $\phi_c(r) = \frac{e^2}{r}$ for e-e case

$= \frac{-e^2}{r}$ for p-e case .

TABLE 4.1A

Proton-electron distribution functions at 10^4°K showing first bound state and total bound state contributions.

r	$g_c(r)$	$g_{1B}(r)$	N	$g_B(r)$	$g_{pe}(r)$
0.0	∞	9.8023	-	-	9.8023
0.5	27.4382	9.3681	2	9.3681	9.3681
1.0	13.7141	8.9338	2	8.9338	8.9338
1.5	9.1427	8.4995	2	8.4995	8.4995
2.0	6.8571	8.0652	2	8.0652	8.0652
2.5	5.4856	7.6309	2	7.6309	7.6309
3.0	4.5714	7.1966	2	7.1966	7.1966
3.5	3.9183	6.7623	3	6.7623	6.7623
4.0	3.4285	6.3280	3	6.3281	6.3281
4.5	3.0475	5.8937	3	5.8939	5.8939
5.0	2.7428	5.4594	3	5.4599	5.4599
5.5	2.4935	5.0251	4	5.0262	5.0262
6.0	2.2857	4.5911	4	4.5931	4.5931
6.5	2.1099	4.1565	5	4.1611	4.1612
7.0	1.9592	3.7222	6	3.7315	3.7317
7.5	1.8285	3.2879	8	3.3068	3.3074
8.0	1.7143	2.8536	11	2.8919	2.8933
8.5	1.6134	2.4194	14	2.4960	2.4994
9.0	1.5238	1.9851	18	2.1346	2.1421

r	$g_c(r)$	$g_{1B}(r)$	N	$g_B(r)$	$g_{pe}(r)$
9.5	1.4436	1.5508	22	1.8271	1.8417
10.0	1.3714	1.1165	26	1.5877	1.6120
10.5	1.3061	0.6822	29	1.4137	1.4489
11.0	1.2467	0.2478	32	1.2888	1.3346
11.5	1.1925	-.1864	34	1.1947	1.2505
12.0	1.1428	-.6207	35	1.1188	1.1842
12.5	1.0971		37	1.0539	1.1286
13.0	1.0549		39	.9961	1.0800
13.5	1.0159		40	.9437	1.0363
14.0	.9796		42	.8955	.9967
14.5	.9458		43	.8509	.9602
15.0	.9143		44	.8094	.9265

TABLE 4.1B

Proton-electron distribution functions including shielding at $10^{4°}$K and showing first bound state and total bound state contributions.

r	$g_{DH}(r))$	$(g_{1B}(r))$	N	$(g_B(r))$	$(g_S(r))$
0.0	∞	9.8023	-	-	9.8023
0.5	27.2799	9.2871	2	9.2894	9.2894
1.0	13.5662	8.7726	2	8.7820	8.7820
1.5	8.9952	8.2589	2	8.2799	8.2799
2.0	6.7099	7.7460	2	7.7833	7.7833
2.5	5.3389	7.2339	2	7.2920	7.2920
3.0	4.4250	6.7225	2	6.8059	6.8059
3.5	3.7724	6.2119	3	6.3252	6.3252
4.0	3.2830	5.7020	3	5.8497	5.8497
4.5	2.9024	5.1929	3	5.3796	5.3796
5.0	2.5981	4.6845	4	4.9149	4.9149
5.5	2.3491	4.1768	4	4.4560	4.4561
6.0	2.1417	3.6698	5	4.0038	4.0039
6.5	1.9663	3.1636	7	3.5597	3.5600
7.0	1.8159	2.6580	9	3.1270	3.1279
7.5	1.6857	2.1531	12	2.7118	2.7140
8.0	1.5718	1.6490	15	2.3246	2.3297
8.5	1.4714	1.1455	19	1.9805	1.9914
9.0	1.3821	.6426	23	1.6949	1.7150

r	$(g_{DH}(r))$	$(g_{1B}(r))$	N	$(g_B(r))$	$g_S(r))$
9.5	1.3023	.1405	27	1.4743	1.5060
10.0	1.2305	-.3610	30	1.3108	1.3548
10.5	1.1655	-.8619	32	1.1885	1.2443
11.0	1.1065		33	1.0926	1.1596
11.5	1.0527		35	1.0128	1.0907
12.0	1.0034		36	.9432	1.0321
12.5	.9580		38	.8804	.9806
13.0	.9162		39	.8226	.9344
13.5	.8775		40	.7687	.8924
14.0	.8416		41	.7181	.8540
14.5	.8082		43	.6705	.8186
15.0	.7770		44	.6255	.7859

TABLE 4.2

The electron-electron distribution functions at 10^4°K

r	$g_C(r)$	$g_{ee}(r)$	$g_{DH}(r)$	$g_S(r)$
0.0	$-\infty$		$-\infty$	
0.5	-27.4282	-3.4176	-27.2799	-3.4017
1.0	-13.7141	-3.2116	-13.3566	-3.1820
1.5	- 9.1427	-3.0192	- 8.9952	-2.9776
2.0	- 6.8571	-2.8411	- 6.7099	-2.7890
2.5	- 5.4856	-2.6769	- 5.3389	-2.6155
3.0	- 4.5714	-2.5255	- 4.4250	-2.4559
3.5	- 3.9183	-2.3858	- 3.7724	-2.3090
4.0	- 3.4285	-2.2569	- 3.2830	-2.1731
4.5	- 3.0476	-2.1377	- 2.9024	-2.0479
5.0	- 2.7428	-2.0274	- 2.5981	-1.9322
5.5	- 2.4935	-1.9252	- 2.3491	-1.8251
6.0	- 2.2857	-1.8304	- 2.1417	-1.7263
6.5	- 2.1098	-1.7423	- 1.9663	-1.6344
7.0	- 1.9591	-1.6605	- 1.8160	-1.5493
7.5	- 1.8285	-1.5845	- 1.6857	-1.4703
8.0	- 1.7143	-1.5137	- 1.5718	-1.3967
8.5	- 1.6134	-1.4477	- 1.4714	-1.3284
9.0	- 1.5238	-1.3862	- 1.3821	-1.2648

r	$g_C(r)$	$g_{ee}(r)$	$g_{DH}(r)$	$g_S(r)$
10.5	- 1.3061	-1.2254	- 1.1655	-1.0992
11.0	- 1.2467	-1.1787	- 1.1065	-1.0513
11.5	- 1.1925	-1.1346	- 1.0527	-1.0066
12.0	- 1.1428	-1.0935	- 1.0034	-0.9647
12.5	- 1.0971	-1.0550	- 0.9580	-0.9252
13.0	- 1.0549	-1.0188	- 0.9162	-0.8885
13.5	- 1.0159	-0.9849	- 0.8775	-0.8540
14.0	- 0.9796	-0.9530	- 0.8416	-0.8215
14.5	- 0.9458	-0.9224	- 0.8082	-0.7910
15.0	- 0.9143	-0.8940	- 0.7770	-0.7622

TABLE 4.3

Proton-electron distribution functions at 2×10^4°K

r	$g_C(r)$	$g_{pe}(r)$	$g_{DH}(r)$	$g_S(r)$
0.0	∞	5.9244	∞	5.9244
0.5	13.7141	5.4901	13.6616	5.4606
1.0	6.8571	5.0559	6.8047	5.0004
1.5	4.5714	4.6218	4.5191	4.5439
2.0	3.4285	4.1884	3.3764	4.0915
2.5	2.7428	3.7563	2.6907	3.6443
3.0	2.2857	3.3275	2.2337	3.2043
3.5	1.9592	2.9057	1.9073	2.7760
4.0	1.7143	2.4978	1.6625	2.3677
4.5	1.5238	2.1164	1.4721	1.9931
5.0	1.3714	1.7791	1.3198	1.6698
5.5	1.2467	1.5033	1.1953	1.4115
6.0	1.1428	1.2947	1.0915	1.2187
6.5	1.0549	1.1436	1.0036	1.0784
7.0	.9796	1.0331	.9284	.9741
7.5	.9143	.9486	.8632	.8928
8.0	.8571	.8806	.8061	.8264
8.5	.8067	.8236	.7558	.7704
9.0	.7619	.7745	.7111	.7219
9.5	.7218	.7315	.6711	.6794
10.0	.6857	.6934	.6351	.6416

r	$g_C(r)$	$g_{pe}(r)$	$g_{DH}(r)$	$g_S(r)$
10.5	.6531	.6592	.6025	.6077
11.0	.6234	.6284	.5729	.5771
11.5	.5963	.6003	.5459	.5493
12.0	.5714	.5748	.5212	.5239
12.5	.5486	.5514	.4984	.5004
13.0	.5275	.5298	.4774	.4792

TABLE 4.4

Electron-electron distribution functions at 2×10^{4}°K

r	$g_c(r)$	$g_{ee}(r)$	$g_{DH}(r)$	$g_S(r)$
0.0	$-\infty$		$-\infty$	
0.5	-13.7141	-2.4644	-13.6616	-2.4560
1.0	- 6.8571	-2.2613	- 6.8047	-2.2461
1.5	- 4.5714	-2.075	- 4.5191	-2.054
2.0	- 3.4285	-1.9065	- 3.3764	-1.8809
2.5	- 2.7428	-1.7546	- 2.6907	-1.7251
3.0	- 2.2857	-1.6183	- 2.2337	-1.5854
3.5	- 1.9592	-1.4959	- 1.9073	-1.4601
4.0	- 1.7143	-1.3861	- 1.6625	-1.3479
4.5	- 1.5238	-1.2875	- 1.4721	-1.2480
5.0	- 1.3714	-1.1989	- 1.3198	-1.1570
5.5	- 1.2467	-1.1192	- 1.1952	-1.0759
6.0	- 1.1428	-1.0475	- 1.0915	-1.0030
6.5	- 1.0549	-0.9829	- 1.0036	-0.9374
7.0	- 0.9796	-0.9247	- 0.9284	-0.8783
7.5	- 0.9143	-0.8719	- 0.8632	-0.8260
8.0	- 0.8571	-0.8242	- 0.8061	-0.7689
8.5	- 0.8067	-0.7809	- 0.7558	-0.7329
9.0	- 0.7619	-0.7415	- 0.7111	-0.6932

r	$g_c(r)$	$g_{ee}(r)$	$g_{DH}(r)$	$g_S(r)$
9.5	-0.7218	-0.7055	-0.6711	-0.6569
10.0	-0.6857	-0.6727	-0.6351	-0.6238
10.5	-0.6530	-0.6426	-0.6025	-0.5935
11.0	-0.6234	-0.6149	-0.5729	-0.5657
11.5	-0.5962	-0.5892	-0.5459	-0.5398
12.0	-0.5714	-0.5656	-0.5212	-0.5164
12.5	-0.5485	-0.5438	-0.4984	-0.4946
13.0	-0.5275	-0.5236	-0.4774	-0.4743
13.5	-0.5079	-0.5049	-0.4580	-0.4554
14.0	-0.4898	-0.4875	-0.4399	-0.4379
14.5	-0.4729	-0.4729	-0.4231	-0.4215
15.0	-0.4571	-0.4714	-0.4075	-0.4063

TABLE 4.5

Proton-electron distribution functions at 3×10^4°K

r	$g_c(r)$	$g_S(r)$	$(g_{DH}(r))$	$(g_S(r))$
0.0	∞	4.5189	∞	4.5189
0.5	9.1427	4.0851	9.1142	4.0682
1.0	4.5714	3.6514	4.5428	3.6203
1.5	3.0476	3.2194	3.0191	3.1771
2.0	2.2857	2.7925	2.2572	2.7421
2.5	1.8286	2.3771	1.8000	2.3221
3.0	1.5238	1.9858	1.4954	1.9303
3.5	1.3061	1.6374	1.2778	1.5855
4.0	1.1428	1.3514	1.1146	1.3061
4.5	1.0159	1.1358	0.9876	1.0971
5.0	.9143	.9811	0.8861	.9470
5.5	.8312	.8694	0.8030	.8380
6.0	.7619	.7852	0.7338	.7551
6.5	.7033	.7185	0.6752	.6892
7.0	.6531	.6635	0.6251	.6346
7.5	.6095	.6170	0.5816	.5884
8.0	.5714	.5770	0.5435	.5485
8.5	.5378	.5420	0.5099	.5137
9.0	.5079	.5112	0.4801	.4830
9.5	.4812	.4838	0.4534	.4557
10.0	.4571	.4593	0.4294	.4312
10.5	.4354	.4371	0.4077	.4092

r	$g_c(r)$	$g_S(r)$	$(g_{DH}(r))$	$(g_S(r))$
11.0	.4156	.4170	0.3879	.3892

TABLE 4.6

Electron-electron distribution functions at 3×10^4°K

r	$g_c(r)$	$g_{ee}(r)$	$g_{DH}(r)$	$g_S(r)$
0.0	$-\infty$			
0.5	-9.1427	-2.0190	-9.1142	-2.0134
1.0	-4.5713	-1.8185	-4.5428	-1.8084
1.5	-3.0476	-1.6376	-3.0191	-1.6239
2.0	-2.2857	-1.4770	-2.2572	-1.4603
2.5	-1.8285	-1.3354	-1.800	-1.3166
3.0	-1.5238	-1.2112	-1.4954	-1.1906
3.5	-1.3061	-1.1024	-1.2778	-1.0802
4.0	-1.1428	-1.0071	-1.1146	-0.9839
4.5	-1.0159	-0.9238	-0.9876	-0.8995
5.0	-0.9143	-0.8506	-0.8861	-0.8257
5.5	-0.8312	-0.7864	-0.8030	-0.7609
6.0	-0.7619	-0.7299	-0.7338	-0.7039
6.5	-0.7033	-0.6801	-0.6752	-0.6538
7.0	-0.6531	-0.6361	-0.6251	-0.6094
7.5	-0.6095	-0.5968	-0.5816	-0.5701
8.0	-0.5714	-0.5621	-0.5435	-0.5322
8.5	-0.5378	-0.5305	-0.5099	-0.5034
9.0	-0.5079	-0.5024	-0.4801	-0.4752
9.5	-0.4812	-0.4769	-0.4534	-0.4496
10.0	-0.4571	-0.4538	-0.4294	-0.4265

r	$g_c(r)$	$g_{ee}(r)$	$g_{DH}(r)$	$g_S(r)$
10.5	-0.4354	-0.4328	-0.4077	-0.4054
11.0	-0.4156	-0.4138	-0.3879	-0.3862
11.5	-0.3975	-0.3959	-0.3699	-0.3686
12.0	-0.3809	-0.3797	-0.3533	-0.3524
12.5	-0.3657	-0.3648	-0.3382	-0.3376
13.0	-0.3516	-0.3509	-0.3242	-0.3238
13.5	-0.3386	-0.3382	-0.3112	-0.3111
14.0	-0.3265	-0.3263	-0.2991	-0.2993
14.5	-0.3153	-0.3152	-0.2879	-0.2883
15.0	-0.3048	-0.3048	-0.2774	-0.2777

TABLE 4.7

Proton-electron distribution functions at 4×10^4°K

r	$g_c(r)$	$(g(r))$	$(g_{DH}(r))$	$(g_S(r))$
0.0	∞	3.7622	∞	3.7622
0.5	6.8571	3.3300	6.8384	3.3184
1.0	3.4285	2.8975	3.4100	2.8768
1.5	2.2857	2.4709	2.2671	2.4436
2.0	1.7143	2.0594	1.6958	2.0284
2.5	1.3714	1.6800	1.3529	1.6458
3.0	1.1428	1.3559	1.1244	1.3268
3.5	.9796	1.1044	0.9612	1.0791
4.0	.8571	.9241	0.8387	.9020
4.5	.7619	.7975	0.7435	.7774
5.0	.6857	.7055	0.6674	.6865
5.5	.6234	.6351	0.6051	.6168
6.0	.5714	.5787	0.5531	.5608
6.5	.5275	.5320	0.5092	.5145
7.0	.4898	.4925	0.4715	.4753
7.5	.4571	.4587	0.4389	.4417
8.0	.4286	.4293	0.4104	.4114
8.5	.4034	.4036	0.3852	.3867
9.0	.3809	.3808	0.3628	.3640
9.5	.3609	.3605	0.3428	.3437

TABLE 4.8

Electron-electron distribution functions at 4×10^{4}°K

r	$g_c(r)$	$g_{ee}(r)$	$g_{DH}(r)$	$g_S(r)$
0.0	$-\infty$		$-\infty$	
0.5	-6.8571	-1.7457	-6.8384	-1.7414
1.0	-3.4285	-1.5475	-3.4100	-1.5400
1.5	-2.2857	-1.3714	-2.2671	-1.3614
2.0	-1.7143	-1.2179	-1.6958	-1.2059
2.5	-1.3714	-1.0852	-1.3529	-1.0718
3.0	-1.1428	-0.9713	-1.1244	-0.9568
3.5	-0.9796	-0.8737	-0.9612	-0.8583
4.0	-0.8571	-0.7901	-0.8387	-0.7740
4.5	-0.7619	-0.7185	-0.7435	-0.7019
5.0	-0.6857	-0.6569	-0.6674	-0.6400
5.5	-0.6234	-0.6038	-0.6051	-0.5866
6.0	-0.5714	-0.5579	-0.5531	-0.5406
6.5	-0.5275	-0.5179	-0.5092	-0.5007
7.0	-0.4898	-0.4830	-0.4715	-0.4662
7.5	-0.4571	-0.4522	-0.4389	-0.4345
8.0	-0.4286	-0.4249	-0.4104	-0.4071
8.5	-0.4034	-0.4005	-0.3852	-0.3828
9.0	-0.3809	-0.3788	-0.3628	-0.3610
9.5	-0.3609	-0.3592	-0.3428	-0.3415

r	$g_c(r)$	$g_{ee}(r)$	$g_{DH}(r)$	$g_S(r)$
10.0	-0.3428	-0.3417	-0.3428	-0.3238
10.5	-0.3265	-0.3257	-0.3085	-0.3078
11.0	-0.3117	-0.3111	-0.2936	-0.2931
11.5	-0.2981	-0.2978	-0.2801	-0.2797
12.0	-0.2857	-0.2855	-0.2677	-0.2675
12.5	-0.2743	-0.2741	-0.2563	-0.2562
13.0	-0.2637	-0.2636	-0.2458	-0.2457
13.5	-0.2540	-0.2539	-0.2360	-0.2361
14.0	-0.2449	-0.2449	-0.2270	-0.2271
14.5	-0.2365	-0.2366	-0.2186	-0.2187
15.0	-0.2286	-0.2289	-0.2107	-0.2108

TABLE 4.9A

Proton-electron distribution functions at 5×10^4°K showing first bound state and total bound state contributions.

r	$(g_c(r))$	$(g_{1B}(r))$	N	$(g_B(r))$	$(g_{e-p}(r))$
0.0	∞	3.2764	-	-	3.2760
0.5	5.4856	2.8371	8	2.8440	2.8470
1.0	2.7428	2.4028	9	2.4120	2.4166
1.5	1.8286	1.9685	12	1.9878	1.9984
2.0	1.3714	1.5342	16	1.5838	1.6099
2.5	1.097	1.1000	20	1.2217	1.2766
3.0	0.9143	0.6656	24	0.9252	1.0197
3.5	0.7837	0.2313	28	0.7020	0.8385
4.0	0.6857	-.2030	30	0.5363	0.7137
4.5	0.6095	-.6373	32	0.4056	0.6248
5.0	0.5486		34	0.2948	0.5576
5.5	0.4987		36	0.1973	0.5045
6.0	0.4571		39	0.1114	0.4611
6.5	0.4220		41	0.0369	0.4248
7.0	0.3918		43	-.0271	0.3938
7.5	0.3657		44	-.0824	0.3672
8.0	0.3429		45	-.1312	0.3440
8.5	0.3227		46	-.1756	0.3235
9.0	0.3048		47	-.2177	0.3054

TABLE 4.9B

Proton-electron distribution functions including shielding at 5×10^{4}°K and showing the total bound state contribution.

r	$g_{DH}(r)$	N	$g_B(r)$	$g_S(r)$
0.0	∞	1	3.2764	3.2760
0.5	5.4724	8	2.8354	2.8384
1.0	2.7296	9	2.3969	2.4016
1.5	1.8153	12	1.9683	1.9793
2.0	1.3582	16	1.5621	1.5892
2.5	1.0830	20	1.1995	1.2569
3.0	0.9011	24	0.9035	1.0021
3.5	0.7705	28	0.6807	.8228
4.0	0.6725	30	0.5152	.6992
4.5	0.5964	32	0.3845	.6109
5.0	0.5354	34	0.2734	.5440
5.5	0.4856	36	0.1750	.4912
6.0	0.4440	38	0.0875	.4479
6.5	0.4089	40	0.0106	.4115
7.0	0.3788	42	-.0563	.3806
7.5	0.3526	44	-.1143	.3540
8.0	0.3298	45	-.1654	.3308
8.5	0.3097	46	-.2116	.3105
9.0	0.2917	47	-.2545	.2924

TABLE 4.10

Electron-electron distribution functions at 5×10^{4}°K

r	$g_c(r)$	$g_{ee}(r)$	$g_{DH}(r)$	$g_S(r)$
0.0	$-\infty$		$-\infty$	
0.5	-5.4864	-1.5555	-5.4724	-1.5521
1.0	-2.7428	-1.3596	-2.7296	-1.3536
1.5	-1.8285	-1.1879	-1.8153	-1.1800
2.0	-1.3714	-1.0408	-1.3582	-1.0314
2.5	-1.0971	-0.9161	-1.0839	-0.9058
3.0	-0.9143	-0.8111	-0.9011	-0.8001
3.5	-0.7837	-0.7229	-0.7705	-0.7113
4.0	-0.6857	-0.5489	-0.6725	-0.6369
4.5	-0.6095	-0.5865	-0.5964	-0.5742
5.0	-0.5486	-0.5338	-0.5354	-0.5213
5.5	-0.4987	-0.4889	-0.4856	-0.4763
6.0	-0.4571	-0.4505	-0.4440	-0.4379
6.5	-0.4220	-0.4174	-0.4089	-0.4046
7.0	-0.3918	-0.3887	-0.3788	-0.3758
7.5	-0.3657	-0.3635	-0.3526	-0.3507
8.0	-0.3429	-0.3413	-0.3298	-0.3283
8.5	-0.3227	-0.3214	-0.3097	-0.3087
9.0	-0.3048	-0.3038	-0.2917	-0.2911
9.5	-0.2887	-0.2880	-0.2757	-0.2753

r	$g_c(r)$	$g_{ee}(r)$	$g_{DH}(r)$	$g_S(r)$
10.0	-0.2743	-0.2739	-0.2613	-0.2611
10.5	-0.2612	-0.2610	-0.2483	-0.2481
11.0	-0.2493	-0.2493	-0.2364	-0.2363
11.5	-0.2385	-0.2385	-0.2256	-0.2255
12.0	-0.2285	-0.2285	-0.2156	-0.2155
12.5	-0.2194	-0.2195	-0.2065	-0.2066
13.0	-0.2110	-0.2111	-0.1981	-0.1982
13.5	-0.2032	-0.2033	-0.1903	-0.1904
14.0	-0.1959	-0.1960	-0.1831	-0.1832
14.5	-0.1892	-0.1893	-0.1763	-0.1765
15.0	-0.1829	-0.1830	-0.1700	-0.1702

TABLE 4.11

The variation in the Debye shielding length, the joining radius and the percentage ionization with temperature for shielded and non-shielded calculations.

TEMP°K	SHIELDING	λ_D	r_s	I
	NO		13.0	.04
10^4	YES	92.21	13.5	.06
	NO		10.5	12.43
1.5×10^4	YES	112.94	10.0	14.55
	NO		9.5	42.76
1.75×10^4	YES	121.99	9.0	46.80
	NO		8.5	71.04
2.0×10^4	YES	130.41	8.0	74.64
	NO		7.0	90.88
2.5×10^4	YES	145.80	7.0	93.06
	NO		6.5	95.16
3×10^4	YES	159.72	6.5	96.68
	NO		5.0	97.44
4×10^4	YES	184.43	5.0	98.34
	NO		4.5	98.25
5×10^4	YES	206.20	4.5	98.85
	NO	-	-	-
8×10^4	YES	260.82	3.0	99.16

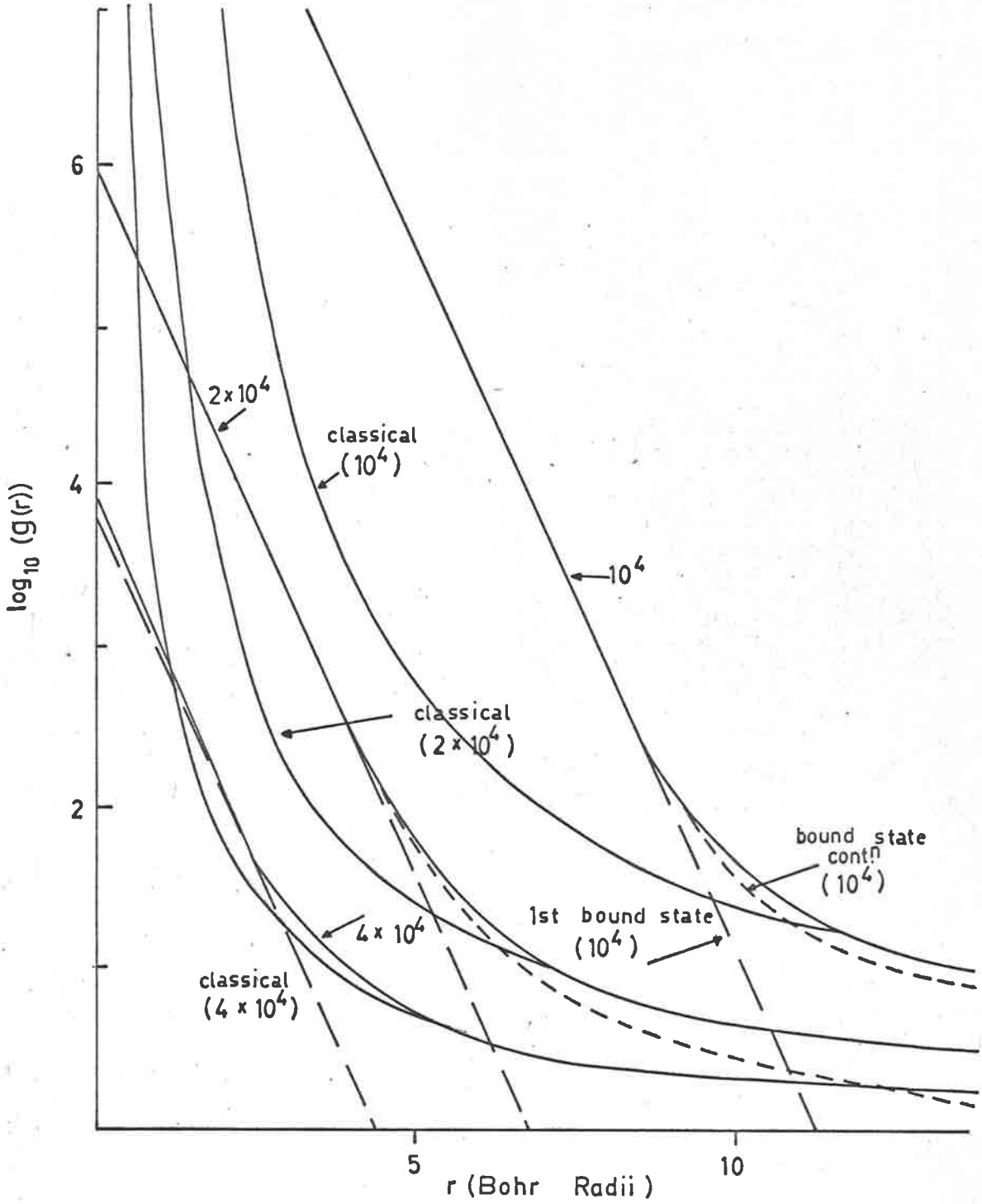

FIG. 4·1 PROTON ELECTRON RADIAL DISTRIBUTION FUNCTIONS SHOWING CONTRIBUTIONS FROM THE FIRST BOUND STATE AND TOTAL BOUND STATES FOR VARIOUS TEMPERATURES. THE CORRESPONDING CLASSICAL RADIAL DISTRIBUTION FUNCTIONS ARE DRAWN FOR COMPARISON.

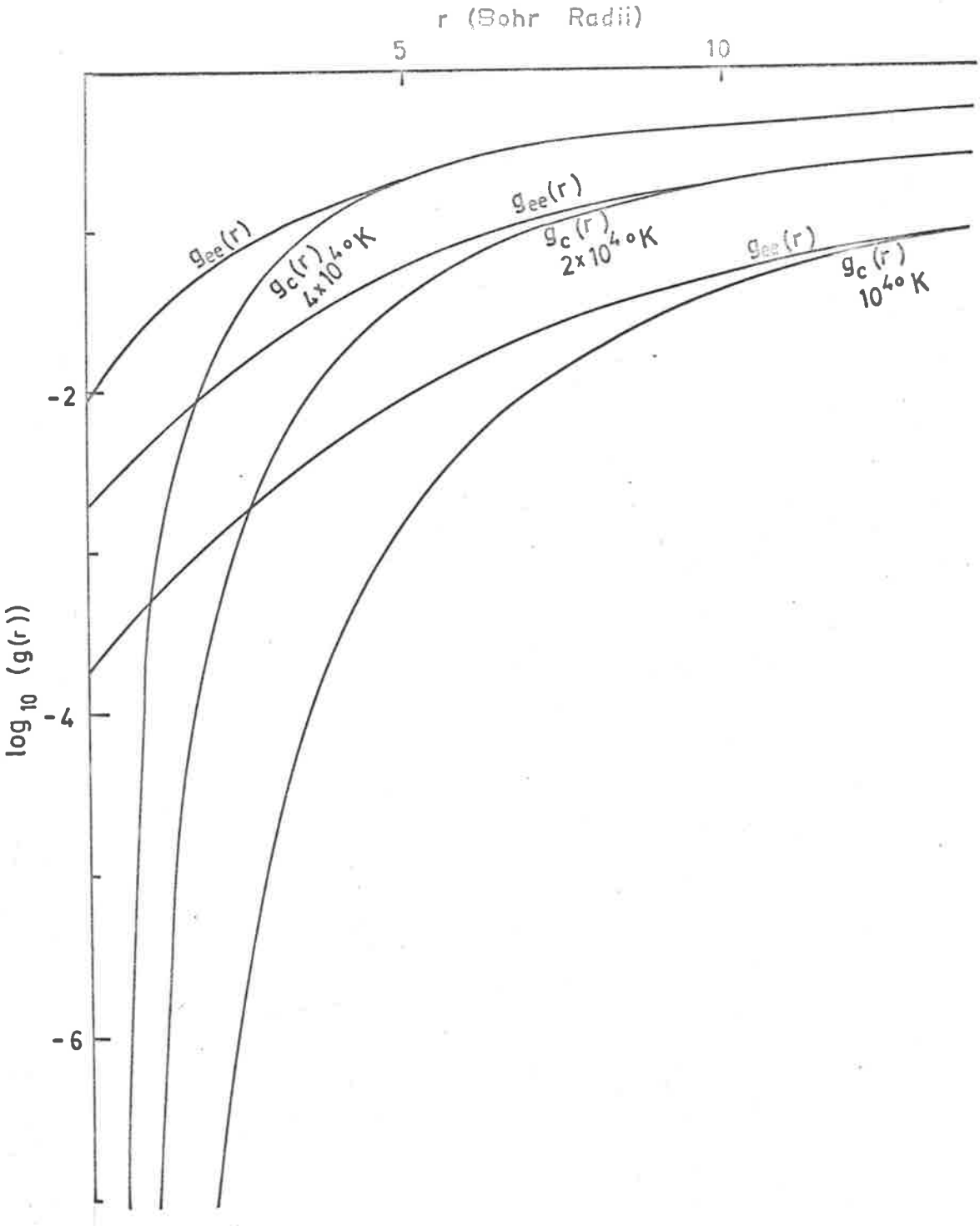

FIG. 4·2 Q.M. ee DISTRIBUTION FUNCTIONS FOR VARIOUS TEMPERATURES COMPARED WITH THEIR CORRESPONDING CLASSICAL DISTRIBUTION FUNCTIONS.

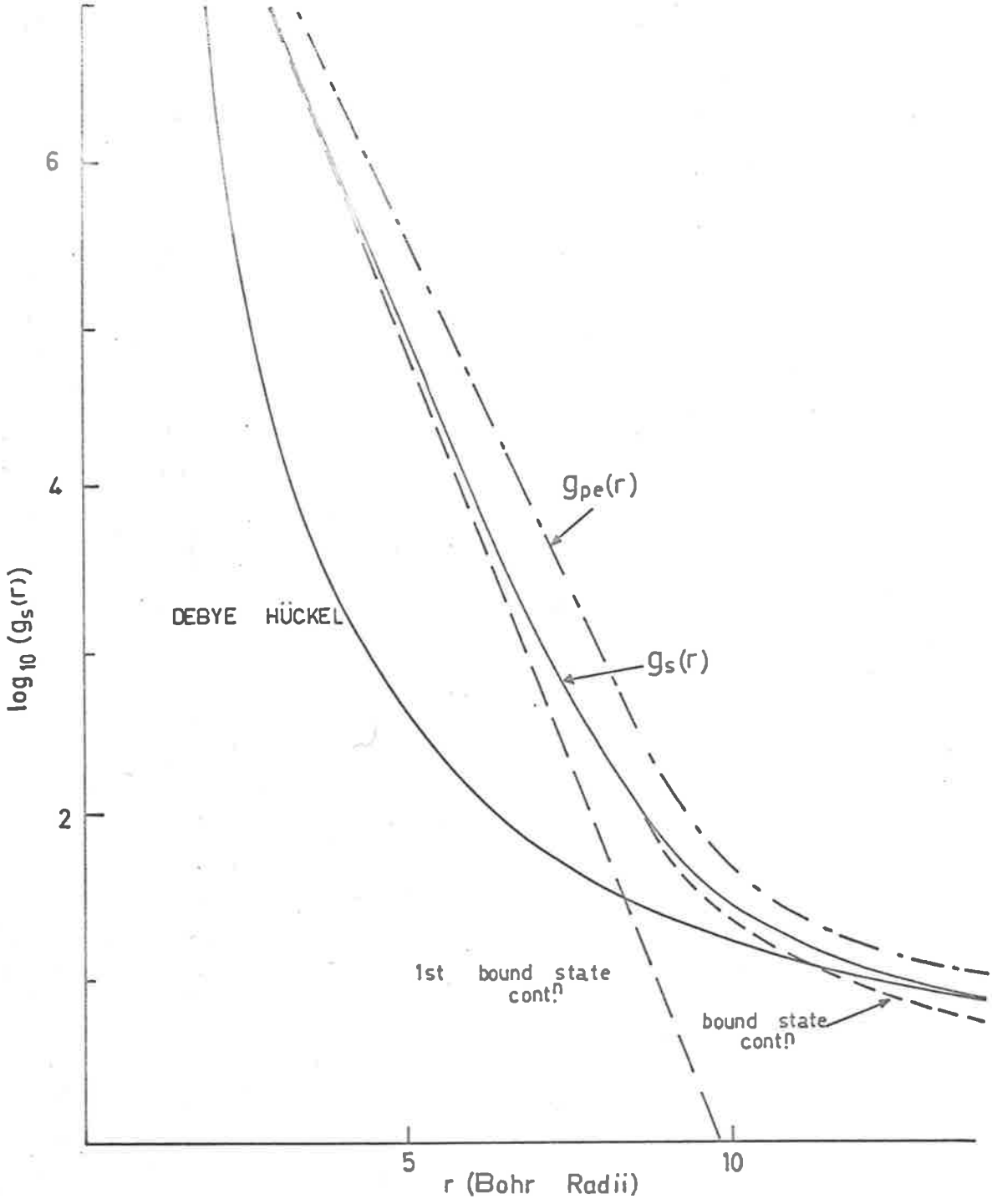

FIG. 4·3 THE PROTON ELECTRON RADIAL DISTRIBUTION FUNCTION WITH A SHIELDING FACTOR INCLUDED, $g_s(r)$, IS COMPARED WITH $g_{pe}(r)$ AND THE DEBYE HÜCKEL DISTRIBUTION FUNCTIONS FOR 10^4°K.

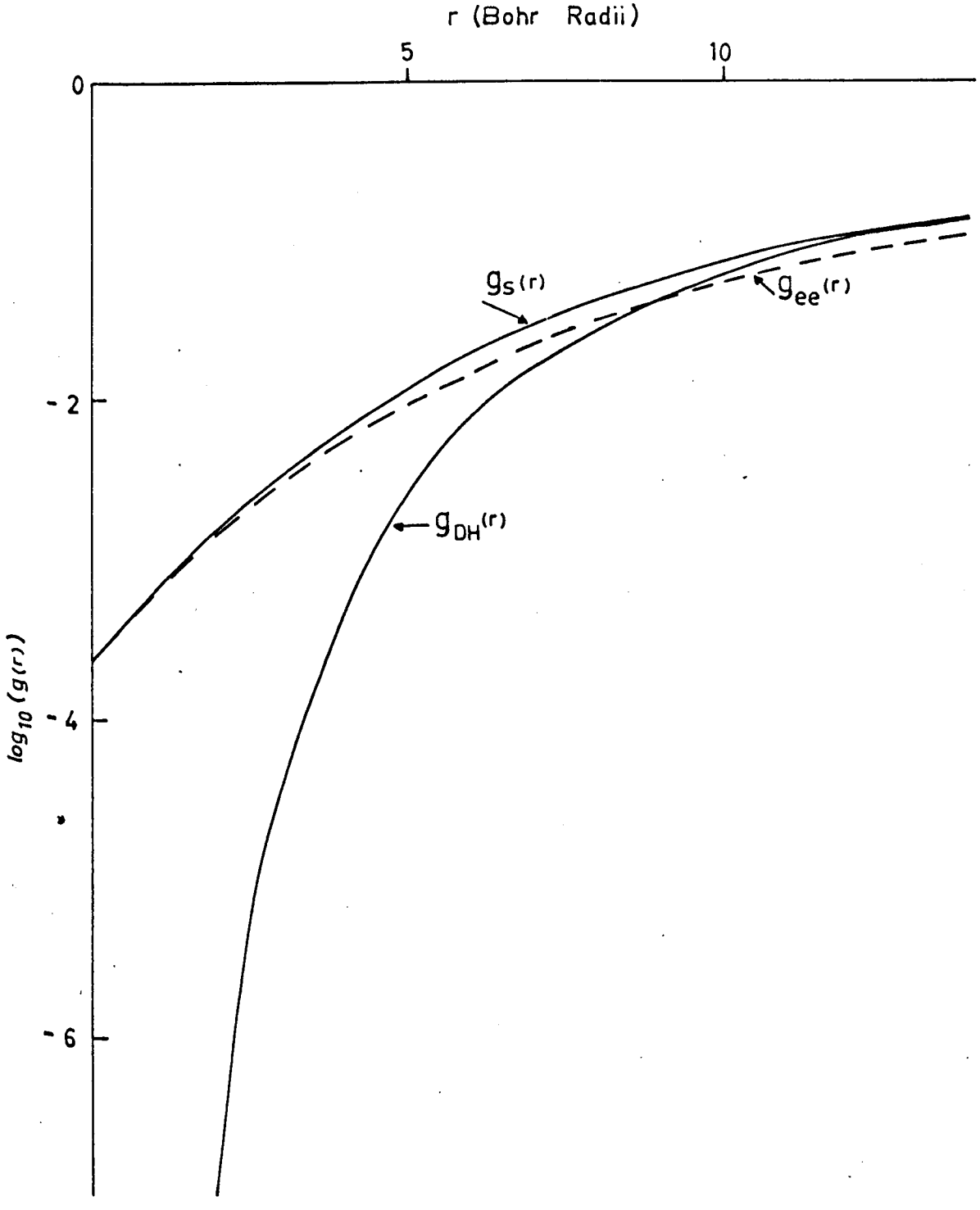

FIG. 4·4 QM DISTRIBUTION FUNCTION FOR ee CASE WITH THE SHIELDING FACTOR INCLUDED $g_s(r)$ COMPARED WITH $g_{ee}(r)$ AND THE CORRESPONDING DH FOR $10^{4\circ}$K.

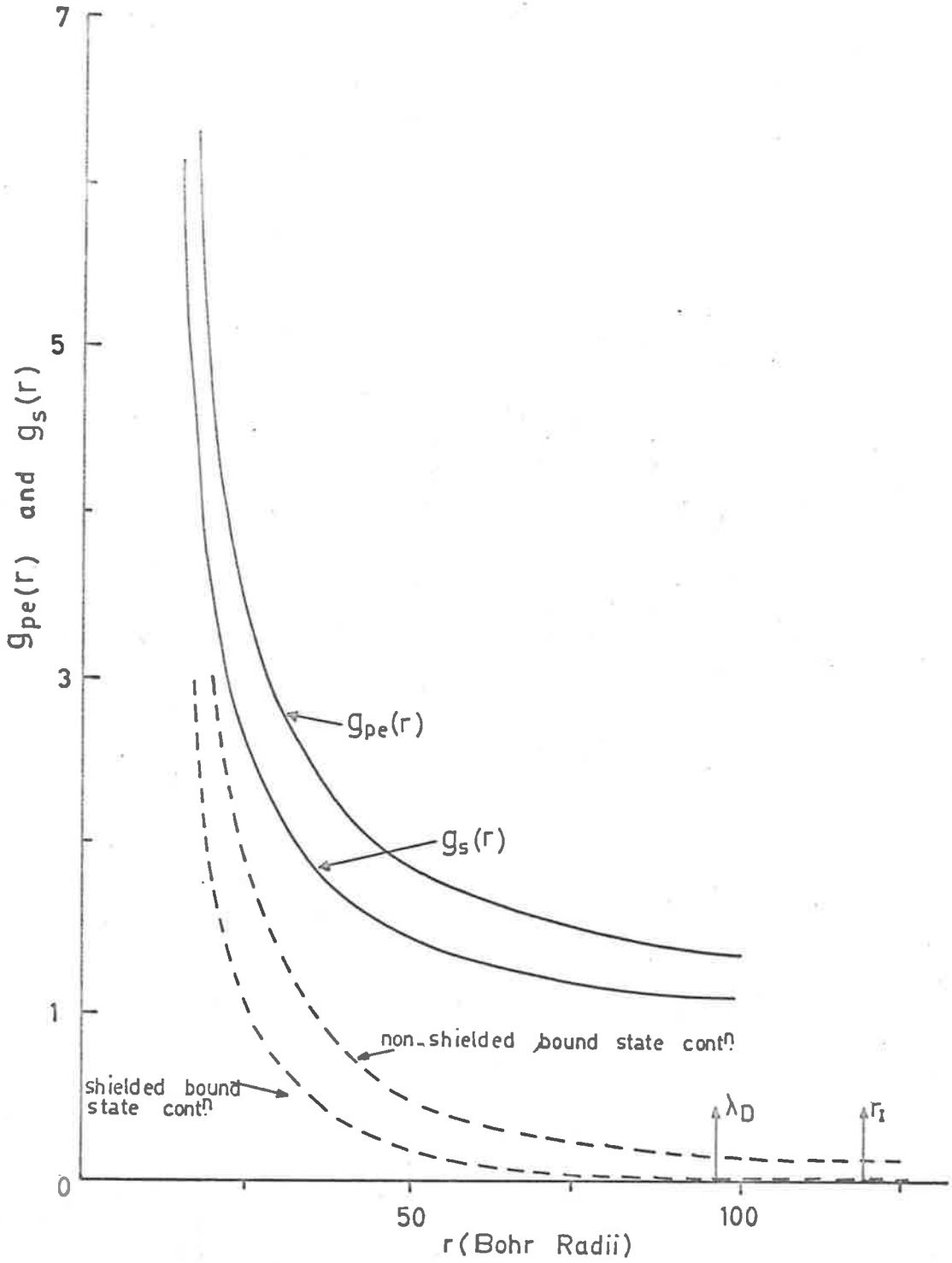

FIG. 4·5 THE SHIELDED AND NON-SHIELDED DISTRIBUTION FUNCTIONS, WITH THEIR CORRESPONDING BOUND STATE CONTRIBUTIONS, TO LARGE RADII AT 10^4°K.

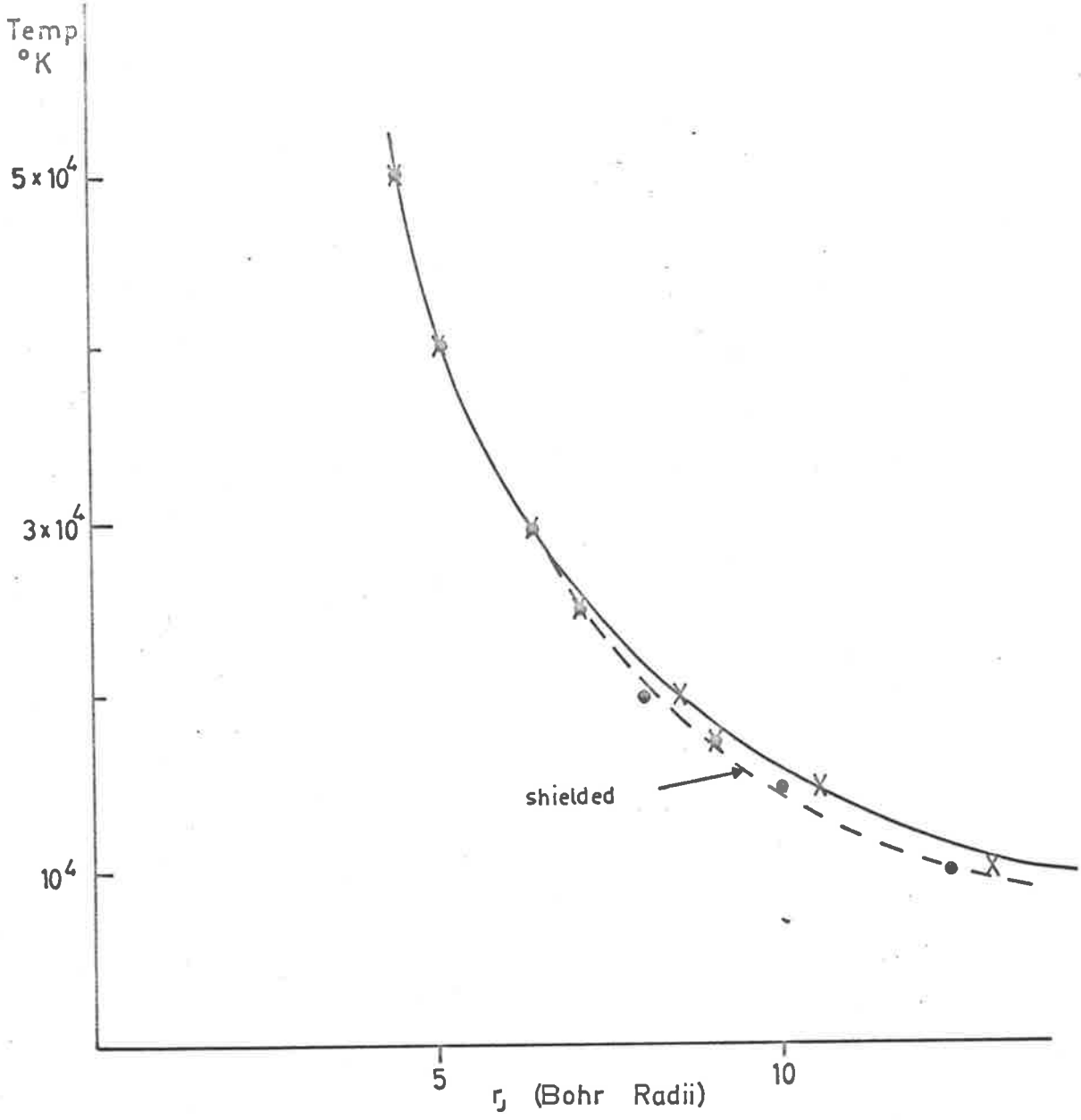

FIG. 4·6 JOINING RADIUS vs TEMPERATURE FOR SHIELDED AND NON - SHIELDED CALCULATIONS.

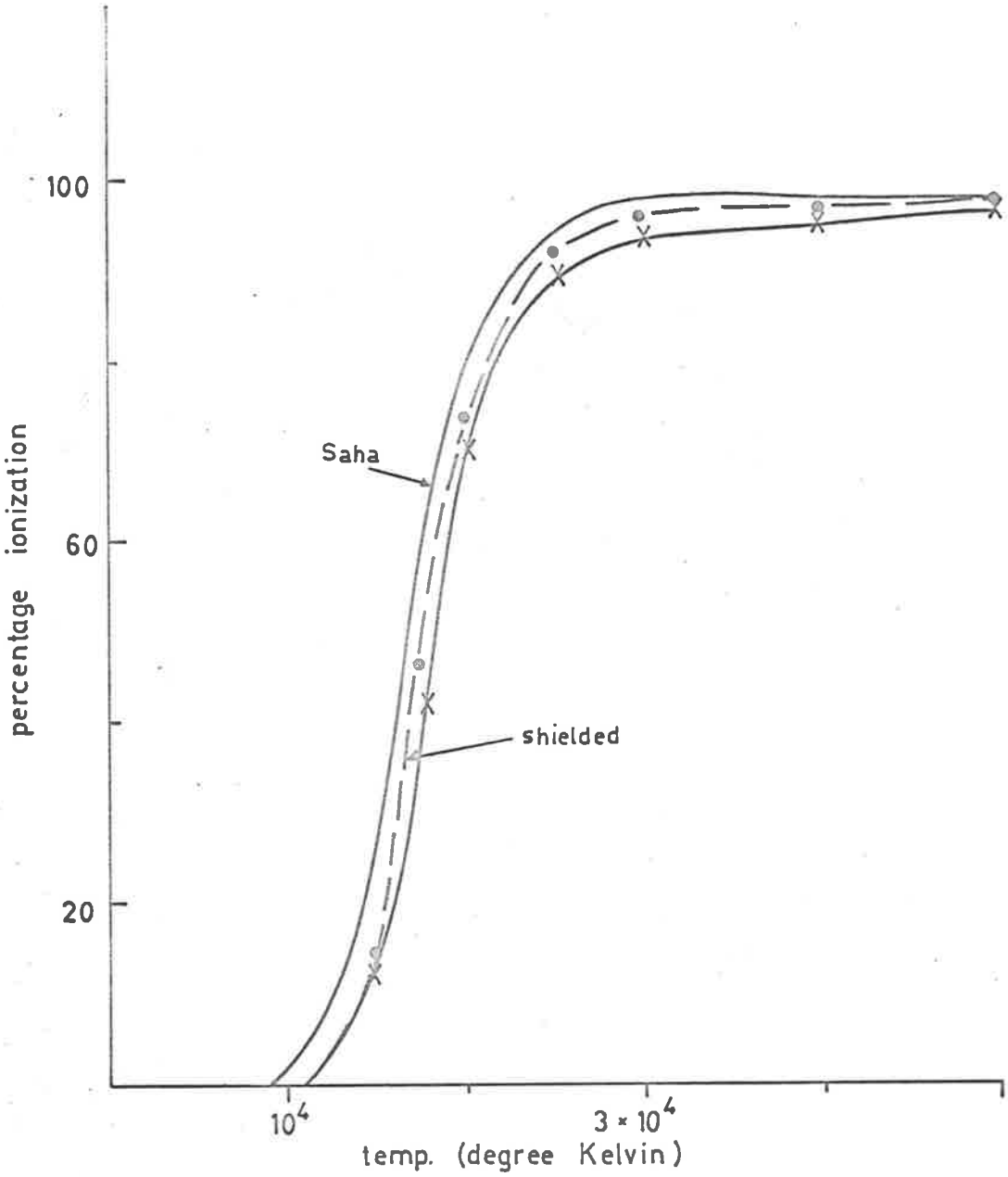

FIG. 4·7 PERCENTAGE IONIZATION GRAPHS FOR SHIELDED AND NON-SHIELDED CASES WITH THE CORRESPONDING SAHA CURVE FOR A PLASMA OF DENSITY 10^{18} e/cc.

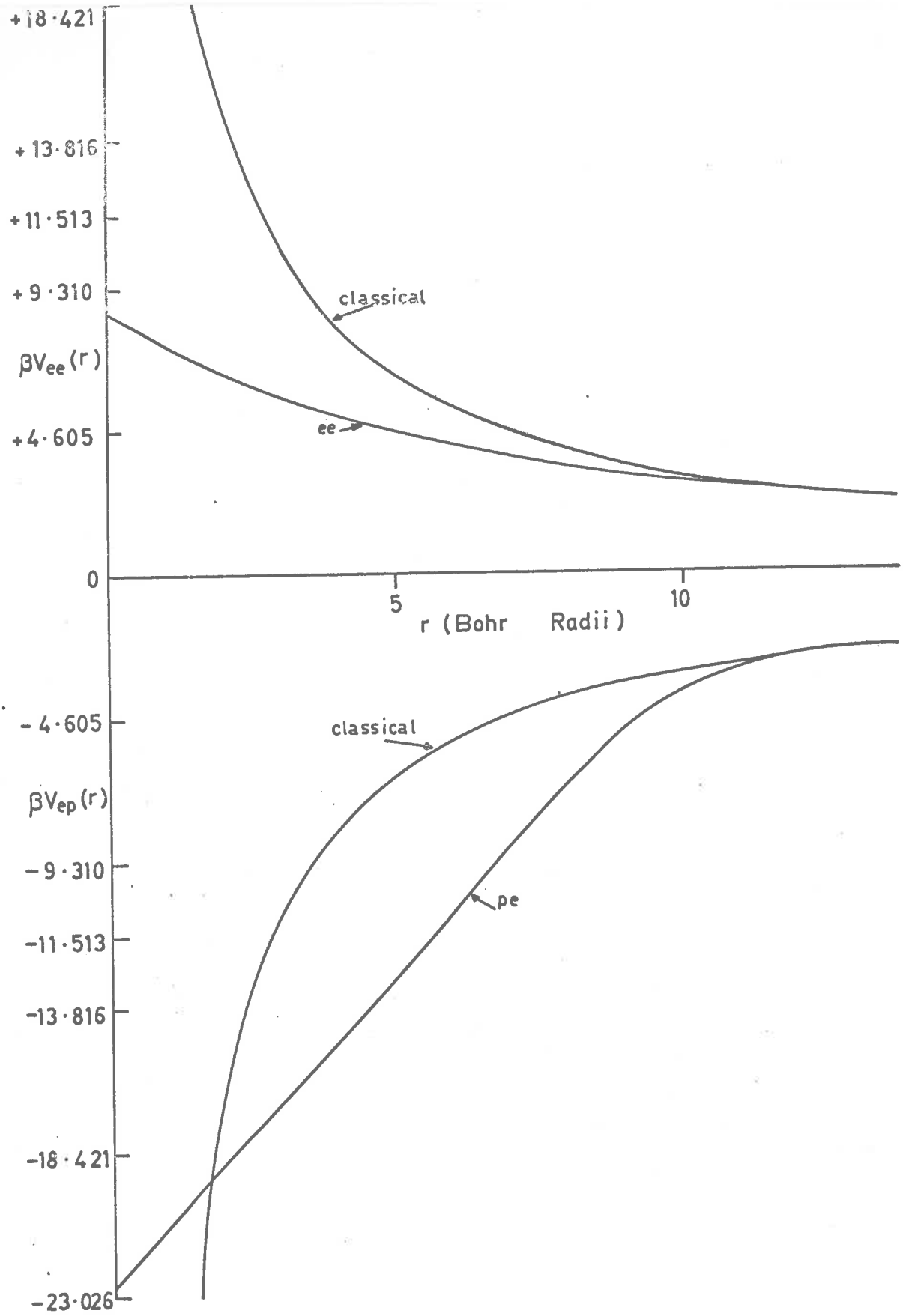

FIG. 4·8 EFFECTIVE POTENTIALS AT 10^4 °K.

4.4 Discussion

The Tables 4.1 - 4.10 with Figs. 4.1 - 4.5 show that for both p-e and e-e pairings, the $g_{QM}(r)$ runs smoothly onto $g_c(r)$ at a certain joining radius r_J. Below r_J there is a marked difference between $g_{QM}(r)$ and $g_c(r)$. At r=0 the QM curve tends to a constant (approximately equal to the first bound state contributio of $(2\pi\beta\hbar^2/m)^{3/2}\exp(15.780/\pi\times10^{-4})/\pi$ for temperatures below 4×10^{4}°K in the p-e case) while the classical curve approaches infinity. For small r and low temperatures the quantum mechanical p-e curve lies close to the first bound state contribution, i.e. $(2\pi\beta\hbar^2/m)^{3/2}\exp\{(15.780/(T\times10^{-4}))-2r\}/\pi$, (where r is in Bohr radii), whilst the correcponding classical curve

$$g_c(r) = \exp\{63.156/(T\times10^{-4}\times2r)\}$$

falls away much more sharply. As the radii increase, other bound states and scattered states start making an appreciable contribution to $g_{pe}(r)$, until at r_J it effectively joins the classical curve. As can be seen from the graphs the e-e case is essentially similar, but in this case no bound states exist, and the log $g_c(r)$ goes to minus infinity.

Figs. 4.1 and 4.5 show that for the p-e case the bound state contribution is quite large, especially at

low temperatures, and for 10^{4}°K even at 50 Bohr radii the bound states contribute 18% of $g_{pe}(r)$ and still contribute 11% at 100 Bohr radii. The value of n at which the bound-states sum terminates is also of interest, and for 10^{4}°K at 10 Bohr radii, 26 terms were needed, at 50 Bohr radii, 84 terms, and at 100 Bohr radii, 110 terms contributed. In a similar fashion the number of terms contributing to the scattering states rose as the radii increased.

The temperature dependence of the both the $g_{ee}(r)$ and $g_{pe}(r)$ is also evident from Figs. 4.1 and 4.2. As the temperature is increased the quantal curve becomes much closer to the classical curve, and for the p-e case the bound state contribution falls off much faster, and the contribution of the first bound state is less important. Comparison of $g_{pe}(r)$ and $g_{ee}(r)$ with recent results obtained by Storer [34] and Storer and Davies [42] give agreement to ±5 in the fourth figure, which is less than the estimated error for these calculations. It should be noted that at higher temperatures than those calculated here, i.e. $>5\times10^{4}$°K, $g_{pe}(0)$ contains important contributions from n>1 states, a feature shown clearly by the results of Storer.

Fig 4.6 shows that the joining radius r_J falls off sharply as the temperature increases from 9×10^{3}°K to

3×10^4°K but at higher temperatures varies only slightly. There is no obvious analytical dependence of r_J on temperature.

The inclusion of the approximate shielding factor in the results of Figs. 4.3 and 4.4 show there is little effect on the general shape of the curve, but that it causes an appreciable change in values, so that now the shielded $g_S(r)$ joins its respective 'D.H.' curve above a certain radius. From Fig 4.6 it can be seen that this joining radius (defined as before, except now the criterion is that $g_S(r)$ approaches within 5% of $g_{DH}(r)$, not $g_c(r)$ as before) only differs from the non-shielded case at temperatures below 3×10^4°K. The effect of the shielding is more pronounced on the total and first bound state contributions, and Fig. 4.5 shows that these fall off appreciably faster than the non-shielded case, especially at large radii. In Fig. 4.5, because the classical curve is nearly identical with $g_{pe}(r)$, and similarly since $g_{DH}(r)$ remains so close to $g_S(r)$, the $g_c(r)$ and $g_{DH}(r)$ are not drawn.

As the quantum mechanical expression for g_{pe} divides it into bound and scattered state contributions, it is possible to obtain the percentage ionization present in the hydrogen gas, and Fig. 4.7 shows that this differs only slightly for the non-shielded and shielded cases.

The effect of shielding is to increase the ionization two or three per cent, which is to be expected, as the shielding precludes some of the bound states. The results agree quite closely with those of Saha [43], the main disagreement being just above 1.5×10^{4}°K where the non-shielded ionization value is only half Saha's value and even the shielded value is 15% below. Also by Saha's theory between 1.5×10^{4}°K and 2×10^{4}°K, 48% of the the ionization occurs, while the quantum mechanical calculation gives 59% without shielding, and 60% with shielding. At 2.5×10^{4}°K the non-shielded theory implies there are twice as many neutral particles as predicted by Saha's results. Saha's original theory, see [44] allowed only for lower bound states in an approximate manner, and has since been improved by a number of authors [17(c)] and [35], to include higher bound states, and some attempt has been made to also allow for shielding effects [23(c)]. The degree of ionization obtained from these refinements is still surprizingly close to the values obtained by Saha.

Fig 4.8 shows that the effective potentials obtained by allowing for quantal effects differ from the classical Coulomb potential at small radii, and are finite at the origin. As the temperature increases the effective potentials become closer to their

corresponding Coulomb potentials, while remaining finite at the origin, the V_{EFF} merge with their corresponding Coulomb potentials at small radii. The difference between the $V_{ee}(r)$ and the $V_{ep}(r)$ is most marked. In the e-e case the inclusion of the quantal effect considerably reduces the repulsive Coulomb potential; whereas for the p-e case there is an increase in the attractive potential from $r=r_s$ to $r=1.5a_o$, then a reduction of the attractive potential for $r=1.5a_o$ to $r=0$.

In conclusion the results are of importance because they show the rather large deviations of the two particle quantal distribution functions from the classical Coulomb theory at short interparticle distances, and because they indicate that below r_J quantum mechanical effects become important for the p-e and e-e cases, especially at low temperatures. Unfortunately the complexity of evaluating Coulomb wave functions over large ranges precludes the calculation of $g_{pp}(r)$, but the quantum effects should be small for this case. An approximate allowance for shielding indicates that results are qualitatively the same, both for e-e and p-e cases, as for no shielding, but the $g_S(r)$ tend to the corresponding $g_{DH}(r)$ instead of joining $g_c(r)$ as for the two particle (i.e. non-shielded) case. The

inclusion of shielding causes changes in the degree of ionization present, but the degree of ionization remains remarkably close to values obtained from the Saha and improved Saha equations. Also from the p-e results one can see some justification for considering the first bound state as the major contribution to the bound states, especially at temperatures below 3×10^{4}°K (for the density 10^{18}e/cc). The decrease in the repulsive Coulomb potential for the e-e interactions is most marked, and in contrast to the p-e case, V_{e-e} never enhances the Coulomb potential. The inclusion of quantum statistics would have most effect on the e-e interactions (see [33]), but should be small relative to the quantum effect calculated.

References to Chapter 4

[1] Born, M. and Oppenheimer, E. (1927) Ann. Physik 84, 457.

[2] Slater, J.C. (1931) Phys. Rev. 38, 237.
(1933) J. Chem. Phys. 1, 687

[3] London, F. (1930) Z. Physik. 63, 245.

[4] Kirkwood, J.G. (1932) Phys. Zeits 33, 39
(1933) Phys. Rev. 44, 31.

[5] Uhlenbeck, G.E. and Gropper, L. (1932) Phys. Rev. 41, 79

[6] Wigner, E. (1932) Phys. Rev. 40, 749

[7] Bethe, E. and Uhlenbeck, G.E. (1937) Physica 4, 915.

[8] Margenau, H., (1930) Phys. Rev. 36, 1782.
(1931) Phys. Rev. 37, 1014 and 1425;
38, 747 and 1785.

[9] DeBoer, J. (1949) Report Progr. Phys. 12, 305.

[10] Coleman, A.J. (1963) Rev. Mod. Phys. 35, 668.

[11] Mayer, J.E. and Band, W. (1947) J. Chem. Phys. 15,141.

[12] In the last ten years papers have appeared by Isihara, A.;Montroll, E.W.; Lee ., T.D. and Yang,C.N.; Fujita, S. and Hirota; Imre, K.; Ozizmir, E.; Rosenbaum, M. and Zweifel, P.; Lee, J.C. and Broyles, A.A.; Hiroike, K.; Jaen, J.K. and Khan, A.A.; Allen, K.R. and Dunn, T.; Lado, F.;

and Larsen, S.Y. and many others.

[13] Fermi, E. (1924) Z. Phys. 26, 54. Assumes bound states do not exist if their energy is > the potential energy of two ions at an average distance apart.

[14] Feix, M.R. in 'Proceedings of the Sixth International Conference on Ionization Phenomena in Gases.' T. Hubert and E. Cremin, Eds. (Bureau des Editions, Centre d'Etudes Nucleaires de Saclay, Paris, 1964). Vol. I p.185. Treats the classical electron gas by a random phase approximation, this however fails at small interparticle distances.

[15] Von Hagenow, K. and Koppe, H. In the conference above Vol. I p.221.

[16] Harris, G.M. (1959) J. Chem. Phys. 31, 211.
(1962) Phys. Rev. 125,1131
(1964) 133, A427.

Calculates new bound state levels by using shielded potentials.

[17](a) Ecker, G. and Weizel, W. (1956) Ann. Physik. 17, 126. Considers shielding on the s states to determine the bound state cut-off.

(b) Ecker, G. and Kroll, W. (1963) Phys. Fluids 6. 62

(c) Ecker, G. and Kroll, W. (1966) Z. Naturforsch 21a 2012,2023.

[18] Kelbg, G. (1954) Ann. Phys. 12, 354. Proposes an effective potential to cut-off the bound states.

[19] Dekeyser, R. (1965) Physica 31, 1405.

[20] Lamb, G.L. (1964) Phys. Rev. Letters. 13, 683.
(1965) Phys. Rev. 140, A1529.
Using the expansion technique of Goldberger and Adams obtainsa convergent correlation function for r> the thermal De Broglie wavelength.

[21] Guernsey, R.L. (1965) Phys. Fluids 7 792.

[22] Oppenheim, I. and Hafemann, D.R. (1963) J. Chem. Phys. 39, 101. Using the relative size of the bound and unbound terms they eliminate the QM divergences.

[23](a) Rouse, C.A. (1967) Phys. Rev. 159, 41.
(b) 163, 62.
(c) Solving the Schroedinger equation for a Yukawa (screened) potential,applies his solutions to equations of state and ionization calculations (preprint).

[24] Montroll, E.W. and Ward, J.C. (1958) Phys. Fluids. 1, 55.

[25] Bloch, C and de Dominicus, C. (1958) J. Nucl. Phys. 7, 459.
Bloch, C. and de Dominicus, C. (1959) J. Nucl. Phys. 10, 181 and 509

[26] De Witt, H. (1962) J. Math. Phys. 3, 1216.
(1966) J. Math. Phys. 7, 616.

[27] Ninham, B.W. Preprint.

[28] Diesendorf, M.O. Private Communication.

[29] ONeil, T. and Rostoker, N. (1965) Phys. Fluids 8, 1109.

[30] Trubnikov, B.A. and Elesin, V.F. (1965) J.E.T.P. 20 866. Includes exchange QM effects, but makes no allowance for shielding.

[31] Dekeyser, R. (1967) Physica 35, 506.

[32] Kremp, P. and Kraeft, W.D. (1968) Ann. Phys. 20, 340.

[33] Matsuda, K. (1968) Phys. Fluids 11, 328.

[34] Storer R.G. (1968) J. Maths. Phys. 9, 964.

[35] Ebeling, W. (1968) Physica 38, 378.

[36] Pauling, L., and Wilson, E.B. "Introduction to Quantum Mechanics" Ch.V, (McGraw-Hill: New York 1935).

[37] Schiff, L.I. 'Quantum Mechanics' Ch.V (McGraw-Hill: New York.1955).

[38] Abramowitz, M. and Stegun, I.A. - "Handbook of Mathematical Functions", Ch.14. (National Bureau of Standards: Washington).

[39] Fröberg, C.E. (1955) Rev. Mod. Phys. 27, 399.

[40] Slater, L.J. 'Confluent Hypergeometric Functions'

[41] N.B.S. Tables of Coulomb Wave Functions AMS 17
Abramowitz, M. Phys. Rev. 98, 1187 (1955).
Abramowitz, M. and Stegun, I.A. Phys. Rev. 98, 1851 (1955).

[42] Storer, R.G. Private Communication
Storer, R.G. and Davies, B. (1968) Phys. Rev. 171, 150.

[43] Saha, M.N. and Saha, N.K. (1934) - "A Treatise in Modern Physics" p.793 (The Indian Press: Calcutta).

[44] Thompson, W.B. (1962) An Introduction to plasma physics p.19 (Pergamon Press: Oxford).

V SOLUTION OF THE MODIFIED PERCUS-YEVICK EQUATION

5.1 A form suitable for solution on a computer

In Chapter III we expressed the PY equation in a form suitable for solution on a computer, and gave an outline of the computer procedure to determine $g_{ab}(r)$ from this equation. We also derived an asymptotic form of the PY equation for large r, which was found to be inconsistent in the second-order terms. It was further shown that the integral term was extremely sensitive to the input potentials and distribution functions at small r. In this section we shall apply the same reasoning to the MPY equation which, in its asymptotic form for large r, has the advantage of self-consistency to all orders. The input potentials and distribution functions will be taken from the accurate quantum mechanical calculations of Chapter IV.

The modified Percus-Yevick equation as proposed by Green [1] has the form

$$g_{ab}\, e_{ab} = 1 + \sum_c n_c \int (g_{bc}-1)\, g_{ac}\, (1-e_{ac})\, d^3x_c$$

$$+ \tfrac{1}{2} \sum_c n_c \sum_d n_d \iint (g_{bc}-1)\, (g_{bd}-1)\, g_{cd}\, g_{ac}\, g_{ad}(1-e_{ac})$$

$$(1-e_{ad})\, d^3x_c\, d^3x_d \qquad (5.1)$$

where $e_{ab} = \exp(\beta\phi_{ab})$, the summations are over the types of particles in the mixture, and the higher order terms have been neglected. In this Chapter, using computer notation, shall refer to the PY term (i.e. the first integration term), as TDTM, and the last integration term as FDTM. Since TDTM was considered in detail in Chapter 3, here emphasis will be placed on FDTM which effectively describes the four-particle interactions. Using an approach similar to that in the 3-particle case, FDTM takes the form

$$\frac{4\pi}{2r^2} \sum_c n_c \sum_d n_d \int_0^\infty \int_0^\infty \int_{|r-s|}^{(r+s)} \int_{|r-u|}^{(r+u)} \int_0^\pi [g_{bc}(t)-1]$$

$$[g_{bd}(v)-1]\, g_{ac}(s)\, g_{ad}(u).\ [1-e_{ac}(s)]\,[1-e_{ad}(u)]$$

$$g_{dc}(w)\, d\theta\, v\,dv\, t\,dt\, u\,du\, s\,ds, \qquad (5.2)$$

where w is defined by the equation

$$2r^2w^2 = 2r^2(s^2+u^2) - (r^2+s^2-t^2)(r^2+u^2-v^2) -$$

$$[4r^2s^2 - (r^2+s^2-t^2)^2]^{\frac{1}{2}} \cdot \qquad (5.2a)$$

$$[4r^2u^2-(r^2+u^2-v^2)^2]^{\frac{1}{2}} \cos\theta \ .$$

The quantities r,s,t,u,v and w refer to the interparticle distances between four particles which are placed at the

vertices of a tetrahedron, viz.

$$r = |\underline{x}_a - \underline{x}_b|,\ s = |\underline{x}_a - \underline{x}_c|,\ t = |\underline{x}_b - x_c|,\ u = |\underline{x}_c - \underline{x}_d|,\ u = |x_b - x_d| \text{ and } w = |\underline{x}_d - \underline{x}_c|,$$

where $\underline{x}_a$, $\underline{x}_b$, $\underline{x}_c$, and $\underline{x}_d$ define the positions of the 4 particles of types a,b,c and d respectively. θ is the angle between the plane $\underline{r}$, $\underline{s}$, $\underline{t}$ and $\underline{r}$, $\underline{u}$, $\underline{v}$, and is related to the length w by (5.2a). It can be seen that w achieves its maximum value (WMAX) when particle c and d are directly opposite each other on either side of $\underline{r}$, and this occurs when $\theta=\pi$. Correspondingly, the minimum value (WMIN) is obtained when $\theta = 0$.

An asymptotic form of FDTM akin to (3.2) can be obtained from the same assumptions, using similar reasoning. Equation (5.2) then becomes

$$2\pi \sum_c n_c \sum_d n_d \int_{-a}^{a} [\beta\, \phi_{ac}(p+y) + \ldots] \left(1 + \frac{p}{r}\right) \int_{-a}^{a} [\beta\phi_{ad}(q+r)+\ldots]\,(1+q/r)\,.$$

$$\int_{|p|}^{p+2r} \epsilon_{bc}(t) \int_{|q|}^{q+2r} \epsilon_{bd}(v) \int_{o}^{\pi} [1+\epsilon_{dc}(w)]\, d\theta\, v\,dv\, t\,dt\, dq\, dp \qquad (5.3)$$

where

$$w^2 = t^2 + v^2 - 2pq + 2(t^2 - p^2)^{\frac{1}{2}} (v^2 - q^2)^{\frac{1}{2}} \cos \theta.$$

This expression can also be obtained by letting $\underline{r}$ become large in the geometrical interpretation of the integral. When it is added to the asymptotic form of the Percus-Yevick equation, it makes the resulting asymptotic equation consistent to second order for charged mixtures, as can be seen from arguments analagous to those of section 3.2.

The numerical evaluation of FDTM as given in (5.2) is based to a large extent on the techniques mentioned in section 3.3. This is to be expected, as FDTM is essentially composed of two parts which are identical to TDTM, but which are modified by the inner integral $\int_0^{\pi} g_{dc}(w)\, d\theta$. In the program (see appendix B) this inner integral is evaluated in terms of w. This is done by using (5.2a) to obtain $d\theta$ in terms of dw. The inner integral then becomes

$$\int_{WMIN}^{WMAX} \left(\frac{g_{dc}(w)}{DEN} \; 2r^2 w \right) dw$$

where we have used the substitution $d\theta = \frac{2r^2 w}{DEN}\, dw$.

However, for the FDTM, although the integrations can be divided into regions and evaluated using a trapezoidal rule as for TDTM, the mesh ratio's that can be used are much smaller due to the higher dimension. Further details of the program for calculation of FDTM are given in the notes with Appendix B.

The application of the MPY equation to a two component (p-e) plasma encounters difficulty in the choice of input, for it can be seen from equation (5.1) that there exist four distribution functions to be calculated, g_{ee}, g_{ep}, g_{pe} and g_{pp}. As it is intended to use an iterative technique to solve the MPY equation, this would mean solving four linked integral equations. Classically, the following identities hold: $-\phi_{ee} = \phi_{pp}$, $g_{ee} = g_{pp}$, $\phi_{pe} = \phi_{ep}$ and $g_{pe} = g_{ep}$. These reduce (5.1) to two linked equations. However, from the quantal considerations of Chapter IV it was shown for small r, that although the effective potentials and distribution functions for interactions between unlike particles were equal (meaning $V_{ep} = V_{pe}$ and $g_{ep} = g_{pe}$ respectively), this was not the case for like particles. For like particles V_{ee} and g_{ee} differ very appreciably for small r from the corresponding V_{pp} and g_{pp}. Furthermore from Chapter IV we could not obtain accurate values for

g_{pp} (and hence V_{pp}) by the same method used for g_{ee}, though it was deduced that for the p-p case the quantal effects should be small, and so g_{pp} is expected to remain close to its corresponding classical curve and V_{pp} close to the corresponding Coulomb potential.

To resolve the difficulty of obtaining accurate input data for like particles at small r, it is found convenient to assume that the combined effect of the e-e and p-p potentials can be represented by reflection of the e-p potential from below to above the r-axis, i.e. $V_L = - V_U$, where V_L refers to the combined effect of the e-e and p-p potentials, and V_U refers to the interaction potential between unlike particles. This assumption, besides alleviating the need for accurate p-p input data, reduces the number of linked integral equations obtained via (5.1) from three to two, and so greatly reduces computational difficulties. From Fig. 4.8 it can be seen that reflection of V_{ep} about the r axis to obtain the combined effect of the e-e and p-p potentials results in a V_L characteristic which differs markedly from the V_{ee} curve, and from the classical curve to which V_{pp} closely approximates. However, since the forces are repulsive, the number of particles of the same charge approaching one another very closely is expected to be small, and the error involved unimportant, at least at

temperatures above 2×10^{4}°K. Below this temperature the number of pairs present may encourage the formation of complex ions for which a more rigorous treatment of quantal effects between like particles (including quantum statistics) would be desirable .

5.2 Outline of the numerical procedure

The evaluation of the PY term and the MPY term has been discussed in some detail in sections 3.3, 5.1, and Appendix B. In this section we shall discuss the iterative procedure adopted in solving the MPY equation. In 1960 Broyles [2] proposed an iterative procedure where an initial trial $g_{ab}^{(o)}(r)$ is inserted in the right-hand side of equation (5.1), the integrations are then performed to give a first-improved trial $g_{ab}^{(1)}(r)$. This can be used to obtain a third trial, and so on. Simple iteration in this fashion did not lead to a convergent sequence and it was found necessary to include a mixing parameter α to secure convergence. Consequently the (n+1)th input was built up using the rule

$$g_{IN}^{(n+1)} = \alpha\, g_{OUT}^{(n)} + (1-\alpha)\, g_{OUT}^{(n-1)} \quad . \quad (5.4)$$

It has been found by Throop and Bearman [3] that the mixing constant α is inversely proportional to the density for LJ fluids, and as the density increases, α decreases,

and hence the rate of convergence becomes appreciably slower. Broyles [2] also pointed out that convergence could be improved if it was assumed that the $g^{(\infty)}$ result is approached exponentially, for then

$$g^{(\infty)} = g^{(j)} + \frac{g^{(j+1)} - g^{(j)}}{1-R} \quad ; \qquad (5.5)$$

where

$$R = \frac{g^{(j+1)} - g^{(j)}}{g^{(j)} - g^{(j-1)}} \quad ,$$

and thus as the solutions approached the final result, the $g^{(\infty)}$ could be predicted.

It is unfortunate that a technique recently proposed by Baxter [4] for the solution of the PY equation does not apply for long-range forces. His method relies on the interparticle potential vanishing beyond some range M, for then the PY equation can be written in a form which depends on the direct correlation function and the radial distribution function over the range (0,M) only. Watts [5] has applied this technique successfully to a Lennard-Jones fluid near the critical region.

In the calculation presented here, the iterative method due to Broyles was used, but several modifications were necessary to obtain convergence, and these will be discussed in the relevant sections. It was decided to initially attempt to solve the MPY equation for a

temperature of 10^{4}°K and density 10^{18}e/cc, and to gradually increase the temperature to obtain results in the region where the DH approximation is valid. The first difficulty is choice of the initial g_{IN} and V_{IN}. It was pointed out in section (5.1) that, by assuming the combined effective potential for like particles was equal to minus the effective potential for unlike particles, the problem is reduced to solving two linked integral equations, and so we chose

$$V_L(r) = V_U(r) = - [\log_{10} (g_{pe}(r))]/\beta, \quad (5.6)$$

where the $\log_{10}(g_{pe}(r))$ are presented in Table 4.1A. Since in Chapter 4 we also determined a distribution function to approximately take into account shielding, it was decided to use those results for g_{IN}, i.e. $\text{Log}_{10} (g_L(r)) = -\text{Log}_{10}(g_U(r)) = -\text{Log}_{10} (g_s(r))$, which can be obtained from Table 4.1B. Thus input will be frequently referred to as the quantum mechanical Debye-Huckel (QMDH) distribution function.

The program in Appendix B does not calculate the distribution function at r=0. To calculate $g_{ab}(0)$ it is necessary to take the limits of the integrals in the MPY equation as r->0, and evaluate the resulting equation

$$g_{ab}(0)\ e_{ab}(0) = 1+4\pi \sum_c n_c \int_o^{LBCUT} [1-e_{ac}(s)]g_{ac}(s)[g_{bc}(s)-1]\, s^2 ds +$$

$$8\pi \sum_c n_c \sum_d n_d \int_o^{LBCUT} (1-e_{ac}(s))g_{ac}(s)[g_{bc}(s)-1]s^2 \int_o^{LBCUT} [1-e_{ad}(u)]\, g_{ad}(u)[g_{bd}(u)-1]u^2 \int_o^{\pi} g_{dc}(w)\, d\theta du ds \,. \qquad (5.7)$$

where $w = (s^2 + u^2 - 2su\cos\theta)^{\frac{1}{2}}$. From this equation it can be seen that the presence of other particles effects the distribution between two particles, even at zero interparticle distance. However, because the effect of the other particles is expected to be small (i.e. the integrals in equation (5.7) are small), it was decided to fix g(0) to the quantal value determined in Chapter IV until the last few iterations. This step should help stabilise the iterative technique. Theoretically of course, g(0) should have no influence on the value of the integrals; however, as $g(\frac{1}{2})$ was obtained as the geometric mean of g(0) and g(1), its value does affect the calculation.

Before commencing a long computer run, extensive hand checks and trial runs to optimize the integration variables were completed. The optimum value chosen

for LACUT, which decides the size of the regions in the integration procedure, was found to be approximately equal to the joining radius mentioned in section 4.4. This means that the regions where the quantal effects become important are treated in greater detail. The mesh ratios chosen for the various regions were determined by accuracy considerations. Graphs of the integral value versus mesh ratio show that the integrals attain a nearly constant value when the mesh ratio becomes sufficiently large. Although it is possible to adopt large mesh ratios for the PY term (TDTM), this is not feasible for the additional MPY term (FDTM) because in this case the five- dimensional integration becomes too time consuming. Thus the choice of the mesh ratios for the regions in FDTM are determined by time limitations. The optimum size of LBCUT for termination of the range of integration has to increase with temperature. This is because it necessarily introduces an error in the calculation of g(r) as r approaches LBCUT, and is consequently chosen to yield accurate values for the integral for $r<3\lambda_D$. Hence LBCUT is of $O(4.\lambda_D)$. Analytical checks for realistic input data proved impossible, though an analytical check for g(r) = const was completed. Several hand

calculations were made for realistic data to confirm that there were no errors in the integration procedure.

The iterative procedure of Broyles was applied to the MPY equation in the form

$$g_u^j(r) = \frac{1 + TDTM + FDTM}{e_u(r)} , \qquad (5.8)$$

where subscript u refers to unlike particles and the superscript j refers to the jth iteration, with a similar equation for like particles. At 10^4°K the iterative process diverged on the second iteration, undergoing extreme fluctuations, especially at small radii. It was further noticed that the sequence of terms in the numerator on the right-hand side of equation (5.8) formed a diverging sequence for small r. This implies that the improved Percus-Yevick equation cannot be applied at this temperature since it forms a diverging sequence. To determine if this was the case at higher temperatures, the temperature was raised in small steps. At 2×10^4°K the iterations also diverge, even if we use a large mixing constant α, and after four iterations $g_L(r) >> 1$, so that FDTM becomes negative, and this results in inadmissible negative distribution functions. At 2.5×10^4°K divergence does not occur until the eighth iteration.

At 3×10^{4}°K several new modifications were introduced to help secure convergence of the iterative procedure. The mixing constant was removed, and a sequence $g^{(IN)}$, $g^{(1)}$, $g^{(2)}$ obtained. From these three values a $g^{(\infty)}$ can be calculated using equation (5.5). This $g^{(\infty)}$ is then used as input to generate another sequence $g^{(IN)}$, $g^{(3)}$, $g^{(4)}$, and another $g^{(\infty)}$ can be determined. In this way it is hoped to obtain a convergent sequence of $g^{(\infty)}$s. However it proved necessary to overcome two difficulties. The first occurs when the R calculated for equation (5.5) is ≈1, for then $g^{(\infty)}$ may become excessively large. This is overcome by testing the values of R obtained, and if $|R-1|$ is less than 0.5 the value of R is replaced by 0.5 (if R is <1), or 1.5 (if R is >1). The second difficulty is that the first $g^{(\infty)}$ calculated seems to overshoot the final $g^{(\infty)}$, and causes the sequence of $g^{(\infty)}$'s to oscillate. This is overcome by using the mixing constant technique to include some of the previous $g^{(\infty)}$; thus a new input $g^{(IN)}$ is obtained from $g_{IN} = \alpha\, g_n^{(\infty)} + (1-\alpha)\, g_{n-1}^{(\infty)}$, where $g_n^{(\infty)}$ is the nth $g^{(\infty)}$ that has been calculated. It is found that the choice $\alpha = \frac{2}{3}$ secures reasonable convergence. A trial run was also made where the input was composed as follows:

$\log(g_{IN}) = \alpha \log(g_n^{(\infty)}) + (1-\alpha) \log(g_{n-1}^{(\infty)})$. This mixing of the logarithmic values improves convergence of the like distribution functions, but has an adverse effect in the unlike case. It does, however, prevent the $g^{(\infty)}$'s obtained from becoming negative, which occasionally occurred for $g_L(r)$ when r is small.

The iterative process proves quite time consuming, one iteration taking approximately 1 hour on the CDC 6400 computer, and for this reason it was decided to move to the temperature of 4×10^4 °K, rather than continue the run at 3×10^4°K, where the results, although convergent for large r values, fluctuated for r<10 Bohr radii, even after 20 iterations. At the higher temperature the iterative technique converges rapidly to give distribution functions identical to four places of decimals after only four iterations. If g(0) is allowed to vary, and not fixed at its quantum mechanical value, this merely alters the results below 5 Bohr radii, and convergence to four decimal places again occurs within four iterations.

By removing the MPY term the program was rearranged to solve the PY equation, and this was applied to a range of temperatures. At 4×10^4°K

convergence to four decimal places was obtained after six iterations. At 3×10^{4}°K however, the PY equation ran into similar, and probably more fundamental difficulties, than the MPY equation. The TDTM became relatively large at small radii, but remained less than unity, and after 36 iterations the $g^{(\infty)}$'s obtained were reasonably consistent. If however this $g^{(\infty)}$ is used as input for the nth iteration, then $g^{(n+1)}$ differs slightly, and $g^{(n+2)}$ differs considerably, although by using equation (5.5) with $g^{(n+1)}$ and $g^{(n+2)}$ a $g^{(\infty)}$ very similar to the $g^{(\infty)}$ used as input is obtained. This means that the final $g^{(\infty)}$ generates a non-convergent sequence on simple iteration. Such behaviour differs from the MPY equation, where the iterations tend to remain fairly stable for large r values, but become erratic at small radii. On further simple iteration of the MPY equation the erratic behaviour at small r gradually effects the whole $g_{ab}(r)$. At temperatures below 3×10^{4}°K, the PY equation produces negative distribution functions. This is a direct result of the inconsistency of the second-order terms when attractive forces are present; for with such forces TDTM is negative, and at these low temperatures the second order TDTM has modulus greater than unity,

and this leads to a negative distribution function. This inconsistency does not occur with the MPY equation, for if TDTM becomes large and negative, FDTM is invariably larger and positive, and so equation (5.8) yields a positive distribution function. However, the divergence of the series 1, TDTM, FDTM soon causes divergence of the iterative technique, and the MPY equation applies over only a slightly greater temperature range than the PY equation.

5.3 Results and discussion

The results obtained by solving the PY and MPY equations for an hydrogenous plasma at 3×10^{4}°K are presented in Table 5.1. They are compared with the initial input data which is labelled QMDH, as it is composed of the Debye-Huckel distribution function at large radii but includes quantal effects at small radii. The QMDH results may contain errors for $r<15$ Bohr radii of less than ±5 in the fourth decimal place, and for $r>15a_o$ they are correct to the fourth decimal place. The PY results are obtained from the final $g^{(\infty)}$ derived from iterations 35 and 36, and only differ from the previous $g^{(\infty)}$ by ±5 in the last figure given in the table. The results of the MPY are similarly obtained, but in this case $g^{(\infty)}$ is derived after only 16 iterations.

It can be seen the errors increase rapidly at small radii, where g(r) can only be given to two decimal places. The results are shown graphically in Fig. 5.1 for like distribution functions, and in Fig. 5.2 for unlike distribution functions.

For 4×10^{4}°K the results are given in Table 5.2 and shown graphically in Figs. 5.3 and 5.4. At this temperature each $g^{(\infty)}$ tabulated is accurate to four decimal places, and further reproduces itself on simple iteration. It will be recalled that the calculation of g(0) was not used in solving the PY equation, and g(0) remained fixed at its quantal value; this particularly proved a stabilizing factor at the lower temperature of 3×10^{4}°K.

It should be noted however, that although the results at 4×10^{4}°K converge to four decimal places, there is an estimated error of approximately ±5 in the fourth decimal place. At small r this is mainly caused by inaccuracies in the evaluation of the integral, especially for the FDTM, where a reasonably small mesh ratio must be used. At larger values of r an error in the fourth decimal figure is caused by the cut-off LBCUT imposed on the integral. At 3×10^{4}°K these errors become quite large at small radii, for in particular FDTM becomes large, and this term is subject

to errors of up to 30%. To improve the accuracy a large mesh ratio is needed in FDTM, and this would involve a considerable increase in computing time.

From Fig. 5.1 it can be seen that the MPY results are very erratic below ten Bohr radii; they become relatively large near the origin, but then fall sharply away at 2-3 Bohr radii, before returning to quite large values at 5 Bohr radii. For $r>10$ the MPY calculation of $g_L(r)$ remains significantly larger than its PY equivalent, a feature which might be predicted from equation (5.8), where as FDTM is always positive the MPY results will invariably be greater than the corresponding PY results. The PY results in turn lie above the QMDH results for $r<150a_o$, but then they gradually fall slightly below the QMDH results. The MPY results, however, remain above the QMDH results for all radii. This means the DH distribution function is between the PY and MPY results for $r>150a_o$, and even allowing for an error of 5 too low in the fourth decimal place in the PY results, this implies g_{QMDH} is surprisingly good. The inclusion of the additional term in the MPY calculation makes an appreciable difference to the distribution functions.

TABLE 5.1

Distribution functions at 3×10^4°K.

	QMDH		PY		MPY	
r	Like	Unlike	Like	Unlike	Like	Unlike
0	3.028×10^{-5}	$3.303\ 10^4$	3.028×10^{-5}	$3.303\ 10^4$	3.52×10^{-3}	$8.49\ 10^4$
1.	2.397×10^{-4}	4.1716×10^3	6.435×10^{-3}	3.508×10^3	$1.51\ 10^{-2}$	$3.98\ 10^3$
2	1.811×10^{-3}	5.5208×10^2	1.587×10^{-2}	5.095×10^2	$1.07\ 10^{-5}$	$5.29\ 10^2$
3	1.174×10^{-2}	8.5173×10	3.638×10^{-2}	8.446×10	$4.84\ 10^{-4}$	$8.41.10$
4	$4.9419.10^{-2}$	2.0235×10	8.000×10^{-2}	2.014×10	$1.40\ 10^{-1}$	$2.00.10$
5	.1130	8.8512	.1397	8.705	.17	8.76
6	.1758	5.6899	.1977	5.600	.19	5.68
7	.2320	4.3112	.2509	4.223	.26	4.290
8	.2828	3.5359	.2997	3.468	.31	3.518
9	.3289	3.0409	.3444	2.986	.36	3.020
10	.3705	2.6990	.3850	2.651	.385	2.679
11	.4081	2.4502	.4207	2.4078	.440	2.432
12	.4432	2.2563	.4570	2.2158	.475	2.243
13	.4740	2.1096	.4885	2.0630	.499	2.092
14	.5022	1.9911	.5143	1.9584	.527	1.975
15	.5280	1.8941	.5400	1.8628	.551	1.879
16	.5515	1.8133	.5628	1.7843	.573	1.800
17	.5731	1.7448	.5834	1.7190	.594	1.734
18	.5931	1.6862	.6047	1.6581	.615	1.672
19	.6115	1.6354	.6216	1.6113	.632	1.627
20	.6285	1.5910	.6372	1.5734	.650	1.591

	QMDH		PY		MPY	
r	Like	Unlike	Like	Unlike	Like	Unlike
25	.6977	1.4334	.7060	1.4160	.7126	1.4315
30	.7477	1.3375	.7535	1.3245	.7588	1.3364
35	.7854	1.2732	.7896	1.2611	.7983	1.2727
40	.8148	1.2273	.8191	1.2217	.8240	1.2270
45	.8382	1.1930	.8410	1.1856	.8475	1.1924
50	.8573	1.1664	.8591	1.1621	.8665	1.1684
60	.8865	1.1281	.8870	1.1220	.8970	1.1308
70	.9076	1.1019	.9087	1.0938	.9162	1.1056
80	.9234	1.0830	.9241	1.0784	.9323	1.0883
90	.9356	1.0688	.9350	1.0654	.9442	1.0755
100	.9453	1.0579	.9457	1.0540	.9540	1.0650
120	.9595	1.0422	.9595	1.0420	.9688	1.0506
140	.9692	1.0318	.9692	1.0310	.9805	1.0400
160	.9761	1.0245	.9759	1.0229	.9870	1.0341
180	.9812	1.0191	.9809	1.0180	.9891	1.0276
200	.9851	1.0152	.9846	1.0147	.9899	1.0201
220	.9880	1.0121	.9874	1.0114	.9926	1.0143
240	.9903	1.0098	.9913	1.0093	.9925	1.0110
260	.9921	1.0080	.9914	1.0078	.9933	1.0092
280	.9935	1.0065	.9933	1.0059	.9944	1.0070
300	.9947	1.0054	.9944	1.0047	.9953	1.0059

	QMDH		PY		MPY	
r	Like	Unlike	Like	Unlike	Like	Unlike
340	.9963	1.0037	.9960	1.0033	.9966	1.0040
380	.9974	1.0026	.9972	1.0022	.9976	1.0029
420	.9982	1.0018	.9984	1.0011	.9981	1.0021
460	.9987	1.0013	.9986	1.0012	.9996	1.0011
500	.9991	1.0009	.9988	1.0009	1.0002	1.0012
540	.9993	1.0007	.9992	1.0004	.9994	1.0006
580	.9995	1.0005	.9996	1.0001	.9996	1.0005
620	.9997	1.0004	.9996	1.0002	.9998	1.0006
660	.9997	1.0003	1.000	.9997	1.0001	1.0011
700	.9998	1.0002	.9998	1.000	.9993	1.0013
740	.9999	1.0001	.9995	1.0004	1.0007	1.0015

(Notes Errors came in MPY about 500)

TABLE 5.2

Distribution functions at 4×10^4°K

	QMDH		PY		MPY	
r	Like	Unlike	Like	Unlike	Like	Unlike
0	$1.730\ 10^{-4}$	5.7811×10^{3}	1.730×10^{-4}	5.7811×10^{3}	$6.440\ 10^{-4}$	$5.645\ 10^{3}$
1	1.3274×10^{-3}	7.5337×10^{2}	2.7907×10^{-3}	7.5199×10^{2}	$2.906\ 10^{-3}$	$7.637\ 10^{2}$
2	9.3755×10^{-3}	1.0666×10^{2}	1.2521×10^{-2}	1.0911×10^{2}	$1.2056\ 10^{-2}$	$1.104\ 10^{2}$
3	4.7097×10^{-2}	2.1233×10	5.3919×10^{-2}	2.0596×10	$5.456\ 10^{-2}$	$2.067\ 10$
4	1.2531×10^{-1}	7.9800	0.1298	8.0012	.1304	8.0186
5	0.2058	4.8585	0.2103	4.8385	.2111	4.8490
6	0.2749	3.6375	0.2793	3.6158	.2780	3.6219
7	0.3347	2.9875	0.3392	2.9661	.3399	2.9708
8	0.3878	2.5787	0.3914	2.5654	.3922	2.5694
9	0.4325	2.3121	0.4369	2.2950	.4377	2.2985
10	0.4734	2.1125	0.4762	2.1038	.4770	2.1069
11	0.5086	1.9661	0.5112	1.9583	.5122	1.9613
12	0.5399	1.8523	0.5425	1.8447	.5436	1.8477
13	0.5678	1.7612	0.5703	1.7540	.5713	1.7566
14	0.5929	1.6866	0.5952	1.6802	.5962	1.6826
15	0.6156	1.6244	0.6178	1.6184	.6188	1.6207
16	0.6361	1.5721	0.6382	1.5663	.6392	1.5685
17	0.6548	1.5273	0.6567	1.5219	.6577	1.5240
18	0.6718	1.4885	0.6740	1.4829	.6750	1.4850
19	0.6874	1.4547	0.6893	1.4496	.6905	1.4517
20	0.7018	1.4250	0.7035	1.4201	.7047	1.4223

	DH		PY		MPY	
r	Like	Unlike	Like	Unlike	Like	Unlike
25	0.7590	1.3175	0.7607	1.3130	.7620	1.3149
30	0.7996	1.2506	0.8008	1.2471	.8020	1.2489
35	0.8298	1.2051	0.8307	1.2023	.8319	1.2039
40	0.8531	1.1772	0.8538	1.1697	.8550	1.1713
45	0.8716	1.1473	0.8722	1.1449	.8735	1.1465
50	0.8866	1.1279	0.8869	1.1261	.8881	1.1276
60	0.9093	1.0997	0.9092	1.0985	.9105	1.1000
70	0.9257	1.0802	0.9256	1.0791	.9268	1.0805
80	0.9380	1.0660	0.9381	1.0647	.9394	1.0662
90	0.9476	1.0553	0.9475	1.0542	.9488	1.0557
100	0.9551	1.0470	0.9550	1.0459	.9564	1.0474
110	0.9612	1.0403	0.9609	1.0396	.9623	1.0411
120	0.9663	1.0349	0.9658	1.0344	.9672	1.0359
130	0.97044	1.0305	0.9700	1.0299	.9715	1.0315
140	0.9739	1.0267	0.9737	1.0260	.9752	1.0276
150	0.9769	1.0236	0.9767	1.0230	.9782	1.0246
170	0.9817	1.0186	0.9814	1.0182	.9830	1.0199
190	0.9853	1.0149	0.9848	1.0147	.9867	1.0166
210	0.9880	1.0121	0.9878	1.0117	.9896	1.0135
230	0.9902	1.0099	0.9899	1.0095	.9914	1.0111
250	0.9919	1.0082	0.9915	1.0080	.9926	1.0091
350	0.9966	1.0034	0.9963	1.0034	.9966	1.0037

r	DH Like	DH Unlike	PY Like	PY Unlike	MPY Like	MPY Unlike
450	0.9985	1.0015	0.9981	1.0016	.9983	1.0017
550	0.9993	1.0007	0.9989	1.0019	.9990	1.0010
650	0.9996	1.0004	0.9994	1.0015	.9994	1.0006
750	0.9998	1.0002	0.9997	1.0002	.9997	1.0003
850	0.9999	1.0001	0.9996	1.0003	.9997	1.0004
950	1.0000	1.0000	0.9998	1.0002	.9999	1.0003

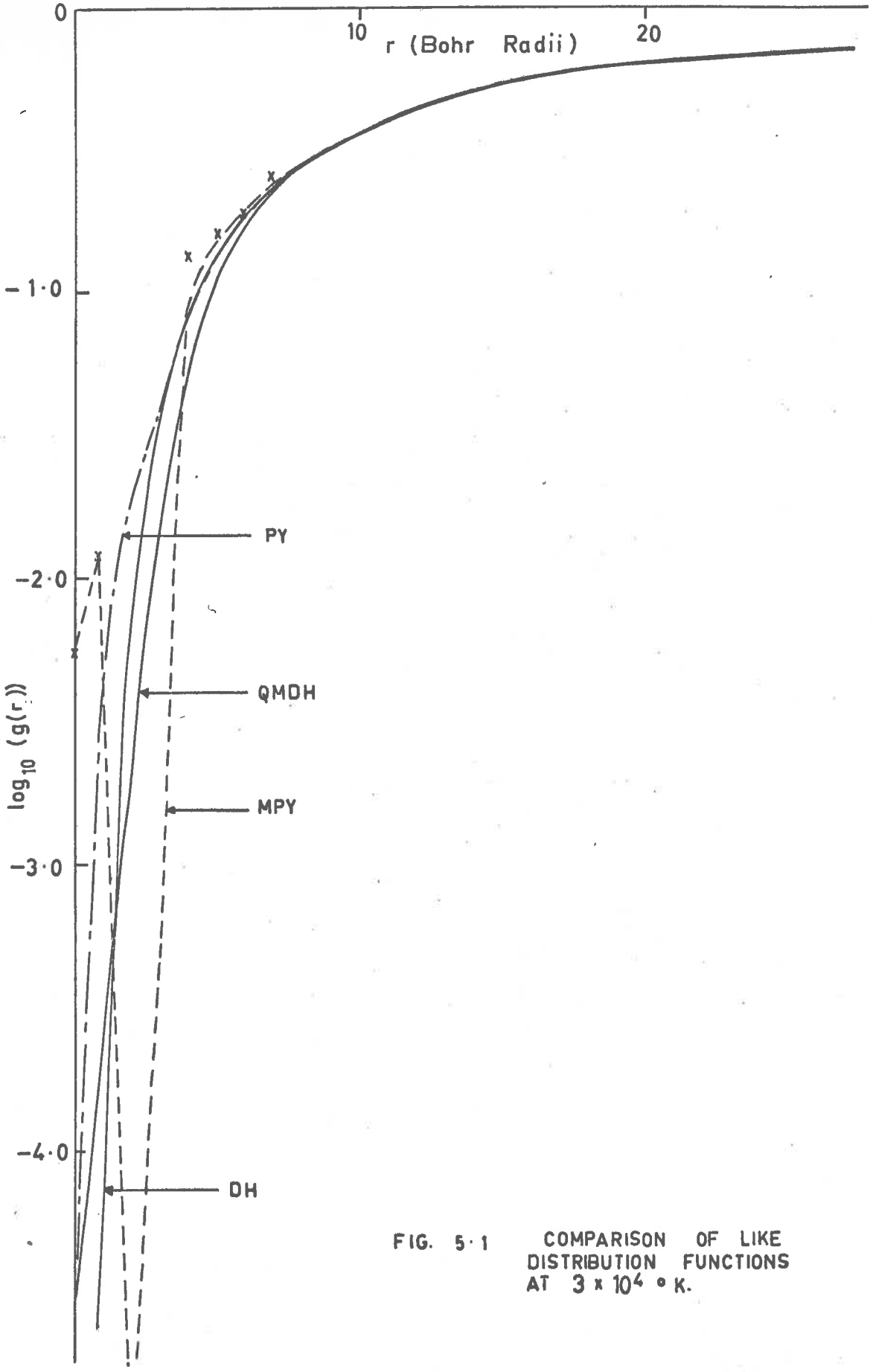

FIG. 5·1 COMPARISON OF LIKE DISTRIBUTION FUNCTIONS AT 3×10^4 °K.

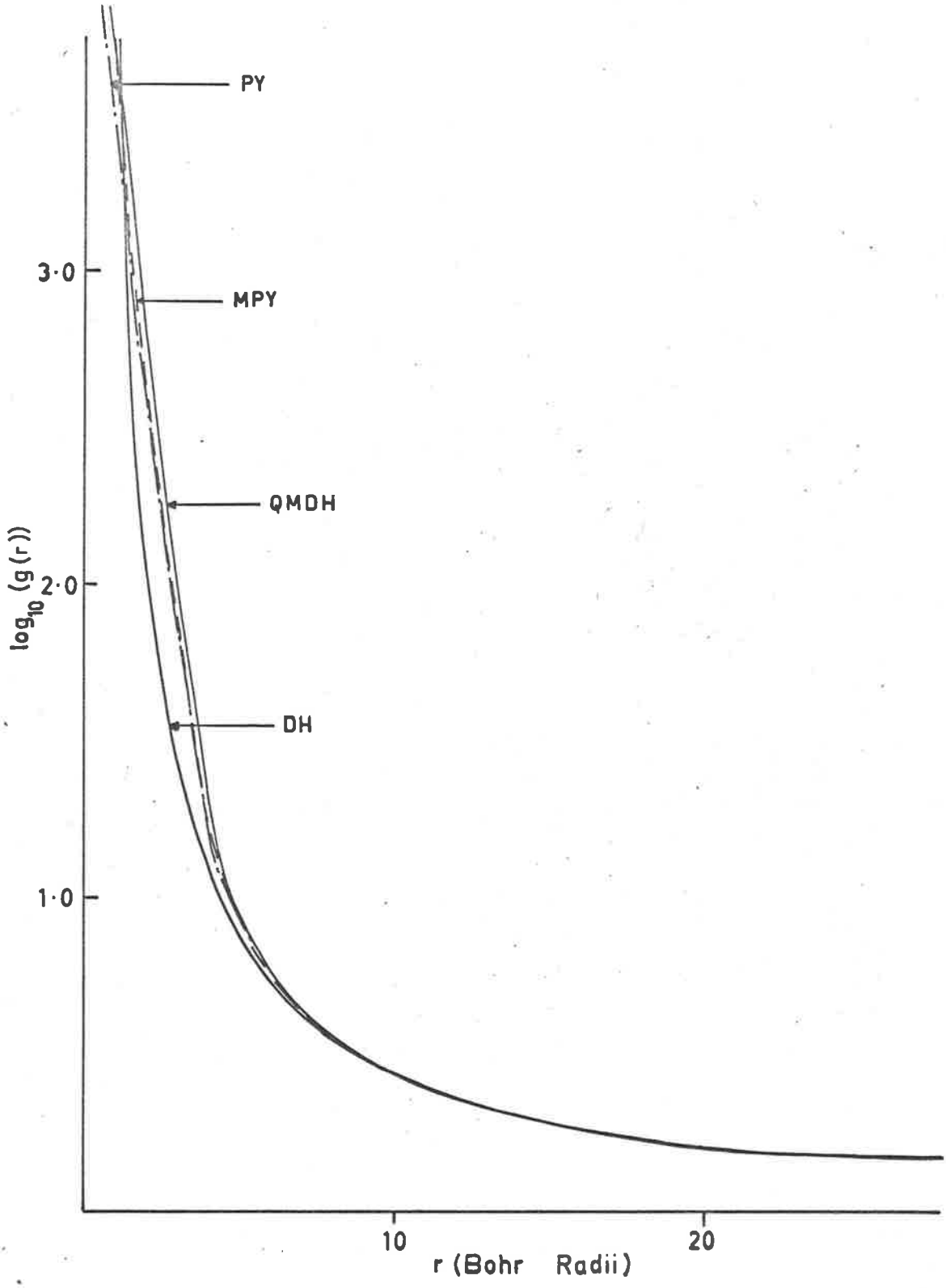

FIG. 5·2 COMPARISON OF UNLIKE DISTRIBUTION FUNCTIONS AT 3×10^4

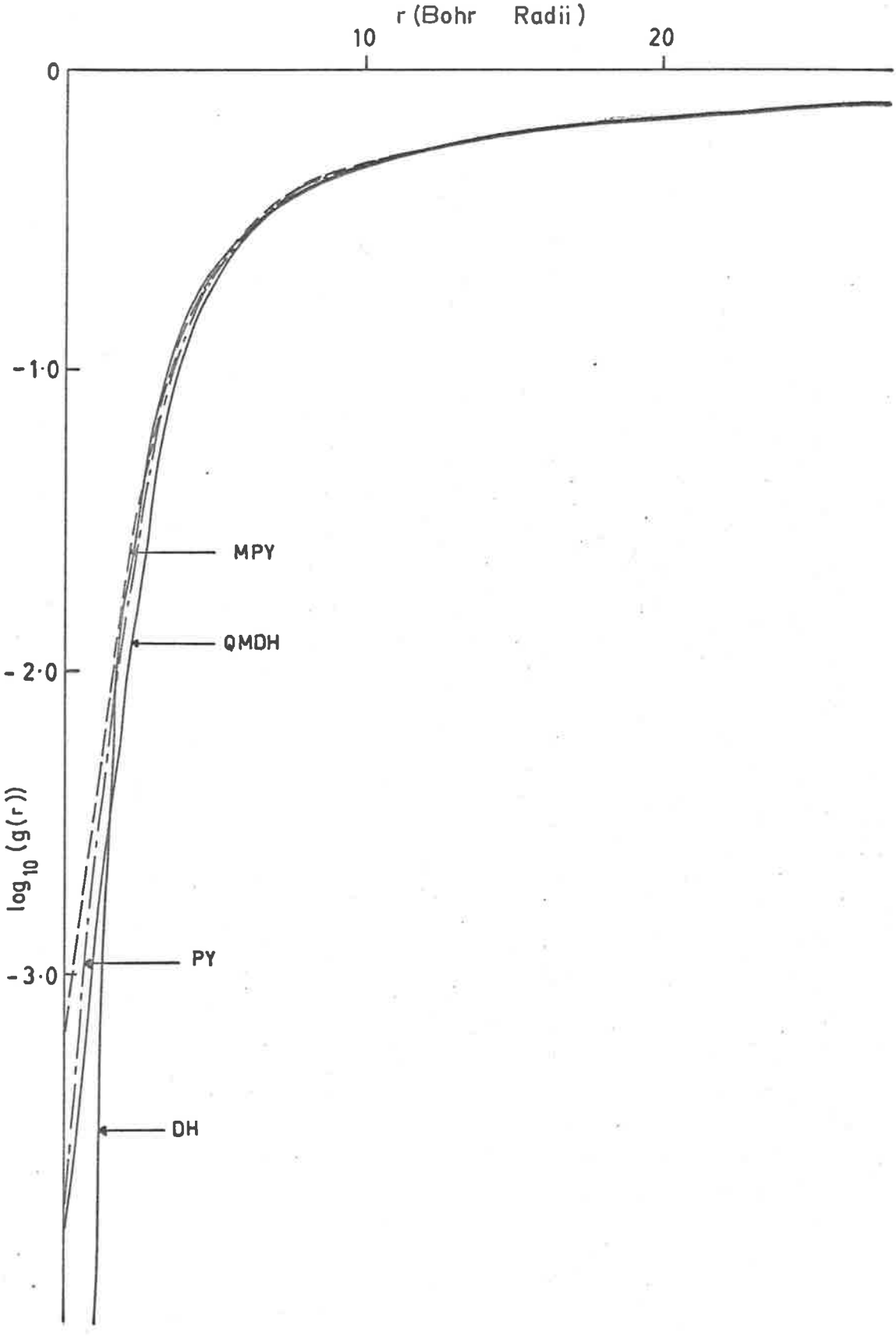

FIG. 5·3 COMPARISON OF LIKE DISTRIBUTION FUNCTIONS AT 4×10^4 °K.

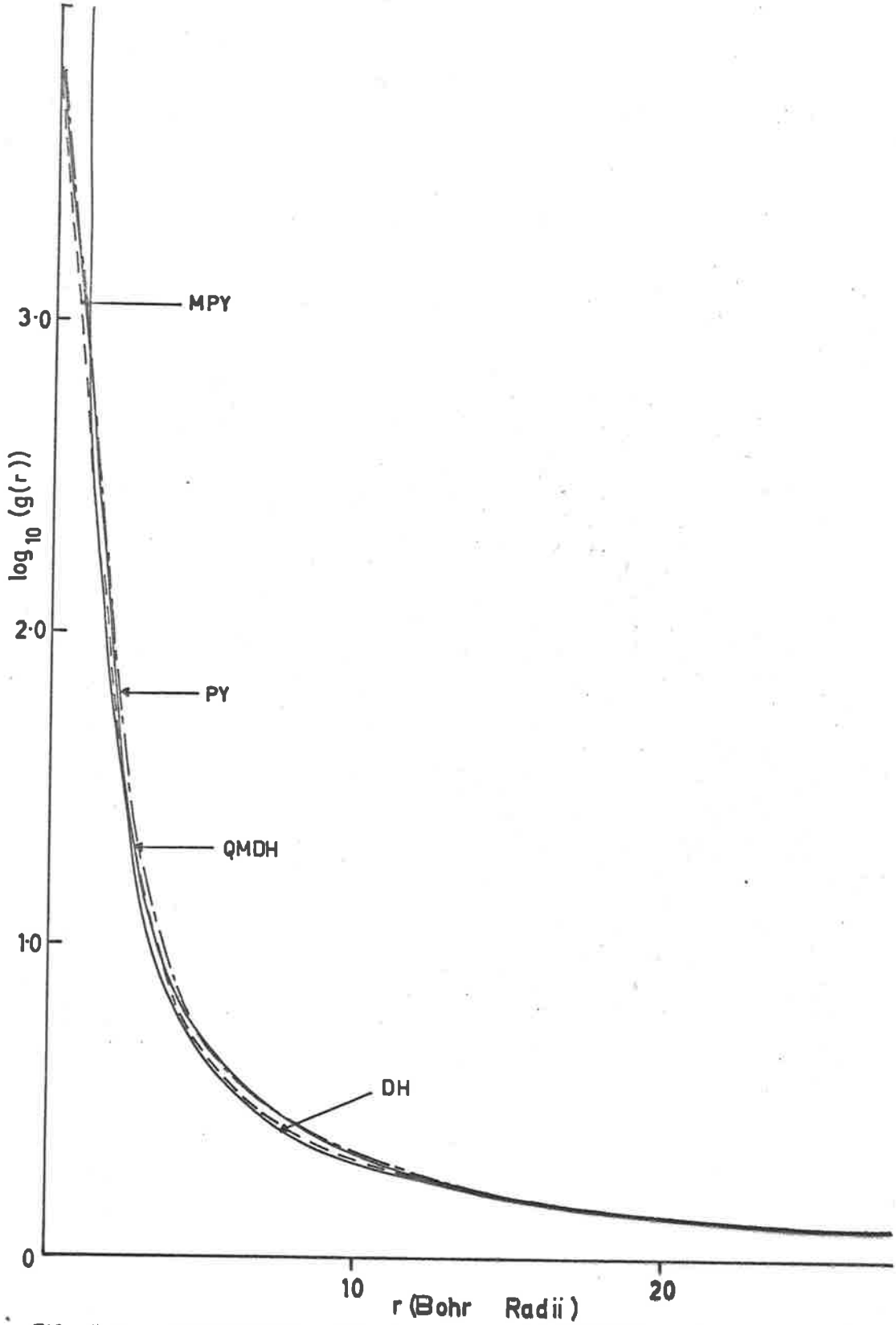

FIG. 5·4 COMPARISON OF UNLIKE DISTRIBUTION FUNCTIONS AT 4×10^4 °K

In Fig. 5.2 (and Table 5.1) for the unlike distribution functions it can be seen that the PY results lie well below the QMDH results. The MPY equation, which should improve on the PY results, lies quite close to the QMDH results, lying below them for $r<50a_o$, except for g(0), and then remaining slightly above them for large r.

An almost identical analysis occurs for the three sets of results given in Table 5.2 at 4×10^4°K. For the like case the PY results remain above the QMDH results for $r<80a_o$, and the MPY results lie above them. Beyond $r = 80a_o$ the QMDH values lie between the MPY and PY values. In the unlike case the PY results remain below the QMDH results, while the MPY results remain smaller for $r<50a_o$, but beyond that become greater than the QMDH results.

Perhaps the most significant feature of the results is the fairly large increase in the value of $g_L(r)$ indicated at small radii. In the Monte Carlo results obtained at 10^4°K it was noted that the peak in $g_L(r)$ at small r was probably due to collisions between ions and pairs. At the higher temperature of 3×10^4°K the quantum mechanical results indicated that the plasma was approximately 90% ionized, and hence there is still a

reasonable chance of a collision between an ion and a pair. As the temperature is lowered the number of pairs increases, at the same time the PY and MPY results start to diverge, which indicates that it is again the formation of pairs which causes the difficulties. However, in the integral equation approach this divergence appears in the following manner. Firstly $g_L(r)$ increases sharply for small r in the evaluation of $g_L^{(1)}(r)$, then on using $g_L^{(1)}(r)$ as input this causes $g_u^{(2)}(r)$ to increase sharply at small r, this in turn increases $g_L^{(3)}(r)$, and the series diverges unless extrapolated back to $g^{(\infty)}$. This difficulty is also associated with the concept of the combined effective potential $V_L = -V_U$, which was introduced in order to reduce the number of linked integral equations in the MPY equation. For the divergence, which initially starts in $g_L(r)$, is very closely connected with the V_L chosen. From such considerations it appears that to rigorously improve upon the results presented at 3×10^{4}°K or to proceed to lower temperatures it is necessary to treat the e-e and p-p interactions separately. In such a procedure the quantal V_{pp} needs to be accurately determined, and for completeness quantum statistical effects should be included in the

calculation of V_{ee}.

In conclusion then the Percus-Yevick integral equation approach can be successfully applied to plasmas when the second order terms remain small, and this occurs when the plasma is fully ionized. The inclusion of higher order terms, as in the MPY equation, alters the results appreciably. However the solution to this equation also becomes unstable as the pairing present in the plasma becomes significant. To extend the region of applicability of the MPY equation it is necessary to obtain accurate quantal effective potentials between the particles, and to solve three linked integral equations. At temperatures above the ionization temperature the method yields accurate distribution functions within a few iterations. The distribution functions obtained for an hydrogenous plasma of 10^{18}e/cc at 3×10^{4}°K are remarkably similar to those obtained by the DH theory, except at small radii.

References to Chapter V

[1] Green, H.S. (1965) Phys. Fluids 8, 1.

[2] Broyles, A.A. (1960) J. Chem. Phys. 33, 456.

[3] Throop, G.J. and Bearman, R.J. (1966) J. Chem. Phys. 44, 1423.

[4] Baxter, R.J. (1967) Phys. Rev. 154, 170.

[5] Watts, R.O. (1968) J. Chem. Phys. 48, 50.

VI CONCLUSION

6.1 Comparison of the two methods

It is unfortunate that the main MC results were obtained for the temperature of 10^4°K, for it was subsequently found that the PY and MPY equations could not be applied at this temperature, and a direct comparison of results became impossible. Another difference in the calculations is that the MC computations were made by taking quantal effects into account only in a rather crude manner, whereas such effects were treated more exactly in the PY and MPY calculations. For these reasons only a broad comparison of the two methods is made, and conclusions pertinent to the presented results are contained in section 6.2. The MC approach has the advantage that the derivation of the method is relatively free of assumptions compared to the PY approach. However, the MC method also exhibits its usual disadvantage, namely, that calculations of accurate distribution functions are very time consuming; and in this temperature range the presence of long-range forces in conjunction with pairing of unlike charges aggravates this situation. On the other hand, while the PY equation can be solved numerically reasonably quickly, to obtain accurate distribution functions; when higher order terms are included to obtain

an improved equation (i.e. MPY), this approach also becomes very time consuming. The improved accuracy of the results is perhaps the main advantage.

6.2 Conclusion

In this work we have applied two of the well-established liquid theories, the Monte Carlo (MC) method and the Percus-Yevick (PY) equation, to a dense hydrogeneous plasma ($n_e = 10^{18}$e/cc) near the ionization temperature. The MC method was applied at 10^4°K, and extensive results of these calculations are presented in the Tables and Figures in Chapter II. From these results it was concluded that quantum mechanical considerations are important at small radii for this temperature, and the cut-off AO used with the Coulomb potential should be replaced by an accurate quantal effective potential at small radii. The results also indicated that the maximum step length Δ used in the MC procedure must be carefully chosen when considering the temperature range corresponding to the transition from the neutral gas to the ionized plasma. For in this region the plasma appears to behave as a mixture of two phases, with the choice of Δ determining which phase dominates in the relatively small sample of configurations selected by the MC procedure.

The initial application of the PY equation, in an asymptotic form for large r, indicated that the PY equation can be successfully applied to systems composed of particles with repulsive interactions at short distances. However, if attractive forces are present, an inconsistency arises in the asymptotic equation. This inconsistency is removed by considering additional terms to the equation such as those suggested by Green. The resulting equation has been termed a modified Percus-Yevick equation (MPY). Further initial investigations into solving the MPY equation for a two-component plasma showed that the integrations involved were highly sensitive to the form of the interparticle potentials and inter-particle distribution functions at small radii. To obtain such accurate two-particle potentials and distribution functions for an hydrogenous plasma it is necessary to include quantal effects. Then, by using accurate two particle potentials in the MPY equation, it should be possible to obtain accurate distribution functions for the many particle system.

The calculation of accurate quantum mechanical two-particle distribution functions has been presented in detail in Chapter IV. The expression obtained for the two-particle distribution function, equation (4.4),

takes the important Heisenberg effect into account, but neglects the smaller quantal effect due to statistics. The computer program written to evaluate (4.4) is listed in Appendix B, and proves extremely efficient for calculations of g_{pe} and g_{ee} over a range of temperatures. However in the p-p case the large increase in the reduced mass of the two-particle system causes computational difficulties, and this particular program is inapplicable. Fortunately the semi-classical WKB approximation may be used there. The quantal calculations of g_{ee} and g_{ep} are presented for the range of temperatures 10^{4}°K to 5×10^{4}°K. Because of the convenient form of equation (4.4), the computer program gives the first bound-state contribution, the number of bound states contributing to $g_{ep}(r)$ to obtain a fixed accuracy, and the total bound-state contribution for that accuracy. It also calculates the percentage ionization present, and the radius, r_J, below which quantal effects become important. The program is further easily modified to include shielding effects in an approximate manner, and hence indicates the form of the distribution function for a many-particle system.

The quantal results show that there are rather large deviations from the classical theory at short

interparticle distances, and that below r_J quantum mechanical effects become important, especially at low temperatures. The approximate allowance for shielding in the calculation of $g_s(r)$ indicates the results are qualitatively the same for this case, but at large radii $g_s(r)$ merges with the Debye-Huckel $g_{DH}(r)$, in contrast to the two-particle $g_{pe}(r)$ case, which merges with the classical $g_c(r)$. The inclusion of shielding also slightly increases the degree of ionization present, which is to be expected, as the shielding precludes some of the bound states. Nevertheless the results showed that either by fully taking account of the bound states, or by attempting to allow for shielding, the degree of ionization was surprisingly close to the values obtained by Saha. Also, the results indicate that there is some justification for considering the first bound state to provide the major portion of the total bound state contribution, especially at temperatures below 3×10^{4}°K.

The accurate two-particle $g_{pe}(r)$, and an associated effective potential $V_{pe}(r)$, were then used as input to the MPY equation. In order to reduce the computer program to a feasible size the input data used for the combined effective potential between like particles was taken to be the reflection of the interparticle potential between unlike particles. This procedure

also avoided the need for a separate calculation of $V_{pp}(r)$.

It was found that the PY and MPY equations could both not be solved at low temperatures, where the integrations on the right-hand side of each of the equations formed a divergent series for small r. In the PY case this also led to negative distribution functions due to the inconsistency of the second-order terms. At temperatures above 3×10^4 it became possible to obtain solutions to both the PY and MPY equations by employing the iteration technique described in Chapter V. Accurate results are presented for 4×10^4°K and somewhat less accurate figures for 3×10^4°K. These results show that the $g_s(r)$ characteristic, obtained by including a Debye-Huckel shielding factor in the two-particle quantal calculation, lies between the PY and MPY curves in the like case for large r. The MPY results are always larger than the PY results.

A close analysis of the divergence in the integrations on the right-hand side of the MPY, showed that it was physically related to the formation of pairs in the plasma. To proceed to lower temperatures it would be necessary to solve three linked integral equations for g_{ee}, g_{pp} and g_{pe}. Further, it would appear desirable

to include quantum statistical effects for the e-e interactions. Because of the sensitive dependence of the integral-equation procedure to the initial input at the low temperatures, in the future it may be preferable to obtain input data by extrapolation of solution at higher temperatures.

In conclusion, both the integral equation approach and the MC method encounter difficulties as the plasma becomes only partially ionized. At temperatures in the region of the ionization temperature, quantal effects play an important role, and should be incorporated into both approaches in a rigorous fashion. For temperatures just below the ionization temperature, indications are that it will be necessary to include three-body interactions. For temperatures above the ionization temperature, and allowing for quantum effects, the PY equation yields approximate distribution functions very economically. They can be improved by solving the MPY equation, as demonstrated in Chapter V.

APPENDIX A

The articles in this appendix were published by the author during the course of this work.

Barker, A. A. (1965). Monte Carlo calculations of the radial distribution functions for a proton-electron plasma. *Australian Journal of Physics 18*(2), 119-134.

On the Percus-Yevick Equation

A. A. BARKER

Reprinted from
THE PHYSICS OF FLUIDS
Volume 9, Number 8, August 1966

On the Percus–Yevick Equation

A. A. Barker
University of Adelaide, Adelaide, South Australia
(Received 10 September 1965; final manuscript received 14 February 1966)

The range of application of the Percus–Yevick equation is analysed using an asymptotic form of the equation. The inconsistencies arising for mixtures of repulsive and attractive forces are removed by considering additional terms to the equation, but the equation still assumes an inconsistent form for many systems of attractive forces.

I. INTRODUCTION

SINCE Percus and Yevick[1] put forward their integral equation to determine radial distribution functions $g_{ab}(r)$ between particles of type a and b, it has been applied very successfully to fluids, i.e., Broyles,[2] and has been extended by Carley[3] to a classical electron gas. However, in trying to apply the equation to a proton–electron plasma, we have found that the equation, to second order in $\phi_{ab}(r)$ (the interparticle potential between particles of type "a" and "b" at a distance "r" apart), can have no asymptotic solution unless additional terms are considered. It is the purpose of this paper to first show how the inconsistency arises, and secondly, subject to various assumptions, to show that the associated difficulties may be overcome if terms suggested by Green[4] are included.

II. AN ASYMPTOTIC FORM OF THE PERCUS–YEVICK EQUATION

The Percus–Yevick equation, generalized for a fluid mixture, has the form

$$g_{ab}e_{ab} = 1 - \sum_c n_c \int (e_{ac} - 1)g_{ac}(g_{bc} - 1)\, d^3x_c, \quad (1)$$

where

$$e_{ab} = \exp(\beta\phi_{ab}),$$

which can be written

$$g_{ab}(r)e_{ab}(r) = 1 - \frac{2\pi}{r}\sum_c n_c \int_0^\infty \int_{|s-r|}^{s+r} [e_{ac}(s) - 1] \cdot g_{ac}(s)[g_{bc}(t) - 1]t\, dt\, s\, ds, \quad (2)$$

where n_c is the number density of particles of type c per unit volume, $\sum_c$ sums over all types of particles in the mixture, and d^3x_c ranges over the volume of particles of the cth type. Broyles[5] rewrote this equation in a form

$$\frac{d}{dr}[rg_{ab}(r)e_{ab}(r)] - 1 = 2\pi \sum_c n_c \int_{-\infty}^{\infty} (s + r)g_{ac}(|s|) \cdot [g_{bc}(|s + r| - 1)][1 - e_{ac}(s)]s\, ds, \quad (3)$$

which is much easier to handle computationally.

To obtain an asymptotic form of the equation for large r, we make the following assumptions: (i) That $\beta\phi_{ab}(r)$ is $O(r^{-n})$ for large r, and for attractive forces it is finite for small r. This assumption excludes gravitational forces, and requires a cutoff at small r for Coulomb forces. It implies that we can express $g_{ab}(r) = 1 + \epsilon_{ab}(r)$, where $\epsilon_{ab}(r)$ will be finite for small r, and will be small for large r; and without it statistical mechanics is probably impossible. (ii) That $\epsilon_{ab}(r)r^m \to 0$ for large r for all m, at any rate for sufficiently small m. (iii) That $|\int_0^\infty \epsilon_{\text{attractive}}(r)\, dr| > |\int_0^\infty \epsilon_{\text{repulsive}}(r)\, dr|$ for mixtures, which in a plasma is a consequence of screening between particles.

Now by assumption (i) we can expand in powers of ϕ for large r, and with retention of terms involving only small powers of ϕ, Eq. (2) becomes

$$[1 + \epsilon_{ab}(r)][1 + \beta\phi_{ab}(r) + \tfrac{1}{2}\beta^2\phi_{ab}^2(r) + \cdots] = 1 + \frac{2\pi}{r}\sum_c n_c \int_0^\infty [1 - e_{ac}(s)][1 + \epsilon_{ac}(s)] \cdot \int_{|s-r|}^{s+r} \epsilon_{bc}(t)t\, dt\, s\, ds \cdots . \quad (4)$$

Changing the variable to $y = s - r$, and neglecting $\epsilon_{ab}(r)$ by assumptions (i) and (ii), Eq. (4) reduces to

$$\beta\phi_{ab}(r) + \tfrac{1}{2}\beta^2\phi_{ab}^2(r) + \cdots = \frac{2\pi}{r}\sum_c n_c \int_{-r}^{\infty} [1 - e_{ac}(y + r)][1 + \epsilon_{ac}(y + r)] \cdot \int_{|y|}^{y+2r} \epsilon_{bc}(t)t\, dt\, (y + r)\, dy \cdots . \quad (5)$$

[1] J. K. Percus and G. J. Yevick, Phys. Rev. 110, 1 (1958).
[2] A. A. Broyles, J. Chem. Phys. 37, 2462 (1962).
[3] D. D. Carley, Phys. Rev. 131, 1406 (1963).
[4] H. S. Green, Phys. Fluids 8, 1 (1965).
[5] A. A. Broyles, J. Chem. Phys. 33, 1068 (1961).

Using assumption (ii) it can be seen that the most important contributions to the right-hand side integral in Eq. (5) arise when y is small, and hence, a cutoff parameter "a" is introduced, where $a < r$ for large r, beyond which contributions to the integral are assumed negligible. Further by assumption (i) the right-hand side is finite, and since r is large and y small, $\epsilon_{ac}(y + r)$ can neglected; so the right-hand side can be expanded in powers of $\phi(y + r)$, to give

$$\beta\phi_{ab}(r) + \tfrac{1}{2}\beta^2\phi_{ab}^2(r) + \cdots$$

$$= 2\pi \sum_c n_c \int_{-a}^{a} [-\beta\phi_{ac}(y+r) - \tfrac{1}{2}\beta^2\phi_{ac}^2(y+r) \cdots] \cdot\left(\frac{y+r}{r}\right) \int_{|y|}^{y+2r} \epsilon_{bc}(t)\, t\, dt\, dy. \quad (6)$$

As there are no general existence theorems for solutions of nonlinear integral equations, even if we obtain agreement in Eq. (6), we cannot be sure an exact solution to Eq. (2) exists. However, if we are able to satisfy the asymptotic equation (6) there may exist a solution to Eq. (2), whereas if (6) has no solution, no exact solution of (2) can exist.

For a system of particles involving attractive forces only, it is evident from Eq. (6) that a solution is impossible, since ϕ_{ac} will always be negative. Also, $\int_{|y|}^{y+2r} \epsilon_{\text{attractive}}(t)\, dt$ is positive for small y by physical considerations, and ϕ_{ab} is negative. Thus, to first order the left-hand side is negative, while the right-hand side is positive; and to second order the left-hand side is positive, while the right-hand side is negative, both orders being mathematically inconsistent. However, by applying the above reasoning to a system of repulsive forces only, we see that ϕ_{ac} becomes positive, while $\int_{|y|}^{y+2r} \epsilon_{bc}(t)\, dt$ becomes negative; so now both first- and second-order agreement in ϕ can be obtained. For a system of mixed forces, several cases arise, for ϕ_{ab} can now be positive or negative, and if ϕ_{ab} is positive, so a particle "a" repels a particle "b," then particle "a" can attract a particle "c" while particle "b" may repel particle "c." (See Table I.) Because many of these cases are unphysical, this paper will be concerned with mixtures of charged particles. Then, if particle "a" repels particle "b" and attracts particle "c," particle "b" will attract particle "c" also. For these charged particle mixtures, first-order agreement follows by the same reasoning as above, but second-order considerations lead to disagreement—on using assumption (iii).

For a Lennard–Jones type of interparticle potential, which is repulsive at short distances, and falls off rapidly, the Percus–Yevick equation applies well, and, in addition to a solution to Eq. (6) being possible, a solution to Eq. (2) has been found. However, for mixed Coulomb interparticle potentials an exact solution is clearly not possible as there is an inconsistency in the second-order terms of Eq. (6).

TABLE I. Summary of the consistency of Eq. (6) for various cases.

Type of force present	Order in ϕ_{ac}	Whether asymptotic Eq. (6) is consistent to this order
Attractive only	First	No
	Second	No
Repulsive only	First	Yes
	Second	Yes
Mixtures (of charges)	First	Yes
	Second	No

III. ADDITIONAL TERMS FOR MIXED FORCES

Green[4] has proposed an integral equation which, compared with the Percus–Yevick equation, contains additional terms. As each term can be expressed in powers of $\phi_{ab}(r)$, which have been assumed to fall off with r, only the first additional term will be considered. The equation for the radial distribution function now becomes

$$g_{ab}e_{ab} = 1 + \sum_c n_c \int (g_{bc} - 1)g_{ac}(1 - e_{ac})\, d^3x_c + \tfrac{1}{2} \sum_c n_c \sum_d n_d \iint (g_{bc} - 1)(g_{bd} - 1)g_{cd}g_{ac}g_{ad} \cdot(1 - e_{ac})(1 - e_{ad})\, d^3x_c\, d^3x_d. \quad (7)$$

Rewriting the "last term" above in terms of interparticle distances, with the same notation as in Eq. (2), we obtain

$$\frac{2\pi}{r^2} \sum_c n_c \sum_d n_d \int_0^\infty \int_0^\infty \int_{|r-s|}^{(r+s)} \int_{|r-u|}^{(r+u)} \cdot\int_0^\pi [g_{bc}(t) - 1][g_{bd}(v) - 1]g_{ac}(s)g_{ad}(u)[1 - e_{ac}(s)] \cdot[1 - e_{ad}(u)]g_{dc}(w)\, d\theta\, v\, dv\, t\, dt\, u\, du\, s\, ds,$$

where

$$2r^2w^2 = 2r^2(s^2 + u^2) - (u^2 + r^2 - v^2)(r^2 + s^2 - t^2) + [4r^2s^2 - (r^2 + s^2 - t^2)^2]^{\frac{1}{2}} \cdot[4r^2u^2 - (r^2 + u^2 - v^2)^2]^{\frac{1}{2}} \cos\theta.$$

If this term is treated in a manner analogous to that adopted in the previous case, an expansion in terms of $\phi(r)$ reduces, for large r, to the following form:

$$2\pi \sum_c n_c \sum_d n_d \int_{-a}^{a} [\beta\phi_{ac}(p+r)\cdots](1+p/r)$$

$$\cdot \int_{-a}^{a} [\beta\phi_{ad}(q+r)\cdots](1+q/r) \int_{|p|}^{p+2r} \epsilon_{bc}(t) \int_{|q|}^{q+2r} \epsilon_{bd}(v)$$

$$\cdot \int_{0}^{\pi} [1+\epsilon_{dc}(w)]\, d\theta\, v\, dv\, t\, dt\, dq\, dp,$$

where

$$w^2 = t^2 + v^2 - 2pq + 2(t^2 - p^2)^{\frac{1}{2}}(v^2 - q^2)^{\frac{1}{2}} \cos\theta.$$

When this term is added to the second-order term of the Percus–Yevick equation, it makes the asymptotic equation consistent to second order for charged particle mixtures, by adopting arguments analogous to those used previously.

IV. CONCLUDING REMARKS

The Percus–Yevick equation can be successfully applied to systems composed of particles with repulsive interactions at short distances. However, if attractive forces are present, for the existence of an asymptotic solution it is necessary that corrections of the type suggested by Green should be included. The main disadvantage of this additional term is that the equation can no longer be expressed in the convenient form of (3), and so computational solution of the equation will be correspondingly more difficult. In the future the author hopes to publish computed radial distribution functions for a proton–electron plasma for various densities and temperatures.

ACKNOWLEDGMENTS

The author is indebted to Professor H. S. Green for many constructive discussions on the above material and to Dr. P. W. Seymour for his useful comments.

Barker, A. A. (1968). A quantum mechanical calculation of the radial distribution function for a plasma. *Australian Journal of Physics, 21*(2), 121-128.

Monte Carlo Study of a Hydrogenous Plasma near the Ionization Temperature

A. A. Barker

Department of Mathematical Physics, University of Adelaide, Adelaide 5000, South Australia

(Received 18 December 1967)

Results of a recent Monte Carlo study of a hydrogenous plasma near the ionization temperature show that distribution functions obtained are unusually sensitive to two parameters. The first is the cutoff imposed at small radii on the Coulomb potential between unlike particles, and it becomes necessary to consider quantum-mechanical effects at these radii. The second is the maximum step length Δ through which the particles are allowed to move in the Monte Carlo procedure. It appears that near the ionization temperature the plasma behaves as a mixture of two phases, one ionized, the other un-ionized, and the magnitude chosen for Δ influences which phase dominates.

THE problem of obtaining distribution functions for long-range forces has been considered by Broyles, Sahlin, and Carley,[1] and Carley[2] has extended the theory to a classical electron gas. Subsequently, a Monte Carlo (MC) study of a one-component plasma has been completed by Brush, Sahlin, and Teller.[3] In this paper the author presents the results of extending the MC procedure, described in detail by Barker,[4] to a two-component plasma, and particularly considers temperatures in the region where ionization occurs. This region is of considerable interest, but is also the most difficult to deal with from the mathematical standpoint. It is found that for a plasma of density $10^{18}e$/cc at a temperature of 10^5°K, acceptable radial distribution functions are obtained using the MC technique, and below 9×10^3°K the particles become paired, forming the neutral gas. However, in the range 10^4–5×10^4°K, the plasma appears to behave as a mixture of two phases, ionized and un-ionized. Which phase dominates is influenced rather sensitively by a parameter Δ.

As the parameter Δ assumes some importance in the following discussion, the manner in which it arises will be briefly discussed. In MC calculations of this type, a number of particles—16 protons and 16 electrons in this case—are placed in a unit cell. This unit cell is surrounded by a network of identical cells, thus enabling the energy of a configuration to be calculated conveniently as described in Refs. 3 and 4. One particle is displaced a random amount, which can have a maximum value Δ. The energy of the new configuration is calculated, and the MC procedure decides if the move is acceptable or not. Each particle is considered in this manner until the system approaches an equilibrium energy level. The criterion for the choice of Δ is usually based on minimizing the rate of approach of the system to equilibrium; however, as is shown below, the results of this calculation indicate that other considerations should also be taken into account.

Another important choice is the cutoff imposed on the attractive Coulomb potential at short radii. The need for this choice is also encountered when trying to solve integral equations with attractive Coulomb forces present. It can be overcome by treating the close interactions quantum mechanically (QM), and Barker[5] and Storer[6] have independently calculated, with close agreement, effective potentials ϕ_e which should be used when unlike particles approach closer than a certain distance r_J, which depends on temperature. However, the MC calculations were completed previous to the calculation of ϕ_e, and the results are presented in Fig. 1, which shows the unlike radial distribution function g_{MC} obtained from iterations 30 000 to 50 000 with $\Delta=12.5a_0$ (a_0 is the Bohr radius), and using the usual Coulomb potential ϕ_C, but with a constant value below $r=2a_0$. A classical distribution function $g_e=e^{\beta\phi_e}$ is drawn for comparison, and the equivalent quantum mechanical case $g_{QM}=e^{\beta\phi_e}$ is also shown. The g_{MC} fails to reproduce g_e at small radii, and this is almost certainly due to too large a choice of the step size Δ, with the result that not enough sample points are considered at short interparticle distances. At higher radii, g_{MC} is well above g_e, which implies that two unlike particles prefer to remain some 25 a_0 apart. This implication is confirmed by a close study of particle movements, from which it is found that two unlike particles tend to move around the cell together.

If Δ is further increased to $50a_0$, then g_{MC} becomes appreciably smaller than g_e, especially for $r<50a_0$, and the particles are found to move in an almost random fashion. The study of the particle movements also explains why the graph of the distribution function between *like* particles has an unusual peak at low radii, which is found to be due to discrete collisions between a pair (effectively neutral) and an ion or electron. The choice of Δ also influences markedly both the rate of approach of the system to equilibrium, and even the equilibrium energy level attained.

Figure 2 shows the variation of the cell energy per particle (16 protons and 16 electrons in the unit cell), with the number of iterations completed (each iteration gives every particle in the unit cell a chance to move a

[1] A. A. Broyles, H. L. Sahlin, and D. D. Carley, Phys. Rev. Letters 10, 319 (1963).
[2] D. D. Carley, Phys. Rev. 131, 1406 (1963).
[3] S. G. Brush, H. L. Sahlin, and E. Teller, J. Chem. Phys. 45, 2102 (1966).
[4] A. A. Barker, Aust. J. Physics 18, 119 (1965).
[5] A. A. Barker, Aust. J. Physics 21 121 (1968).
[6] R. G. Storer, J. Math. Phys. 9, 964 (1968).

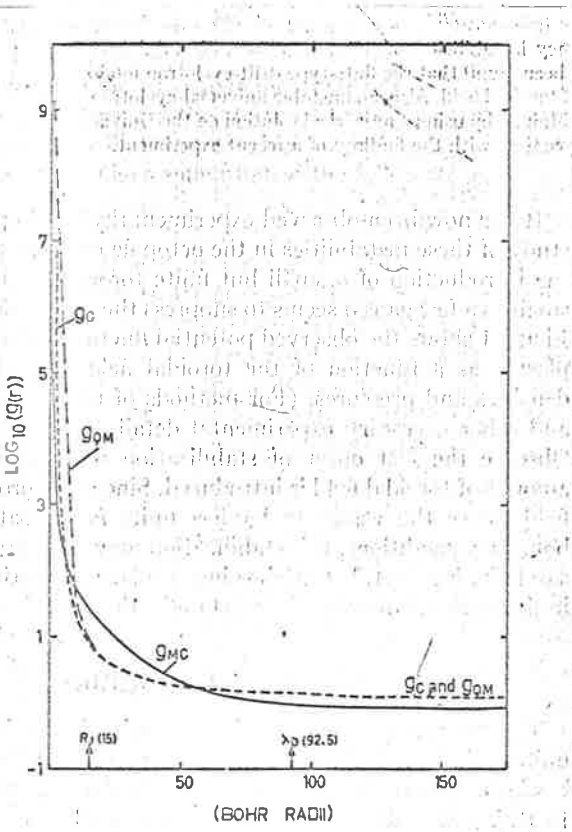

FIG. 1. The radial distribution functions, (drawn on a log scale), for a hydrogenous plasma of density 10^{18} e/cc and temperature 10^4°K, taken from iterations 30 000 to 50 000.

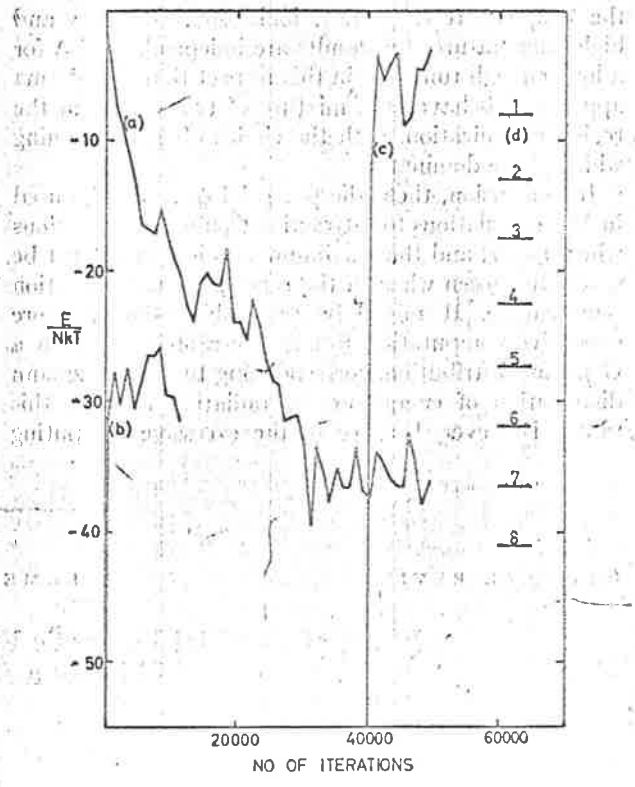

FIG. 2. Approach to equilibrium: (a) from a random initial configuration of protons and electrons with $\Delta=12.5a_0$; (b) from a configuration of pairs approximately equidistant from each other, with $\Delta=12.5a_0$; (c) as for (b) but $\Delta=50a_0$; (d) levels showing approximately the number of pairs existing at this energy.

maximum distance Δ). In (b) and (c) it can be seen that the equilibrium energy is extremely sensitive to Δ, and (a) and (b) show that approximate equilibrium energy is reached faster by approaching from an ordered configuration. Pairing is said to occur when the potential energy between a proton and electron is greater than the ionization energy (this occurs when they are less than $2a_0$ apart), and (d) shows approximately the number of pairs in the unit cell at that energy. The study of particle movements mentioned confirms that the degree of pairing depends on Δ. Previous MC calculations[3,4,7] have emphasized that results should be independent of Δ, and the magnitude of Δ has been chosen empirically by considering the rate of convergence of the system to equilibrium. It has been found that $\Delta \approx L/(3N) \approx 5.0a_0$ in this case, where L is the unit-cell length, and N is the number of particles in the cell, has the right order of magnitude to secure near optimum convergence. However, in the region near the ionization point it appears as if Δ is analogous to a limit of the energy of quanta absorbed or emitted from the radiation field, and if Δ is small, one particle may move slightly away from the interacting particle, but rarely escapes fully; whereas if Δ is relatively large the particles completely separate. This behavior is peculiar to the temperature range near ionization, as at low and high temperatures the results are independent of Δ for a long enough run. It is in this respect that the plasma appears to behave as a mixture of two phases in the region of ionization, with the choice of Δ determining which phase dominates.

In conclusion, then, the potential ϕ_e should be used in MC calculations for attractive Coulomb interactions where $r<r_J$; and the maximum step length Δ must be carefully chosen when in the range near the ionization temperature. It might be preferable (though more expensive computationally) to use a step size with a Gaussian distribution, corresponding to the Boltzmann distribution of energy in the radiation field, in this range. However, because of the excessive computing time involved (3000 iterations taking 1 h on a CDC 6400 computer), distribution functions should be obtained more economically in this region by solving a modified Percus-Yevick equation[8] and calculations using this approach are at present being carried out. It is hoped by comparing these results with the MC results to resolve the dilemma of the choice of Δ, and hence improve the MC results.

The author wishes to acknowledge the helpful suggestions of Professor H. S. Green and Dr. P. W. Seymour on this work. The MC results were completed under a generous grant from the Australian Institute of Nuclear Science and Engineering.

[7] W. W. Wood and T. R. Parker, J. Chem. Phys. 27, 720 (1957).

[8] A. A. Barker, Phys. Fluids 9, 1590 (1966).

APPENDIX B

FORTRAN PROGRAMMES

1. To evaluate the QM distribution functions

The program listing is for the calculation of $g_{pe}(r)$, for r varying from $.5a_o$ to $117a_o$ in steps of one half Bohr radii. The prefix or suffix HBR signifies the variable expressed in half Bohr radii, and BR signifies Bohr radii. The program only needs slight modifications to calculate $g_{ee}(r)$. The charge term SHZ becomes -1, the reduced mass REDM becomes 0.5, and the bound state calculation (statements 20 to 16) is removed, with several minor program changes.

A separate fortran program was written to calculate the first bound state contribution and evaluate the distribution functions at zero radii, but as it is mainly a simplification of the program listed, it is not included. Two additional programmes were run to check the values of the bound and scattered contributions by using alternative techniques as discussed in section 4.2. These were run only for select r values, and are also not listed.

2. To solve a Modified Percus-Yevick equation

The program reads the results of the last run from tape, transfers them to another tape using the 'Father-daughter' procedure, and begins this calculation using the $g_{ab}(r)$ derived in the previous iteration. Suppose for definiteness the jth iteration (ITER) has been read in, i.e. $g^{(j)}(r)$, where $g^{(j)}(r)$ refers to both like and unlike cases. The variable LA is given the value 1 to denote interactions between like particles, and 2 to denote interactions between unlike particles. LC and LD are used in a similar role during the Σ_c and Σ_d. The equation is programmed for the computer in the form:-

GO(LA,LR+1) = (1+TDTM+FDTM)/EXP(PZ(LA,LR+1)

where LR is the radius in Bohr radii (1 is added in indices to avoid storage difficulties when r=0).

TDTM is the PY term:

$$= \frac{2\pi}{r} \sum_c n_c \int_o^{LRF} \int_{Is-LR1}^{s+LR} [1-e_{ac}(s)].g_{ac}(s)[g_{bc}(t)-1]tdt.sds$$

for $e_{ac}(r)$ = exp [PZ(LAC,LR+1)]

$g_{ac}(r)$ = exp[GZ(LAC,LR+1)] .

FDTM is the additional term suggested by Green:

$$= \frac{2\pi}{r^2} \sum_c nc \sum_d nd \int_0^{LRF} \int_0^{LRF} \int_{|LR-S|}^{LR+S} \int_{|LR-U|}^{LR+U} \int_0^{\pi}$$

$$[g_{bc}(t)-1]\,[g_{bd}(v)-1]\; g_{ac}(s)\; g_{ad}(u)\; [1-e_{ad}(u)]\, g_{dc}(w)$$

$$d\theta v dv\; t dt\; u du\; s ds \text{ for}$$

$$2r^2w^2 = 2r^2(s^2+u^2) - (u^2+r^2-v^2)\,(r^2+s^2-t^2)$$

$$+ 4[r^2s^2-(r^2+s^2-t^2)^2]^{\frac{1}{2}}\; [4r^2u^2-(r^2+u^2-v^2)^2]^{\frac{1}{2}}\; \cos\theta\ .$$

The TDTM and FDTM are decomposed into terms obtained by completing the respective summations to give

```
TDTM = TDCON*[TD(LA,1) + TD(LA,2)]
FDTM = FDCON*[FD(LA,1,1) + FD(LA,1,2) +
              FD(LA,2,1) + FD(LA,2,2)] .
```

The two dimensional integration contained in TD(LA,LC) is carried out in the DO loop from statement 109 to 102, and the five dimensional integration contained in FD(LA,LC,LD) is completed in the DO loop from statement 102 to 92.

As described in section 3.3, the integration procedure finally adopted was a simple trapezoidal rule. The mesh ratio used (MHS, MHU and MHZ for the 5D case, and MHT and MHF for the 2D case) were altered according to the region of integration, i.e. to MHI (5D) and MTI (2D)

for the "inner" region, to MH(5D) and MHT(2D) for the "main" region and to MHLR(5D) and MTLR(2D) for the "large r" region. The procedure used to obtain g(r) for non-integer values of LR was to do a linear interpolation between GZ(LA,LR+1) and GZ(LA,LR+2), i.e. on the logs of g(r).

The final GO(LA,LR+1) obtained is stored (statement 188), and the GO(LA,LR+1) is returned to the start of the program as g_{j+1}. A similar iteration is made but the GO(LA,LR+1) derived are now stored as g_{j+2}, (statement 195) and then used to obtain a g_∞ as described in section 5.2 (see statements 195 to 173). The value of g_∞ may be mixed (as in 199) with the g_j read in initially to obtain the next g_{IN}, or may be used directly as input for the next series of iterations, g_{IN}, g_{j+3}, g_{j+4}, to obtain the next estimate of g_∞. On each iteration the main results are printed out (204) and written on tape (171).

The program used for the PY calculation is essentially the same as the one listed (but does not contain the time consuming 5D calculation) and so is not presented. Small programmes to calculate g(o) from equation (5) and the thermodynamic integrals I and J referred to in Chapter 5 are also omitted.

```
C
C     FORTRAN PROGRAM TO EVALUATE THE  Q.M.  DISTRIBUTION FUNCTIONS
      PROGRAM SMLR (INPUT,OUTPUT)
      DIMENSION A(300),B(300),G(300),F(300),COULF(300) ,COULT(300),
     1C(300),BP( 300) ,PL(300)
      READ1,NSHBR,NDHBR,NHBMX,MESHR,NSHZ,TEMP,BTMLM,UPLIM
    1 FORMAT(5I5,3F10.3)
      RJOIN=250.    $    DENIS=0.    $    SCS=0.       $NUMAC=10000
      RNMDE=1.0E18     $    REDM=1.0
      RNMDE=1.0E18
      FLDBR=SQRT(1.38044*TEMP*1.0E22/(8.*3.14159*RNMDE*4.80286**2*5.2917
     1 **2))
      BE= (15.780/(TEMP*.0001))
      CONBR=3.1578/(TEMP*.00001)
      CSTBRS=1.5787/(TEMP*.00001*REDM)
      CONST=SQRT((1.38044*9.1083*5.29172**2*TEMP*1.0E-6*REDM/(2*3.14159*
     1 1.05443**2))**3)
      PI=3.14159 $    A0=1.   $   A0CUB=B/(2*A0**3*4*3.14159)
      FLAMD=2*FLDBR $   API=2./((2.*PI)**2)   $   NHBR=NSHBR-NDHBR
   11 NHBR=NHBR+NDHBR
      R=NHBR     $    RSQ=R*R
      M=0   $   SCATS=0.
      N=0     $    RTFAC=1.0     $    SUMB=0.          $    I=0
      RANGE=UPLIM-BTMLM      $    TNVAL=RANGE/MESHR
      IF(NSHZ)55,55,56
   55 SHZ=1.
      GOTO20
   56 SHZ=1./EXP(NHBR/(2*FLDBR))
   20 N=N+1
      FNSQ=N*N     $    TSUM=0.    $    R=NHBR     $ RO=R*SHZ/N $    K=0
      PL(1)=RO**(N-1)
      IF(N.NE.1)23,24
   23 RTFAC=RTFAC*SQRT((2.*N-2.)*(2.*N-3.))
   24 RTAK=1./(FNSQ*RTFAC)
      IF(PL(1))21,28,28
   21 PLT  =-PL(1)
      GOTO29
   28 PLT=PL(1)
   29 TERM=RTAK*PLT
      TSUM=TERM*TERM
      IF(K.GE.(N-1))30,31
   31 K=1
      PL(2)=2*(N-1)*RO**(N-2)-PL(1)
      IF(PL(2))33,34,34
   33 PLT  =-PL(2)
      GOTO43
   34 PLT=PL(2)
   43 TERM=RTAK*SQRT(2.*N-3)*PLT
      TSUM=TSUM+TERM*TERM
      IF(K.GE.(N-1))30,44
   44 K=K+1
      M=K+1
      PL(M)=((2.*N-2.*K+1.)/(2.*N-K))*((2.*(N-K)/RO)-(N/(N-K+1.)))*PL(M
     1-1)-((N-K)*(K-1.)*PL(M-2))/((N-K+1.)*(2.*N-K))
      RTAK=RTAK*SQRT((2.*N-K)/K)
      IF(PL(M))45,46,46
```

```
C                                                                    PA
   45 PLT  =-PL(M)
      GOTO47
   46 PLT=PL(M)
   47 TERM=RTAK*SQRT(2.*N-2.*K-1)*PLT
      TSUM=TSUM+TERM*TERM
      IF(K.GE.(N-1))30,44
   30 ENY=EXP((BE*SHZ*SHZ/FNSQ)-RO)
      SUMB   =SUMB   +TSUM*ENY
      BNDG=SUMB*SHZ**3*AOCUB/CONST     $ BNDGL=ALOG(BNDG)/2.30259
      IF((TSUM*ENY).LE.(SUMB/NUMAC ))16,20
   16 IF(NHBR.LT.(RJOIN+10))64,62
   64 I=I+1
      FK=BTMLM+RANGE*(2*I-1)/(2.*MESHR)      $FKSQ=FK*FK
      ALPHA=(-1.00263*SHZ)*REDM/FK                  $  ALPSQ=ALPHA*ALPHA
      FKR=FK*NHBR/2.     $  FKRSQ=FKR*FKR
      CA=ALPHA/FKR   $   THE=FKR-ALPHA*ALOG(2.*FKR)    $   DP=ALPHA*FKR
      WT=FKSQ/EXP(CSTBPS*FKSQ)$   TPA=PI*2*ALPHA
      LCN=FKR+ABS(ALPHA)+20
      IF(FKR.LT.10.0)17,40
   40 PART=0.
      S=0.
   27 S=S+1
      T1=ALPHA/S   $  T2=ATAN(ALPHA/S)   $  TE=T1-T2
      IF(ABS(TE).LE.ABS(PART/100000.))25,26
   26 PART=PART+TE
      GOTO27
   25 SIGZ=-.577215665*ALPHA+PART
      NC=1     SNCT=1       $   L=0     $  AX=0.   $  THETZ=THE+SIGZ
      G(1)=(AX+ALPSQ)/(2.*FKR)  $  F(1)=CA/2.
      GS=0.+G(1)        $   FS=1.+F(1)      $  K=0
   18 K=K+1
      A(K)=(2*K+1)*CA/(2.*K+2. )
      B(K)=(AX-K*(K+1)+ALPSQ)/((2*K+2)*FKR)
      G(K+1)=A(K)*G(K)+B(K)*F(K)
      IF(ABS(G(K+1)).GT.ABS(G(K)))35,14
   35 IF(ABS(G(K)).GT.1.0E-100)13,14
   13 NCT=-1
   14 GS=GS+G(K+1)
      F(K+1)=A(K)*F(K)-B(K)*G(K)
      FS=FS+F(K+1)
      IF(ABS(F(K+1)).GT.ABS(F(K)))36,18
   36 IF(ABS(F(K)).GT.1.0E-100)15,18
   15 IF(NCT.EQ.-1)22,18
   22 COULZ      =GS*COS(THETZ)+FS*SIN(THETZ)
      GOTO19
   17 L=0
      BP(1)=DP          $   BP(2)=(2*DP**2-FKRSQ)/6.
      BPS=1+BP(1)+BP(2)              $   NP=1
   41 NP=NP+1
      BP(NP+1)=(2*DP*BP(NP)-FKRSQ*BP(NP-1))/((NP+1)*(NP+2.))
      BPS=BPS+BP(NP+1)
      IF(ABS(BP(NP+1)).LE.ABS(BPS/10000.))42,41
   42 CZ=EXP(-PI*ALPHA)*SQRT(-TPA/(EXP(-TPA)-1))
      COULZ=BPS*FKR*CZ
```

```
C                                                                       PA
      19 COULT(LCN)=0.0
         COULT(LCN-1)=1.0E-200 $    L=LCN
      38 L=L-1
         AX=L*(L+1)      $    Z=2.*L+1       $     LSQ=L*L
         COULT(L  -1)=(Z*(ALPHA+AX/FKR)*COULT(L  )-L*SQRT((L+1)**2+ALPSQ)
        1 *COULT(L  +1))/((L+1)*SQRT(LSQ+ALPSQ))
         IF(L  .LE.2)37,38
      37 COUTZ=(3*(ALPHA+2/FKR)*COULT(1)-SQRT(4+ALPSQ)*COULT(2))/(2*SQRT(
        11+ALPSQ))
         CAL=COULZ/COUTZ
         SUMS=COULZ**2/FKRSQ
         L=0
      39 L=L+1
         Z=2.*L+1
         COULF(L  )=CAL*COULT(L  )
         TERN=Z*COULF(L  )**2/FKRSQ
         SUMS=SUMS+TERN
         IF(L.GE. (LCN     ))32,39
      32 FUNC=WT*SUMS
         SCATC=TNVAL*FUNC
         SCATS=SCATS+SCATC
         IF(I.GE.MESHR)12,16
      12 SCATG=API*SCATS  /CONST
         GR=BNDG+SCATG   $  GRL=ALOG(GR)/2.30259   $ SCTGL=ALOG(SCATG)/2.302
         IF(NSHZ)59,59,58
      59 CLASL=2*CONBR/NHBR
         CLAS=EXP(CLASL)
         PRINT2,NHBR,BNDG,BNDGL,SCATG,SCTGL,GR,GRL,CLAS,N
       2 FORMAT(I5,7E15.7,I5)
         IF(ABS((GR-CLAS)/CLAS).LT..05)57,63
      57 IF(RJOIN.LT.200)63,77
      77 RJOIN=NHBR
         GOTO63
      58 DHUCL=2*CONBR*SHZ/NHBR
         DHUC=EXP(DHUCL)
         PRINT2,NHBR,BNDG,BNDGL,SCATG,SCTGL,GR,GRL,DHUC,N
         IF(ABS((GR-DHUC)/DHUC).LT..05)65,63
      65 IF(RJOIN.LT.200)63,76
      76 RJOIN=NHBR
      63 SCION=RSQ*SCATG
         SCS=SCS+SCION   $   DENI=RSQ*GR   $   DENIS=DENIS+DENI
         GOTO11
      62 NUMAC=100
         IF(NSHZ)68,68,69
      68 CLASL=2*CONBR/NHBR
         CLAS=EXP(CLASL)
         CLASL=CLASL/2.30259
         SCION=RSQ*(CLAS-BNDG)
         SCS=SCS+SCION   $   DENI=RSQ*CLAS $   DENIS=DENIS+DENI
         ZION=SCS*100/DENIS
         PRINT5,NHBR,N,BNDG,BNDGL,CLAS,CLASL,SCION,SCS,DENI,DENIS,ZION
       5 FORMAT(2I5,9E11.3)
         GOTO54
      69 DHUCL=2*CONBR*SHZ/NHBR
```

```
C
      DHUC=EXP(DHUCL)
      SCION=RSQ*(DHUC-BNDG)
      SCS=SCS+SCION    $   DENI=RSQ*DHUC $    DENIS=DENIS+DENI
      DHUCL=DHUCL/2.30259
      ZION=SCS*100/DENIS
      PRINT5,NHBR,N,BNDG,BNDGL,DHUC,DHUCL,SCION,SCS,DENI,DENIS,ZION
   54 IF(NHBR.GE.NHBMX)52,11
   52 PRINT1,NSHBR,NDHBR,NHBMX,MESHR,NSHZ,TEMP,BTMLM,UPLIM
      PRINT4,FLDBR,BE,CSTBRS,CONST,CONBR,RJOIN,ZION
    4 FORMAT(8E14.6 )
      STOP
      END
```

M LENGTH INCLUDING I/O BUFFERS

ON ASSIGNMENTS

ENT ASSIGNMENTS

=	001522	2	=	001570	4	=	001501	5	=	001575
=	000116	12	=	001126	13	=	000637	14	=	000640
=	000667	16	=	000427	17	=	000705	18	=	000566
=	000770	20	=	000150	21	=	000212	22	=	000674
=	000174	24	=	000206	25	=	000543	26	=	000540
=	000516	28	=	000214	29	=	000216	30	=	000376
=	000227	32	=	001114	33	=	000244	34	=	000246
=	000630	36	=	000660	37	=	001043	38	=	000774
=	001073	40	=	000514	41	=	000720	42	=	000750
=	000250	44	=	000271	45	=	000346	46	=	000351
=	000353	52	=	001441	54	=	001434	55	=	000136
=	000140	57	=	001205	58	=	001215	59	=	001142
=	001301	63	=	001271	64	=	000436	65	=	001261
=	001304	69	=	001360	76	=	001267	77	=	001213

AMES AND LENGTHS

LE ASSIGNMENTS

=	001660	ALPHA	=	007154	ALPSQ	=	007155	API	=	007123
=	007177	AQ	=	007120	AQCUB	=	007121	B	=	002334
=	007113	BNDG	=	007150	BNDGL	=	007151	BP	=	005744
=	007204	BTMLM	=	007102	C	=	005270	CA	=	007160
=	007212	CLAS	=	007224	CLASL	=	007223	CONBR	=	007114
=	007116	COULF	=	004140	COULT	=	004614	COULZ	=	007203
=	007211	CSTBRS	=	007115	CZ	=	007206	DENI	=	007230
=	007105	DHUC	=	007226	DHUCL	=	007225	DP	=	007162
=	007147	F	=	003464	FK	=	007152	FKR	=	007156
=	007157	FKSQ	=	007153	FLAMD	=	007122	FLDBR	=	007112
=	007140	FS	=	007202	FUNC	=	007215	G	=	003010
=	007220	GRL	=	007221	GS	=	007201	I	=	007134
=	007143	L	=	007176	LCN	=	007165	LSQ	=	007210
=	007127	MESHR	=	007077	N	=	007131	NC	=	007174
=	007175	NDHBR	=	007075	NHBMX	=	007076	NHBR	=	007124
=	007205	NSHBR	=	007074	NSHZ	=	007100	NUMAC	=	007107
=	007166	PI	=	007117	PL	=	006420	PLT	=	007145

```
      C
      C          FORTRAN PROGRAM TO SOLVE A MODIFIED PERCUS-YEVIC EQUATION

            PROGRAM MPRO (INPUT,OUTPUT,XOPPY16,TAPE16=XOPPY16,XOPPY17,TAPE17
           1 =XOPPY17)
      C      ALL UNITS IN BOHR RADII      COPY2
03            COMMON GT(3,2,1010)
03            DIMENSIONFD(2,2,2),FSUM(20),  TD(2,2),TDS ( 30),
           1 GZ(2,2020),PZ(2,2020),GO(2,1010),R(2,1010)    ,TDT(2,2)
           2 ,COT1(2,2),COT2(2,2)
03            LBCUT=2010 $ ITST= 65 IDEBM=189 $ LRF=1000$ INTL=20 $ IDEBL=190
11            ITEM=0     $    IDEBP=IDEBL+1    $    LRP=LRF+1
16       203 READ  (17)ITER,MHT,LACUT,LRF,INTL,MHI,LTPJR,TEMP,
           1   ((PZ(LZ,IZ),LZ=1,2), IZ=1,LBCUT),((GZ(LX,IX),LX=1,2),IX=1,LBCUT)
           2 ,(((GT(LP,LQ,LT),LP=1,3),LQ=1,2),LT=1,IDEBM)
           3 ,(((GT(LP,LQ,LT),LP=1,3),LQ=1,2),LT=IDEBP,LRP,INTL)
31            PRINT10,ITER,ITST,GZ(1,60),GZ(2,60),GT(1,1,2),GT(1,2,2) ,GZ(2,601)
           1, GT(1,1,201),GT(1,2,201),GT(3,1,2),GT(3,2,2) ,GT(3,2,501)
65        10 FORMAT(2I5,10E12.4)
65            WRITE (16)ITER,MHT,LACUT,LRF,INTL,MHI,LTPJR,TEMP,
           1   ((PZ(LZ,IZ),LZ=1,2), IZ=1,LBCUT),((GZ(LX,IX),LX=1,2),IX=1,LBCUT)
           2 ,(((GT(LP,LQ,LT),LP=1,3),LQ=1,2),LT=1,IDEBM)
           3 ,(((GT(LP,LQ,LT),LP=1,3),LQ=1,2),LT=IDEBP,LRP,INTL)
00            IF(ITER.EQ.ITST)208,219
05       219 IF(ITER.GT.ITST)209,203
12       208 READ  3,LRS,LRE,LRD,MTI,MHT,MTLR,LACUT,LRF,ITCUT,INTL,MHI,MH,
           1 MHLR,LTPJR
52         3 FORMAT(14I5)
52            READ  4,TEMP
60         4 FORMAT( F10.2,2F10.4,4E12.4)
      C       CON = BETA*E**2(BOHR RAD)
00            CON=3.1578/(TEMP*.00001)  $ DENS=1.0E18*(5.29172E-9)**3
05            PI=3.14159       $   TPI=2*PI  $   LACSQ=LACUT*LACUT
13            DEBL=SQRT(1/(CON*8*PI*DENS))                    $  LTPT=LTPJR+1
14            ITEBL=(DEBL+10)/10    $   IDEBL=10.*ITEBL  $   IDEBM=IDEBL-1
15            PRINT 3,LRS,LRE,LRD,MTI,MHT,MTLR,LACUT,LRF,ITCUT,INTL,MHI,MH,
           1 MHLR,LTPJR
54            PRINT 4,TEMP           ,DEBL,CON,DENS
70       201 ITER=ITER+1
72            LR=LRS         $   LRD=1
74            GZ(1,1)=ALOG(.0006429) $   GZ(2,1)=ALOG(5644.0)
81            ITEM=ITEM+1
82       205 LR=LR+LRD
84            IF(LR.EQ.IDEBL)108,109
90       108 LRD=INTL
92       109 LRSQ=LR*LR   $   TRSQ=2.*LRSQ
96            TDCON=TPI*DENS/LR   $  FDCON=TPI*DENS*DENS*2/LRSQ
05             DO 102 LA=1,2
06             DO 102 LC=1,2
07             IF((LA*LC).EQ.2)125,126
14       125  LAC=2
15            GO TO 127
16       126  LAC=1
17       127  IF(LC.EQ.2)128,129
24       128  LBC=2
25            GOTO191
26       129 LBC=1
```

```
C                                                                       PA
7       191 TDS(MHT)=0.
1           MHF=MTI    $    LLM=0    $    ULM=LACUT    $    CTR=-3
6       192 WS=(ULM-LLM)/MHF       $    I=1
3       181  S=LLM   +(2*I-1)*WS/2
4           IF(S.LT.LRF)186,187
1       186 NS=S+1
4           PZS=PZ(LAC,NS)+(S+1-NS)*(PZ(LAC,NS+1)-PZ(LAC,NS))
1           GZS=GZ(LAC,NS)+(S+1-NS)*(GZ(LAC,NS+1)-GZ(LAC,NS))
3           GOTO185
3       187 NST=S/INTL
6           NSL=INTL*NST+1        $    NSU=INTL*(NST+1)+1
3           PZS=PZ(LAC,NSL)+(S-NSL+1)*(PZ(LAC,NSU)-PZ(LAC,NSL))/INTL
0           IF(S.LT.LRF)183,184
5       183 GZS=GZ(LAC,NSL)+(S-NSL+1)*(GZ(LAC,NSU)-GZ(LAC,NSL))/INTL
3           GOTO185
3       184 GZS=0.
4       185 TS=(1-EXP(PZS))*WS*S*EXP(GZS)
5            TDLL3=ABS(LR-S)          $    TDUL3=LR+S
2           IF(CTR.GT.0)182,103
7       182 TDUL3=LACUT
1           GOTO107
1       103 IF(CTR.LT.-2)107,115
7       115 IF(TDLL3.LT.LACUT)104,105
5       104  TDLL3=LACUT
7       105 IF(TDUL3.GT.LRF)106,107
5       106 TDUL3=LRF
7       107 WT=(TDUL3-TDLL3)/MHF    $    K=1
4       161  T=TDLL3+(2*K-1) *WT/ 2
5           IF(T.LT.IDEBL)162,163
2       162 NT=T+1
5           GZT=GZ(LBC,NT)+(T+1-NT)*(GZ(LBC,NT+1)-GZ(LBC,NT))
2           GOTO165
2       163 NTT=T/INTL
5           NTTL=INTL*NTT+1    $    NTTU=INTL*(NTT+1)+1
2           GZT=GZ(LBC,NTTL)+(T-NTTL+1)*(GZ(LBC,NTTU)-GZ(LBC,NTTL))/INTL
7       165 TDS(MHT)=TDS(MHT)+TS          *T*WT*(EXP(GZT)-1)
1           K=K+1
3           IF(K.GT.MHF)160,161
0       160 I=I+1
2           IF(I.GT.MHF)180,181
7       180 IF(CTR.LT.-2)193,194
6       193 MHF=MHT    $    LLM=LACUT    $ ULM=LRF+LR   $ CTR=-1 $ COT1(LA,LC)
          1 =TDS(MHT)
1           GOTO192
2       194 IF(CTR.LT.0)197,102
5       197 MHF=MTLR   $    LLM=LR-LACUT    $    ULM=LR+LACUT $ CTR=1 $ COT2(LA,
          1 LC)=TDS(MHT)
            IF(LLM.LT.LACUT)112,192
5       112 LLM=LACUT
            GOTO192
```

```
C
50      102  TD(LA,LC)=TDS(MHT)
61           DO92 LA=1,2
63           DO92 LC=1,2
64           IF(LC.EQ.2)12,13
70        12 LBC=2
71           GOTO14
72        13 LBC=1
73        14 IF((LA*LC).EQ.2)17,19
01        17 LAC=2
02           GOTO15
03        19 LAC=1
04        15 IF(LC.EQ.1)95,95
11        95 DO92 LD=1,2
13           GOTO97
13        96 LD=2    $    FD(LA,2,1)=FD(LA,1,2)
16        97 IF(LD.EQ.2)20,69
23        20 LBD=2
24           GOTO77
25        69 LBD=1
26        77 IF((LD*LC).EQ.2)78,79
34        78 LDC=2
35           GOTO89
36        79 LDC=1
37        89 IF((LD*LA).EQ.2)93,94
45        93 LAD=2
46           GOTO91
47        94 LAD=1
50        91 FSUM(MH)=0.
52           MHS=MHI   $    SMIN=0.    $    SMAX=LACUT    $    CTS=-3
57        82 WS=(SMAX-SMIN)/MHS        $    I=1
64        81 S=SMIN+(2*I-1)*WS/2
75           FDLL3=ABS(LR-S)   $    FDUL3=LR+S
02           IF(CTS.GT.0.)62,63
06        62 FDUL3=LACUT
10           GOTO27
10        63 IF(CTS.LT.-2)27,57
16        57 IF(FDLL3          .LT.LACUT)21,49
24        21 FDLL3=LACUT
26        49 IF((FDUL3).GT.LRF  )25,27
04        25 FDUL3=LRF
06        27 WT=(FDUL3-FDLL3)/MHS
12            SSQ= S* S
13           C6= TRSQ* SSQ
15           IF(S.LT.IDEBL)87,88
12        87 NS=S+1
15           PZS=PZ(LAC,NS)+(S+1-NS)*(PZ(LAC,NS+1)-PZ(LAC,NS))
12           GZS=GZ(LAC,NS)+(S+1-NS)*(GZ(LAC,NS+1)-GZ(LAC,NS))
14           GOTO22
14        88 NS=S/INTL
17           NSL=INTL*NS+1    $    NSU=INTL*(NS+1)+1
14            PZS=PZ(LAC,NSL)+ (S-NSL+1  )*(PZ(LAC,NSU)-PZ(LAC,NSL))/INTL
11           IF(S.LT.LRF)26,28
16        26  GZS=GZ(LAC,NSL)+ (S-NSL+1  )*(GZ(LAC,NSU)-GZ(LAC,NSL))/INTL
14           GOTO22
```

```
C
454       28 GZS=0.
455       22 FS=EXP(GZS)*(1-EXP(PZS))*WS*S
467          MHU=MHI   $    UMIN=0.    $    UMAX=LACUT    $    CTU=-3
474       72 WU=(UMAX-UMIN)/MHU    $    J=1
501       71 U=UMIN+(2*J-1)*WU/2     $    K=1
513          FDLL4=ABS(LR-U)    $    FDUL4=LR+U
520          IF(CTU.GT.0.)52,53
524       52 FDUL4=LACUT
526          GOTO24
526       53 IF(CTU.LT.-2)24,67
534       67 IF(FDLL4          .LT.LACUT)30,31
542       30 FDLL4=LACUT
544       31 IF((FDUL4).GT.LRF   )23,24
552       23 FDUL4=LRF
554       24 WV=(FDUL4-FDLL4)/MHU
560           USQ= U* U
561          C7= TRSQ* USQ
563          C1=C6+C7
565          IF(U.LT.IDEBL)43,44
572       43 NU=U+1
575          PZU=PZ(LAD,NU)+(U+1-NU)*(PZ(LAD,NU+1)-PZ(LAD,NU))
612          GZU=GZ(LAD,NU)+(U+1-NU)*(GZ(LAD,NU+1)-GZ(LAD,NU))
624          GOTO29
624       44 NU=U/INTL
627          NUL=INTL*NU+1    $    NUU=INTL*(NU+1)+1
634           PZU=PZ(LAD,NUL)+ (U-NUL+1   )*(PZ(LAD,NUU)-PZ(LAD,NUL))/INTL
651          IF(U.LT.LRF)54,55
656       54  GZU=GZ(LAD,NUL)+ (U-NUL+1   )*(GZ(LAD,NUU)-GZ(LAD,NUL))/INTL
674          GOTO29
674       55 GZU=0
675       29 FSU=EXP(GZU)*FS *(1-EXP(PZU))*U*WU
710       61 T=FDLL3+(2*K-1)*WT/(2.)      $    L=1
721          TSQ=T*T
723          C2=LRSQ+ SSQ-TSQ
726          C4=SQRT(2*C6-C2*C2)
734          IF(T.LT.IDEBL)48,56
741       48 NT =T+1
744          GZT=GZ(LBC,NT)+(T+1-NT)*(GZ(LBC,NT+1)-GZ(LBC,NT))
761           GOTO32
761       56 NT=T/INTL
764           NTL=NT*INTL+1    $    NTU=INTL*(NT+1)+1
772           GZT=GZ(LBC,NTL)+ (T-NTL+1   )*(GZ(LBC,NTU)-GZ(LBC,NTL))/INTL
006       32 FSUT=FSU*(EXP(GZT)-1)*WT*T
015       51 V=FDLL4+(2*L-1)*WV/(2.)
025          IF(V.LT.IDEBL)59,64
032       59 NV =V+1
035          GZV=GZ(LBD,NV)+(V+1-NV)*(GZ(LBD,NV+1)-GZ(LBD,NV))
052          GOTO42
052       64 NV=V/INTL
055          NVL=INTL*NV+1    $    NVU=INTL*(NV+1)+1
062           GZV=GZ(LBD,NVL)+ (V-NVL+1   )*(GZ(LBD,NVU)-GZ(LBD,NVL))/INTL
077       42 FSUTV=FSUT *(EXP(GZV)-1)*WV*V
106          VSQ=V*V
117          C3= USQ+LRSQ-VSQ
```

```
      C
13          C5=SQRT(2.*C7-C3*C3)
20          C8=C3*C2
22          C9=C4*C5
24          WMIN=SQRT(ABS(C1-C8-C9)/TRSQ)
33          WMXT=SQRT((C1-C8+C9)/TRSQ)
41          IF(WMIN.GT.LBCUT)47,37
47       37 IF(WMXT.LE.LACUT)33,34
55       33 MHZ=MH    $    WMAX=WMXT    $    CT=+1
62          GOTO18
62       34 IF(WMIN.LT.LACUT)16,38
70       16 MHZ=MHI   $    CT=-1
73          WMAX=LACUT
75          GOTO18
75       38 IF(WMXT.GT.LBCUT)36,39
03       36 WMAX=LBCUT
05          GOTO18
05       39 WMAX=WMXT
07       18 WW=(WMAX-WMIN)/MHZ      $    M=1
14       41 W=(2*M-1)*WW/(2)     +WMIN
24          IF(W.LT.IDEBL)65,66
31       65 NW =W+1
34          GZW=GZ(LDC,NW)+(W+1-NW)*(GZ(LDC,NW+1)-GZ(LDC,NW))
51          GOTO45
51       66 NW =W/INTL
54          NWL=INTL*NW+1    $    NWU=INTL*(NW+1)+1
61           GZW=GZ(LDC,NWL)+ (W-NWL+1  )*(GZ(LDC,NWU)-GZ(LDC,NWL))/INTL
76       45 DEN=SQRT((C4*C5)**2-(C8-C1+TRSQ*W*W)**2)
07          DELW=W*2*TRSQ*WW*EXP(GZW)/DEN
.6          FSUM(MH)=FSUTV*DELW+FSUM(MH)
21       35 M=M+1
23          IF(M.GT.MHZ)40,41
30       40 IF(CT.LT.0.)46,47
34       46 MHZ=MH    $    WMIN=LACUT    $CT=+1
-1          GOTO38
-1       47 L=L+1
-3          IF(L.GT.MHU)50,51
50       50 K=K+1
52          IF(K.GT.MHS)60,61
57       60 J=J+1
61          IF(J.GT.MHU)70,71
66       70 IF(CTU.LT.-2)73,74
74       73 MHU=MH    $    UMIN=LACUT    $    UMAX=LRF+LR  $    CTU=-1
73          GOTO72
74       74 IF(CTU.LT.0.)75,76
80       75 MHU=MHLR $    UMIN=LR-LACUT    $    UMAX=LR+LACUT    $    CTU=+1
87          IF(UMIN.LT.LACUT)68,72
84       68 UMIN=LACUT
86          GOTO72
86       76 I=I+1
90          IF(I.GT.MHS)80,81
95       80 IF(CTS.LT.-2)83,84
93       83 MHS=MH    $    SMIN=LACUT    $    SMAX=LRF+LR  $    CTS=-1
92          GOTO82
93       84 IF(CTS.LT.0.)85,92
```

```
C                                                                       P
57        85 MHS=MHLR $   SMIN=LR-LACUT   $   SMAX=LR+LACUT   $   CTS=+1
66           IF(SMIN.LT.LACUT)58,82
73        58 SMIN=LACUT
75           GOTO82
75        92 FD(LA,LC,LD)=FSUM(MH)
12           DO204 LA=1,2
14           TDTM=TDCON*(TD(LA,1)+TD(LA,2))
17           FDTM=FDCON*(FD(LA,1,1)+FD(LA,1,2)+FD(LA,2,1)+FD(LA,2,2))
24           GIN=EXP(GZ (LA,LR+1))   $   PIN=EXP(PZ(LA,LR+1))
37           GO(LA,LR+1)=(1+TDTM+FDTM)/PIN
46       204 PRINT 7,LA,LR              ,TDCON,FD(LA,1,1),FD(LA,1,2),FD(LA,2,2),FD
              1TM,  TD(LA,1) ,TD(LA,2),TDTM,PIN,GIN,GO(LA,LR+1)
10         7 FORMAT(2I5,11E10.3)
10           IF(LR.LT.LRE)205,206
15       206 GO(1,1)=EXP(GZ (1,1))   $   GO(2,1)=EXP(GZ (2,1))
22           IF(ITEM.EQ.1)188,189
26       189 IF(ITEM.EQ.2)195,209
33       188 DO207 LR=1,IDESM
35           GT(1,1,LR+1)=   (GZ(1,LR+1))  $ GT(2,1,LR+1)=ALOG(GO(1,LR+1))
52           GT(1,2,LR+1)=   (GZ(2,LR+1))  $ GT(2,2,LR+1)=ALOG(GO(2,LR+1))
67            GT(3,1,LR+1)=0.0   $   GT(3,2,LR+1) =0.0
72           GZ(1,LR+1)=GT(2,1,LR+1)
76       207 GZ(2,LR+1)= GT(2,2,LR+1)
05           DO175 LR=IDESL,LRF,INTL
07           GT(1,1,LR+1)=   (GZ(1,LR+1))  $ GT(2,1,LR+1)=ALOG(GO(1,LR+1))
24           GT(1,2,LR+1)=   (GZ(2,LR+1))  $ GT(2,2,LR+1)=ALOG(GO(2,LR+1))
-1            GT(3,1,LR+1)=0.0   $   GT(3,2,LR+1) =0.0
-4           GZ(1,LR+1)=GT(2,1,LR+1)
00       175 GZ(2,LR+1)= GT(2,2,LR+1)
07           GOTO171
00       195 DO199 LR=1,IDESM
02           GT(3,1,LR+1)=ALOG(GO(1,LR+1) )
01           GT(3,2,LR+1)=ALOG(GO(2,LR+1))
01           R(1,LR+1)=(GT(3,1,LR+1)-GT(2,1,LR+1))/(GT(2,1,LR+1)-GT(1,1,LR+1))
02           R(2,LR+1)=(GT(3,2,LR+1)-GT(2,2,LR+1))/(GT(2,2,LR+1)-GT(1,2,LR+1))
02           IF(ABS(1-R(1,LR+1)).LT.0.50)131,132
01       131 IF(R(1,LR+1).GT.1.0)143,144
01       143 R(1,LR+1)=1.5
05           GOTO132
05       144 R(1,LR+1)=0.5
01       132 GINF1      =GT(2,1,LR+1)+(GT(3,1,LR+1)-GT(2,1,LR+1))/(1-R(1,LR+1))
04           IF(ABS(1-R(2,LR+1)).LT.0.50)133,148
05       133 IF(R(2,LR+1).GT.1.0)145,146
05       145  R(2,LR+1)=1.5
01           GOTO148
01       146 R(2,LR+1)=0.5
05       148 GINF2      =GT(2,2,LR+1)+(GT(3,2,LR+1)-GT(2,2,LR+1))/(1-R(2,LR+1))
00           GTOR1=EXP(GT(1,1,LR+1))  $   GTOR2=EXP(GT(1,2,LR+1))
07           GTTR1=EXP(GT(2,1,LR+1))   $   GTTR2=EXP(GT(2,2,LR+1))
05           GINR1=EXP(GINF1)   $   GINR2=EXP(GINF2)
01           PRINT5,LR,GTOR1        ,GTTR1        ,GO(1,LR+1) , R(1,LR+1),GINR1,
               1      LR,GTOR2        ,GTTR2        ,GO(2,LR+1) , R(2,LR+1),GINR2
02         5 FORMAT( I5,5E12.4, I5,5E12.4)
02           GZ(1,LR+1)= 00.67*GINF1  +  0.33*GT(1,1,LR+1)
02       199 GZ(2,LR+1)= 00.67*GINF2  +  0.33*GT(1,2,LR+1)
```

```
      C                                                                 P
32          DO173 LR=IDEBL,LRF,INTL
34          GT(3,1,LR+1)=ALOG(GO(1,LR+1))
43          GT(3,2,LR+1)=ALOG(GO(2,LR+1))
53          R(1,LR+1)=(GT(3,1,LR+1)-GT(2,1,LR+1))/(GT(2,1,LR+1)-GT(1,1,LR+1))
54          R(2,LR+1)=(GT(3,2,LR+1)-GT(2,2,LR+1))/(GT(2,2,LR+1)-GT(1,2,LR+1))
74          IF(ABS(1-R(1,LR+1)).LT.0.50)135,136
03      135 IF(R(1,LR+1).GT.1.0)139,140
13      139 R(1,LR+1)=1.5
17          GOTO136
17      140 R(1,LR+1)=0.5
23      136 GINF1      =GT(2,1,LR+1)+(GT(3,1,LR+1)-GT(2,1,LR+1))/(1-R(1,LR+1))
36          IF(ABS(1-R(2,LR+1)).LT.0.50)137,138
47      137 IF(R(2,LR+1).GT.1.0)141,142
67      141  R(2,LR+1)=1.5
63          GOTO138
63      142 R(2,LR+1)=0.5
67      138 GINF2      =GT(2,2,LR+1)+(GT(3,2,LR+1)-GT(2,2,LR+1))/(1-R(2,LR+1))
02          GTOR1=EXP(GT(1,1,LR+1))   $   GTOR2=EXP(GT(1,2,LR+1))
11          GTTR1=EXP(GT(2,1,LR+1))   $   GTTR2=EXP(GT(2,2,LR+1))
17          GINR1=EXP(GINF1)   $   GINR2=EXP(GINF2)
23          PRINT5,LR,GTOR1        ,GTTR1        ,GO(1,LR+1) , R(1,LR+1),GINR1,
          1       LR,GTOR2        ,GTTR2        ,GO(2,LR+1) , R(2,LR+1),GINR2
64          GZ(1,LR+1)= 00.67*GINF1   +  0.33*GT(1,1,LR+1)
72      173 GZ(2,LR+1)= 00.67*GINF2   +  0.33*GT(1,2,LR+1)
03          ITEM=0
64      171 PRINT6,ITER,GO(1,1),GO(2,1)
.6        6 FORMAT(1H1, I5,2E12.4)
.6          WRITE (16)ITER,MHT,LACUT,LRF,INTL,MHI,LTPJR,TEMP,
          1   ((PZ(LZ,IZ),LZ=1,2), IZ=1,LBCUT),((GZ(LX,IX),LX=1,2),IX=1,LBCUT)
          2 ,(((GT(LP,LQ,LT),LP=1,3),LQ=1,2),LT=1,IDEBM)
          3 ,(((GT(LP,LQ,LT),LP=1,3),LQ=1,2),LT=IDEBP,LRP,INTL)
11          IF(ITER.GE.ITCUT)209,201
16      209 STOP
.0          END

AM LENGTH INCLUDING I/O BUFFERS
0

ION ASSIGNMENTS

MENT ASSIGNMENTS
  =  003663    4     =  003665    5     =  003710    6     =  003721
  =  003702    10    =  003656    12    =  001170    13    =  001172
  =  001173    15    =  001204    16    =  002170    17    =  001201
  =  002207    19    =  001203    20    =  001223    21    =  001324
  =  001455    23    =  001552    24    =  001554    25    =  001334
  =  001436    27    =  001336    28    =  001454    29    =  001675
  =  001542    31    =  001544    32    =  002006    33    =  002155
  =  002162    35    =  002321    36    =  002203    37    =  002147
  =  002175    39    =  002205    40    =  002330    41    =  002214
  =  002077    43    =  001572    44    =  001624    45    =  002276
  =  002334    47    =  002341    48    =  001741    49    =  001326
  =  002350    51    =  002015    52    =  001524    53    =  001526
```